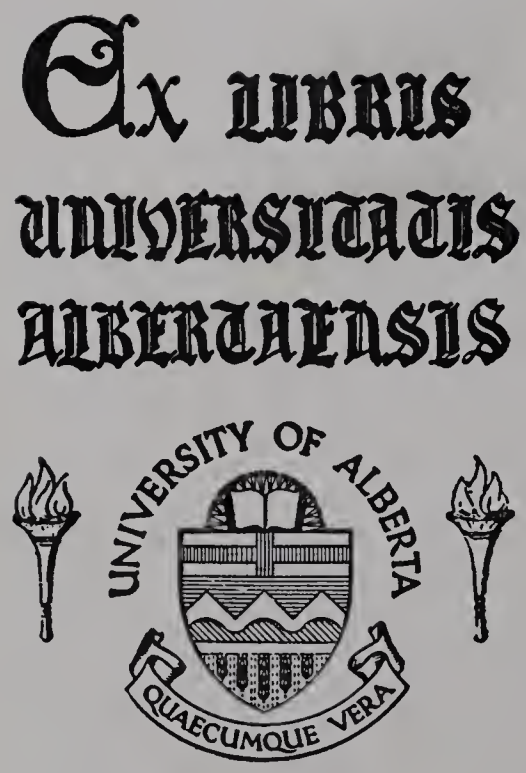

University of Alberta
Printing Department

THE UNIVERSITY OF ALBERTA

LONGITUDINAL STRAIN DISTRIBUTION IN DELAMINATED TIMBER BEAMS

by

EUGENE FREDERICK COLLINS

A THESIS

SUBMITTED TO THE FACULTY OF GRADUATE STUDIES

IN PARTIAL FULFILMENT OF THE REQUIREMENTS FOR THE DEGREE OF

MASTER OF SCIENCE

DEPARTMENT OF CIVIL ENGINEERING

EDMONTON, ALBERTA

APRIL 1966

UNIVERSITY OF ALBERTA

FACULTY OF GRADUATE STUDIES

The undersigned certify that they have read, and recommend to the Faculty of Graduate Studies for acceptance, a thesis entitled LONGITUDINAL STRAIN DISTRIBUTION IN DELAMINATED TIMBER BEAMS submitted by EUGENE FREDERICK COLLINS in partial fulfilment of the requirements for the degree of Master of Science.

ABSTRACT

Thirteen Douglas Fir beams were tested in an investigation of the effect of delamination on the longitudinal strain distribution in glue laminated timber beams. An attempt was made to determine the horizontal shear stress distribution from the longitudinal strain distribution. Ten delaminated beams, 3" x 6" in cross section and 6'-2" long were extensively instrumented and strains recorded at loads up to failure. These beams contained artifical mid-depth delaminations of various lengths located symmetrically with respect to midspan. Two types of delamination were investigated. In one type the wood surfaces at the delaminated section were in contact; whereas in the other type the surfaces were not in contact.

Beam test results indicate non-linear longitudinal strain distributions exist at intact sections in the vicinity of the delamination. The extent of this warping is dependent on the ratio of delamination length to beam length. Horizontal shear stress distributions, derived from the strain distributions were on the whole unsatisfactory due to the difficulty in accurately defining the strain distribution across the section depth. The strains measured at delaminated sections agree with theoretical values for low delamination to beam length ratios. This agreement is not as satisfactory for higher ratios. Strain distributions indicate no appreciable friction exists between contacting delamination surfaces.

ACKNOWLEDGEMENTS

The author wishes to express his sincere thanks to the following persons for their assistance in this investigation.

J. Longworth, Professor of Civil Engineering for his guidance, advice and criticism throughout the testing program and in the preparation of this thesis.

Western Archrib Structures Ltd., Edmonton, for providing the test specimens.

Mr. H. Panse, and staff of the Department of Civil Engineering for their assistance during the testing program.

Miss H. Wozniuk for typing the manuscript.

TABLE OF CONTENTS

TABLE OF CONTENTS (Continued)

LIST OF TABLES

LIST OF FIGURES

5.1	[illegible]	47
5.2	[illegible]	51
5.3	[illegible]	53
6.1	[illegible]	61
6.2	[illegible]	64
6.3	[illegible]	67
7.1	[illegible]	71
7.2	[illegible]	74
7.3	[illegible]	77
8.1	[illegible]	81
8.2	[illegible]	84
8.3	[illegible]	87

LIST OF FIGURES (Continued)

LIST OF PLATES

CHAPTER I

INTRODUCTION

1-1 Definition of Delamination

Delamination is a term used to define the separation of wood surfaces at glued joints. If the separation is in the wood, even though very close to the glued joint, it is termed wood failure or checking.

1-2 Causes of Delamination

The wide spread use of quality control in laminating plants combined with an accumulation of experience in glue laminated timber fabrication has decreased the possibility of faulty manufacture of glulam members. However, delamination when caused by faulty manufacture is the result of a defective glued joint. The most obvious cause of this defective joint is the absence of glue on adjacent laminations, which is quite improbable with the use of mechanical glue spreaders. A more conceivable cause of the joint defect is the non-rectangularity of adjacent laminations. The resulting separation of the lamination edges produces a minor delamination, which may increase in width under service conditions.

Shrinkage is a major cause of delamination. Stress produced by deformation may be built up as a result of this shrinkage. Dietz, Grinsfelder and Reissner (1946)* developed a mathematical analysis of the stresses produced by shrinkage or swelling in a beam composed of

---

*References are listed in the Bibliography

two laminations. Their analysis indicated that high stresses can be induced by relatively small changes in moisture content.

In this paper two cases are considered. The first case is that of a beam with two laminations, one of which is subjected to a uniform moisture change. This moisture change tends to increase or decrease the lamination width while the other lamination remains unchanged. As a result transverse shear stresses develop with a distribution as shown in FIGURE 1.1A. The maximum intensity of stress at the edge of a lamination is:

$$\tau_{max} = 0.7 e \alpha \sqrt{E_x G_{xy}}$$

where $e = \alpha (M_2 - M_1)$

α = coefficient of moisture expansion

M_1 = initial moisture content

M_2 = final moisture content

E_x = modulus of elasticity parallel to the glue line

G_{xy} = shear modulus in plane of beam cross section

Using accepted material properties for Douglas Fir, Dietz, Grinsfelder and Reissner determined the magnitude of stresses produced by a 4% change in moisture content. The resulting maximum transverse shear stress developed was 165 psi for edge grain laminations and 240 psi for flat grain laminations.

The second case considers a moisture change over the total depth of the two layer beam. In this case only normal stresses develop perpen-

GLUE LINE STRESSES RESULTING FROM MOISTURE CONTENT VARIATIONS

[AFTER DIETZ, GRINDSFELDER AND REISSNER]

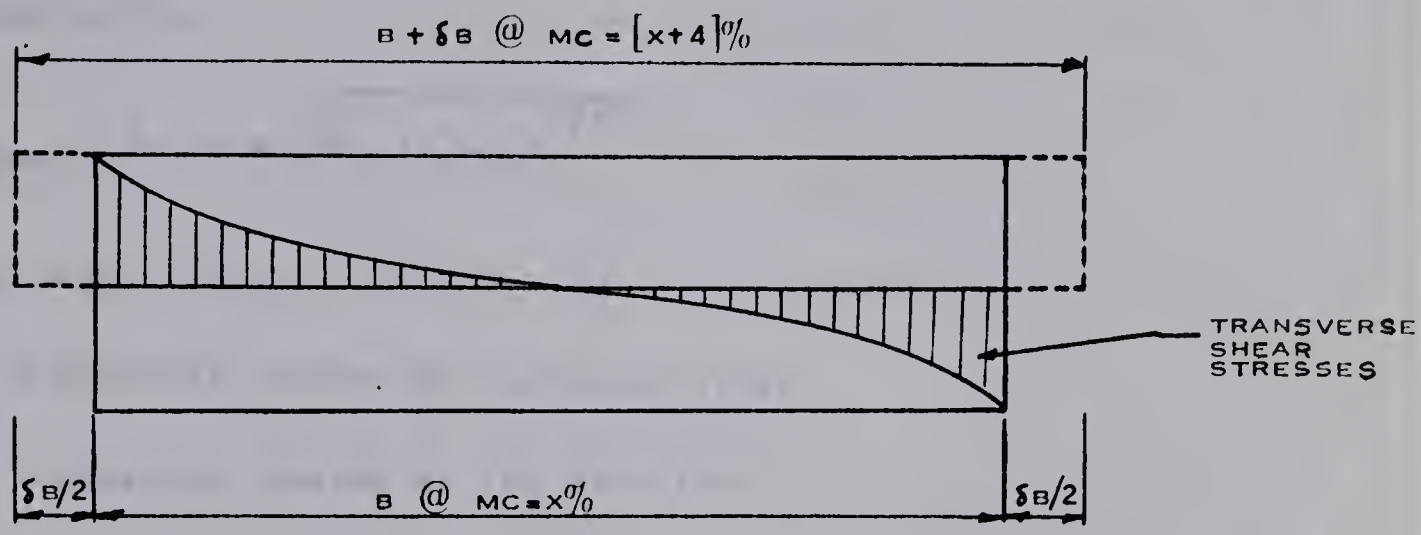

[A] CASE ONE

CROSS SECTION THROUGH BEAM WITH ONE LAMINATION TENDING TO EXPAND UNIFORMLY DUE TO UNIFORM INCREASE IN MOISTURE CONTENT.

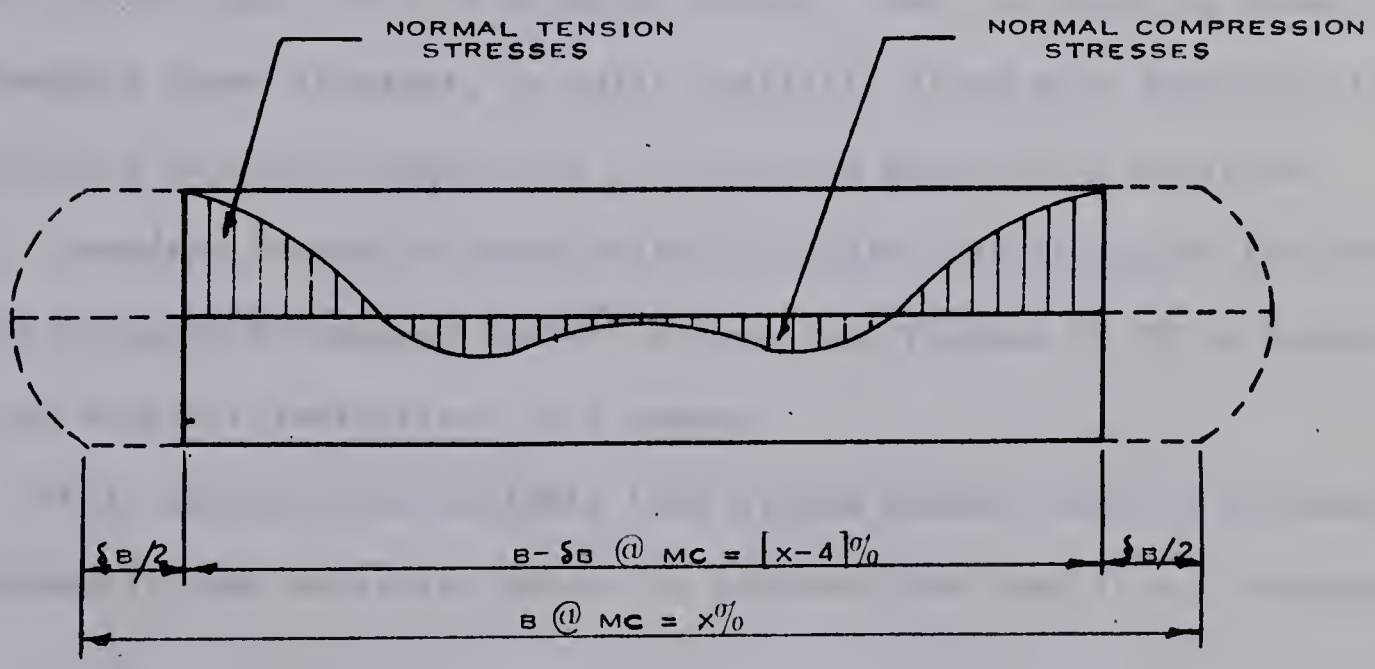

[B] CASE TWO

CROSS SECTION THROUGH BEAM WHEN BOTH LAMINATIONS CONTRACT DUE TO A PARABOLIC DECREASE IN MOISTURE CONTENT.

FIGURE 1.1

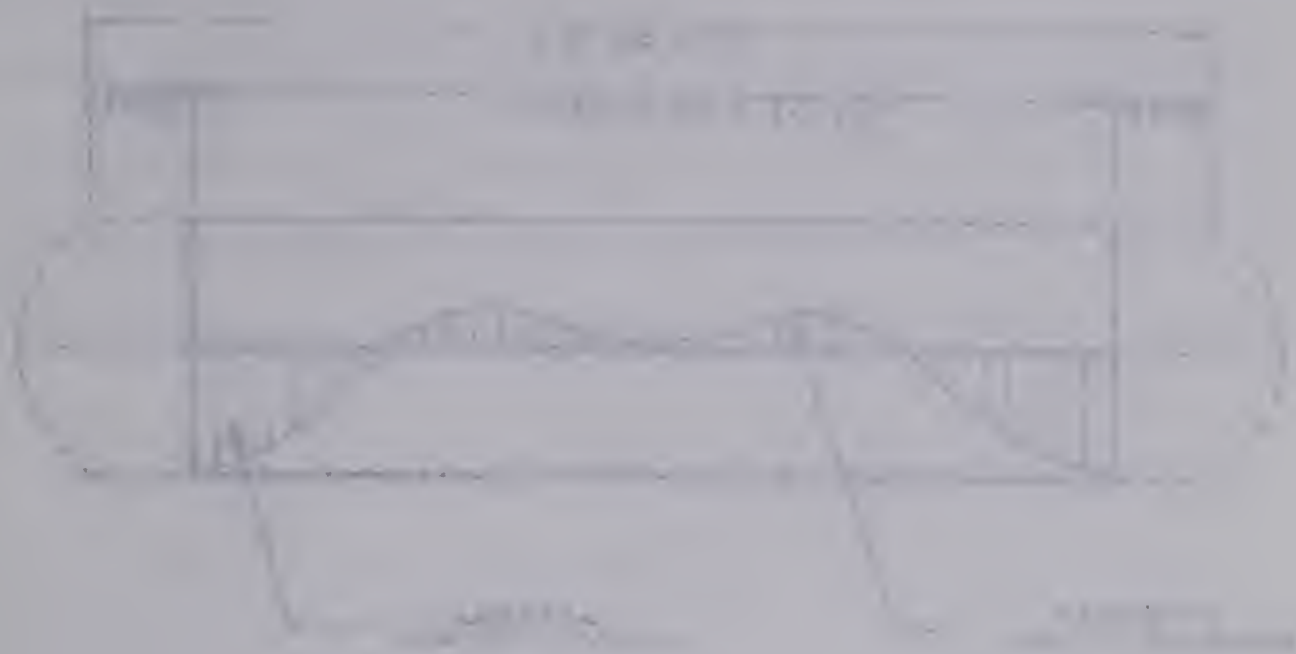

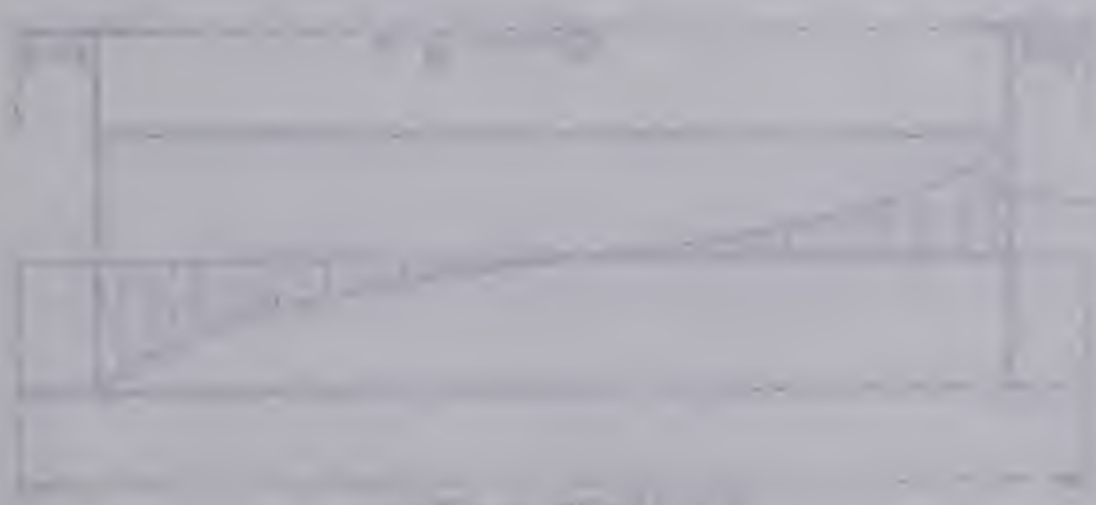

dicular to the glue line, with a distribution as shown in FIGURE 1.1B. For wood, an anisotropic material, the maximum normal stress at the edge of the lamination is:

$$\sigma_{max} = 0.45 e \alpha \sqrt{E_x (E_y G_{xy})^{1/2}}$$

where $e = \alpha (M_2 - M_1)$

M_2 = moisture content at the outer fiber

M_1 = moisture content at the glue line

E_y = modulus of elasticity perpendicular to the glue line

A 4% change in moisture content results in a maximum normal stress of 235 psi for edge grain laminations and 370 psi for flat grain laminations.

For the majority of beams composed of several laminations, the usual condition is intermediate between these two cases of moisture change and grain orientation. The 4% moisture change, used in computing normal and transverse shear stresses, is quite realistic since most specifications commonly allow adjacent laminations to differ by about 4% in moisture content. Canadian Standards Association 0122-1959 "Specification for Glue Laminated Softwood Structural Timber" allows a difference of 5% in moisture content of adjacent laminations in a member.

Field observations indicate that glulam members tend to delaminate more frequently when moisture content is reduced than when it is increased.

1-3 Forces in Delaminated Glulam Beams

In an intact glulam beam the total compressive or tensile force at any cross section can be computed by the simple flexure formula. This

$$\sigma_{\bar{x}} = \frac{\sigma}{\sqrt{n}}$$

force must be resisted by the horizontal shearing forces on the area of the neutral surface, between the support and the cross section in question. When a delamination exists at the cross section, equilibrium between flexural forces and the summation of horizontal shearing forces must satisfy equilibrium requirements. However, the computation of the flexural force is made more difficult due to the presence of the delamination through the cross section.

Huggins, Aplin and Palmer (1964) developed a theoretical method of analysis to determine the flexural compressive and tensile forces, at any interior section of a glulam beam containing a full width delamination. The following simplifying assumptions were made:

1. A plane transverse section at the end of the delamination remains plane after bending.
2. The radii of curvature of the portions of the beam below and above the delamination are equal.
3. The moduli of elasticity in compression and tension parallel to the grain are equal.
4. No friction exists between the two delamination portions of the beam.

Since the two portions of the delaminated beam have the same radius of curvature;

$$\frac{1}{\rho} = \frac{M_T}{EI_T} = \frac{M_B}{EI_B}$$

This implies that the bending moments in the top and bottom portions of the beam are proportional to the respective moments of inertia.

For a beam subjected to a single concentrated load as shown in FIGURE 1.2, bending moment is a linear function of vertical shearing force. Therefore, shear forces in the top and bottom portions of the beam will be proportional to the respective moments of inertia. From FIGURE 1.2 it follows that:

$$I_T = \frac{1}{12} b(kd)^3$$

$$I_B = \frac{1}{12} b\left[(1-k)d\right]^3$$

$$\frac{M_T}{M_B} = \frac{V_T}{V_B} = \frac{(kd)^3}{\left[(1-k)d\right]^3}$$

$$M_T = \frac{k^3}{(1-k)^3} M_B$$

$$V_T = \frac{k^3}{(1-k)^3} V_B$$

If the total shear force across a delaminated section is known, V_T and V_B can be computed.

In order to satisfy the condition of horizontal equilibrium the compressive force C must be equal to the tensile force T at a transverse section in a delaminated glulam beam. (FIGURE 1.2). All quantities in-

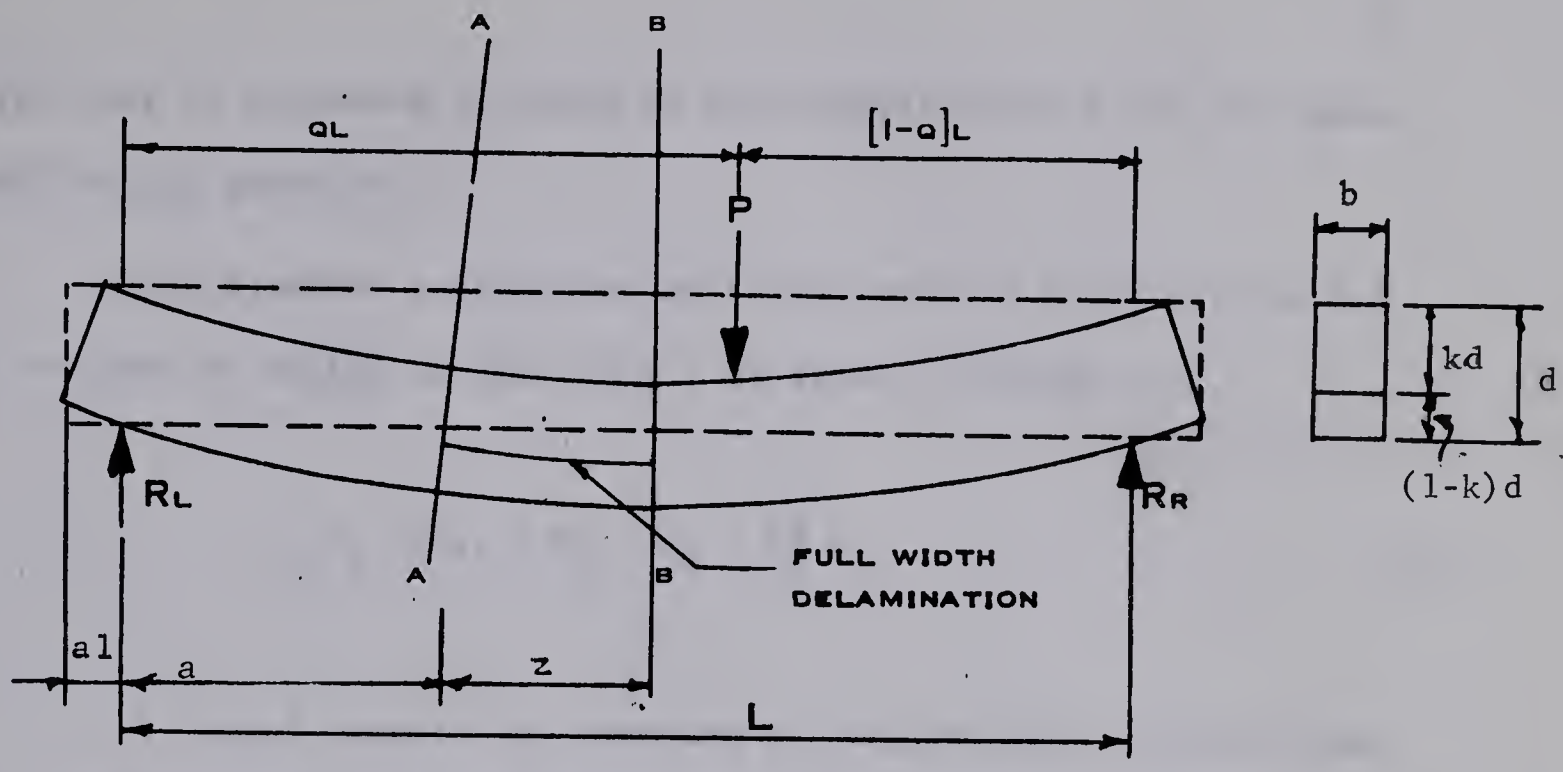

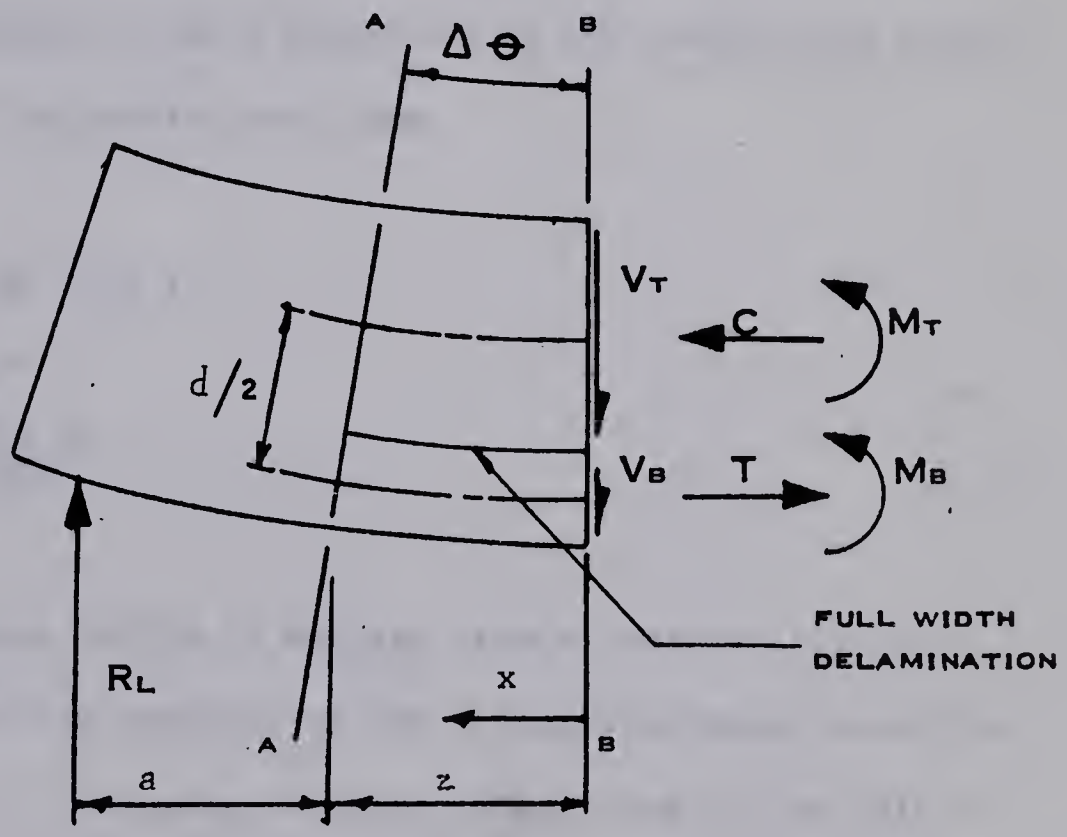

FORCES IN A DELAMINATED GLULAM BEAM

FIGURE 1.2

volved may be expressed in terms of the tensile force T and the upper beam bending moment M_T.

One equation is obtained by taking moments about section B-B on the line of action of the force T as shown in FIGURE 1.2.

$$R_L\ (a+z)\ -\ M_T\ -\ M_B\ -\ \frac{Cd}{2} = 0 \qquad (1.1)$$

A second equation is obtained by considering two expressions for the angle change $\Delta\theta$. This angle change is the change in slope of the elastic curve between section A-A and section B-B in FIGURE 1.2. If M_{TX} is the bending moment in the top portion of the beam at any point, a distance X to the left of section B-B, then:

$$M_{TX} = M_T\ -\ V_T\ X$$

$$\Delta\theta = \int_o^z \frac{M_{TX}\ d_x}{EI_T} \qquad (1.2)$$

Another expression for $\Delta\theta$ is derived from a consideration of strains in the top and bottom portions of the delaminated beam, under the action of forces C and T . Assuming the part of the beam to the left of section A-A is rigid, the change in length at mid-depth of the top portion of the beam due to the compressive force C will be:

$$\frac{CZ}{A_T E}$$

Similarly, for the bottom portion of the beam the change in length due to the tensile force T will be:

$$\frac{TZ}{A_B E}$$

The change in length of the bottom portion of the beam relative to the top portion of the beam is therefore:

$$\frac{CZ}{A_T E} + \frac{TZ}{A_B E}$$

This relative change in length divided by half the total beam depth gives another expression for the angle change $\Delta\theta$.

$$\Delta\theta = \frac{2}{d}\left[\frac{CZ}{A_T E} + \frac{TZ}{A_B E}\right] \tag{1.3}$$

Combining expressions 1.2 and 1.3 we obtain:

$$\frac{2Z}{d}\left[\frac{C}{A_T E} + \frac{T}{A_B E}\right] = \int_0^z \frac{M_{TX}\, d_x}{EI_T} \tag{1.4}$$

From the simultaneous solution of Equations 1.1 and 1.4 the tensile force T and bending moment M_T can be evaluated. Subsequently, after the determination of bending moment M_B and compressive force C , the distribution of stress or strain can be found at any delaminated cross section. With the compressive force C known an average horizontal shear stress along the undelaminated length of the plane, in which the

$$\frac{\partial}{\partial t}\left[\frac{\partial^2}{\partial x^2}+\frac{\partial^2}{\partial y^2}\right]\frac{\partial \psi}{\partial x}$$

$$\frac{\partial}{\partial t}\left[\frac{\partial^2}{\partial x^2}+\frac{\partial^2}{\partial y^2}\right]$$

$$\frac{\partial \psi}{\partial x}$$

$$\frac{\partial \psi}{\partial x}$$

delamination occurs, can be computed.

1-4 Shear Stress Concentration in Delaminated Glulam Beams

There are two methods of analysis which may be applied to postulate a stress concentration factor for the shear stress near the end of a delamination.

The first method is based on work by Guyon (1960) related to anchorage zone stresses in post-tensioned prestressed concrete beams. Considering local stresses near the end surface of a homogeneous, isotropic, prismatic member produced by a concentrated load acting on this end surface, Guyon determined influence coefficients for calculating shear stresses along the member. A loading condition very similar to the condition analysed by Guyon exists in a vertical plane at the end of a delamination in a glue laminated beam. The flexural stress distribution in the two portions of a delaminated beam, proposed by Huggins, Aplin and Palmer, satisfies this condition of concentrated loading when the stress distribution is sub-divided into a series of concentrated loads, extending across the beam depth. (FIGURE 1.3).

However, Guyon's solution for anchorage zone shear stresses is only approximate as indicated by Iyengar (1962). Iyengar investigated the problem of anchorage zone stresses by employing a two dimensional model. The resulting solution, an Airy stress function, has been evaluated by Lee (1964). The resulting influence lines for shear stresses at various positions along the neutral axis of a beam are shown in FIGURE 1.4. This second method of computing shear stress concentrations has the one disadvantage, in that it can be applied only to the case

FORCES AND STRESSES AT THE TERMINATION OF A DELAMINATION

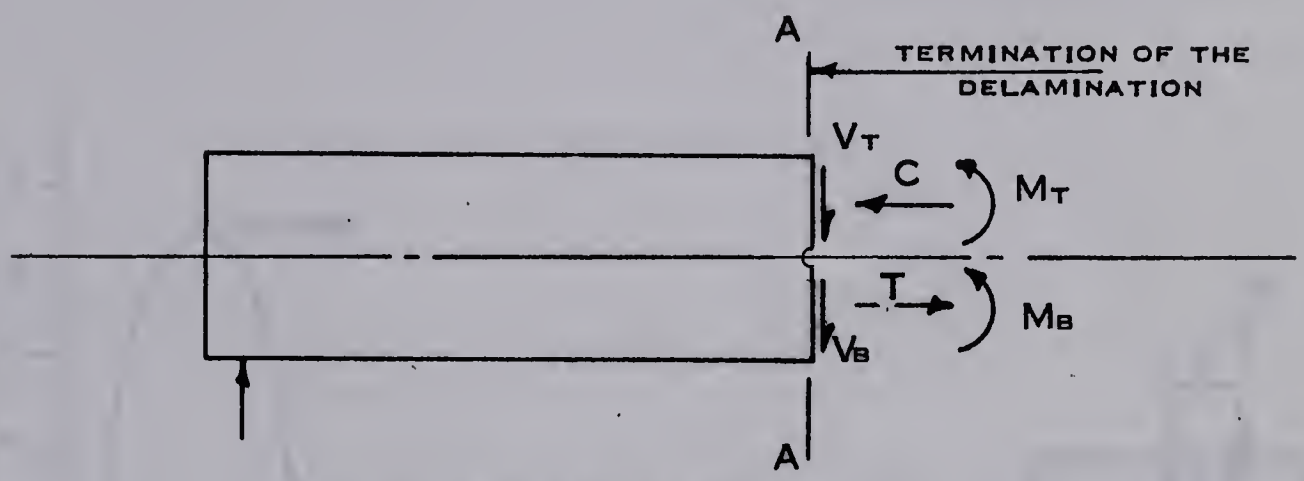

MOMENTS AND FORCES

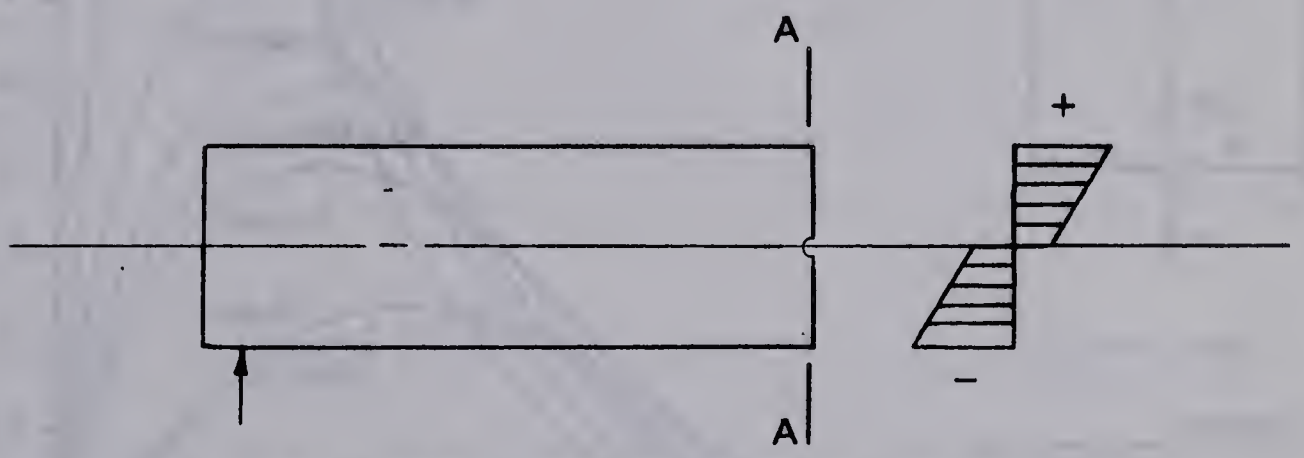

FLEXURAL STRESS DISTRIBUTION

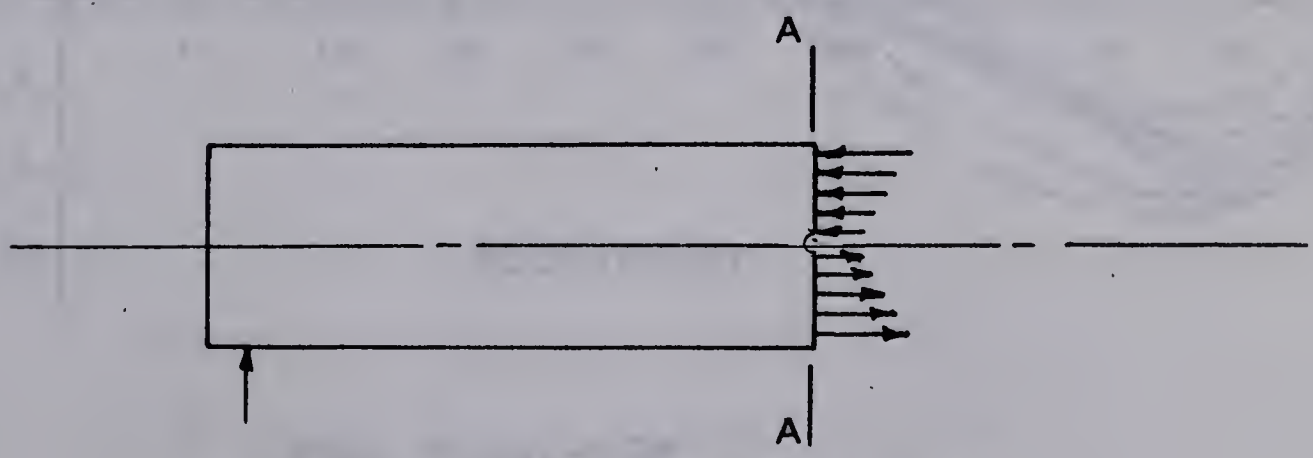

EQUIVALENT CONCENTRATED LOADS

FIGURE 1.3

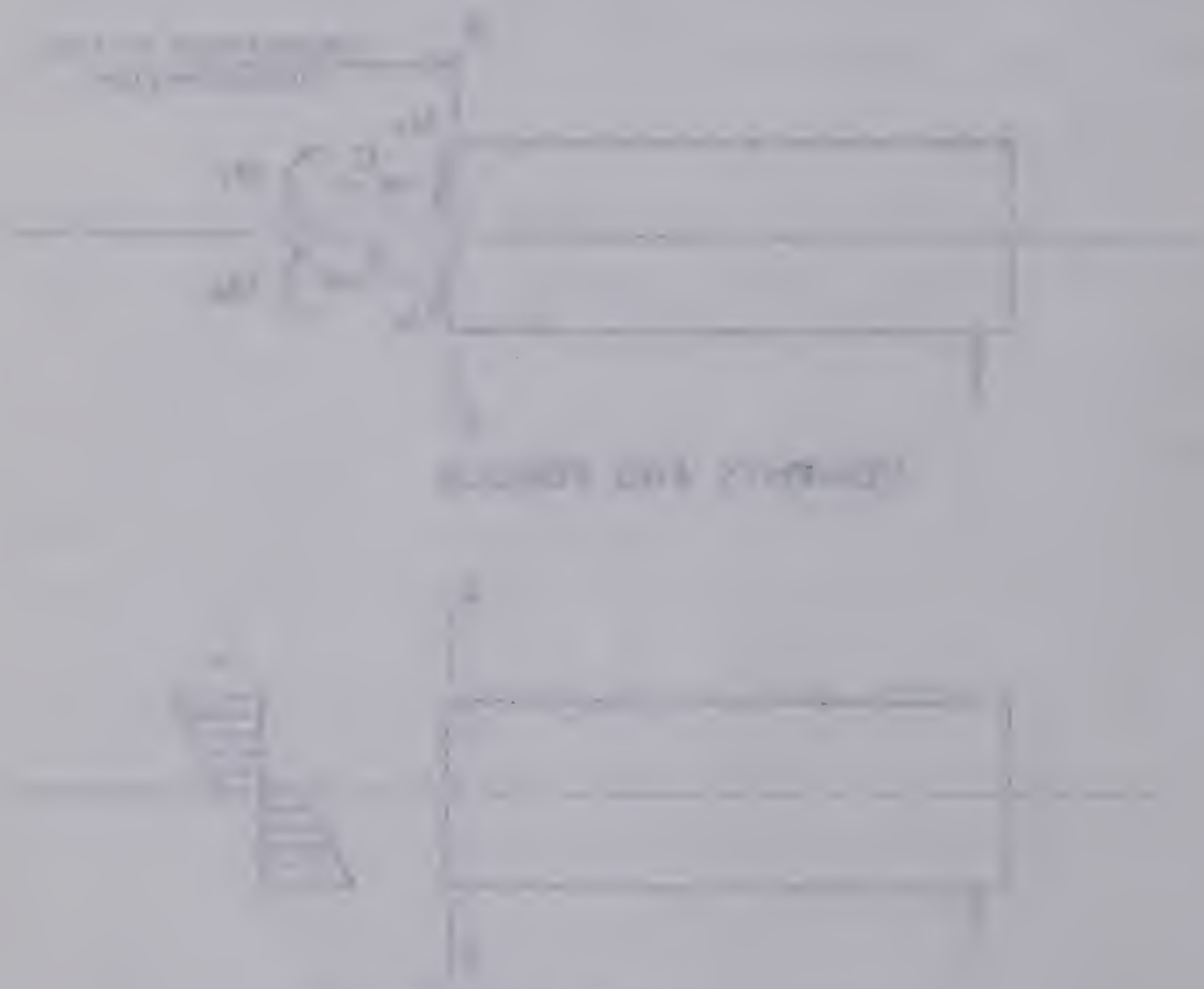

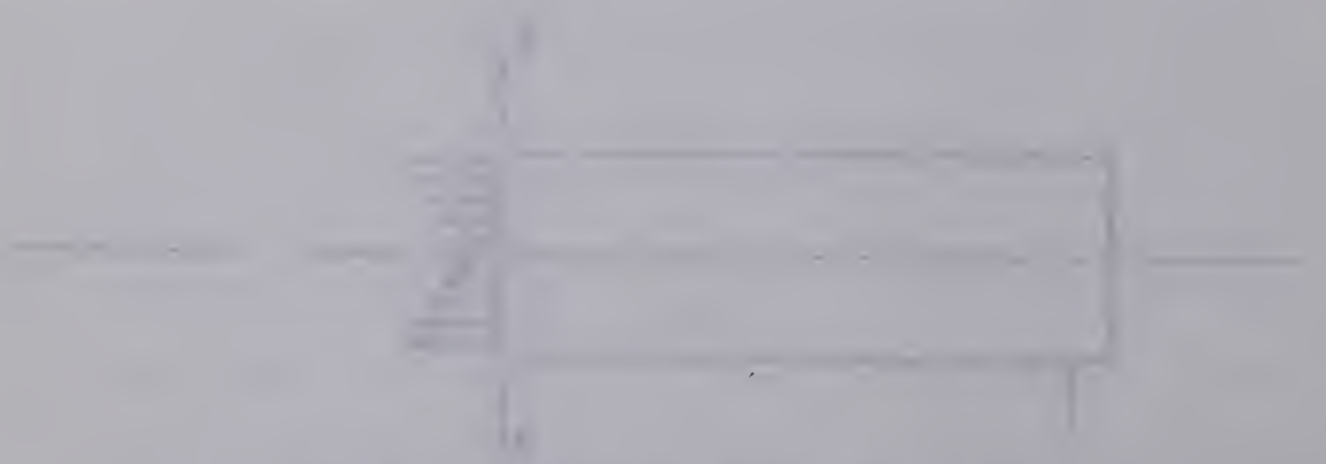

INFLUENCE LINES FOR SHEAR STRESSES

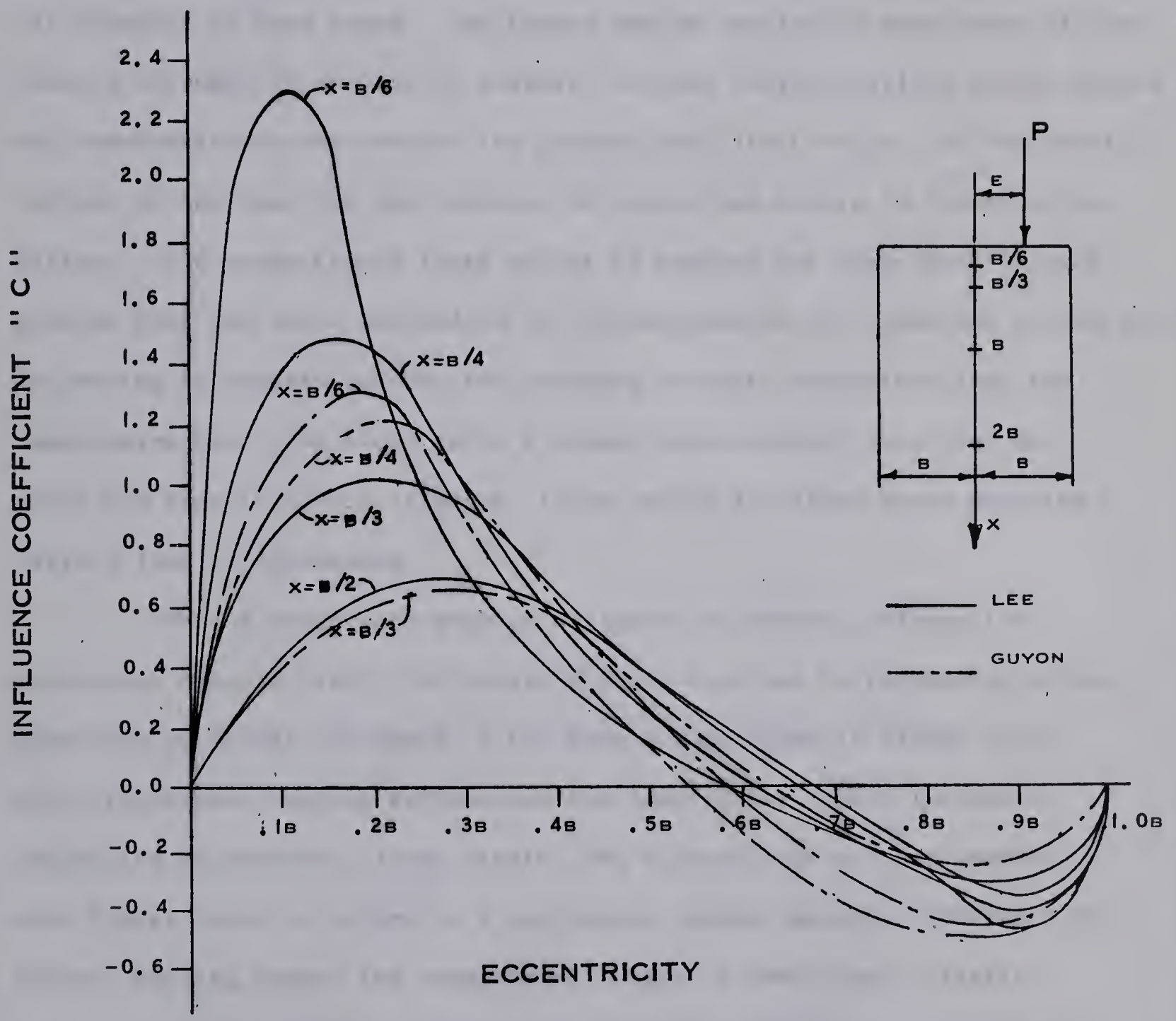

$$\text{Shear Stress} = \frac{CP}{2B}$$

FIGURE 1.4

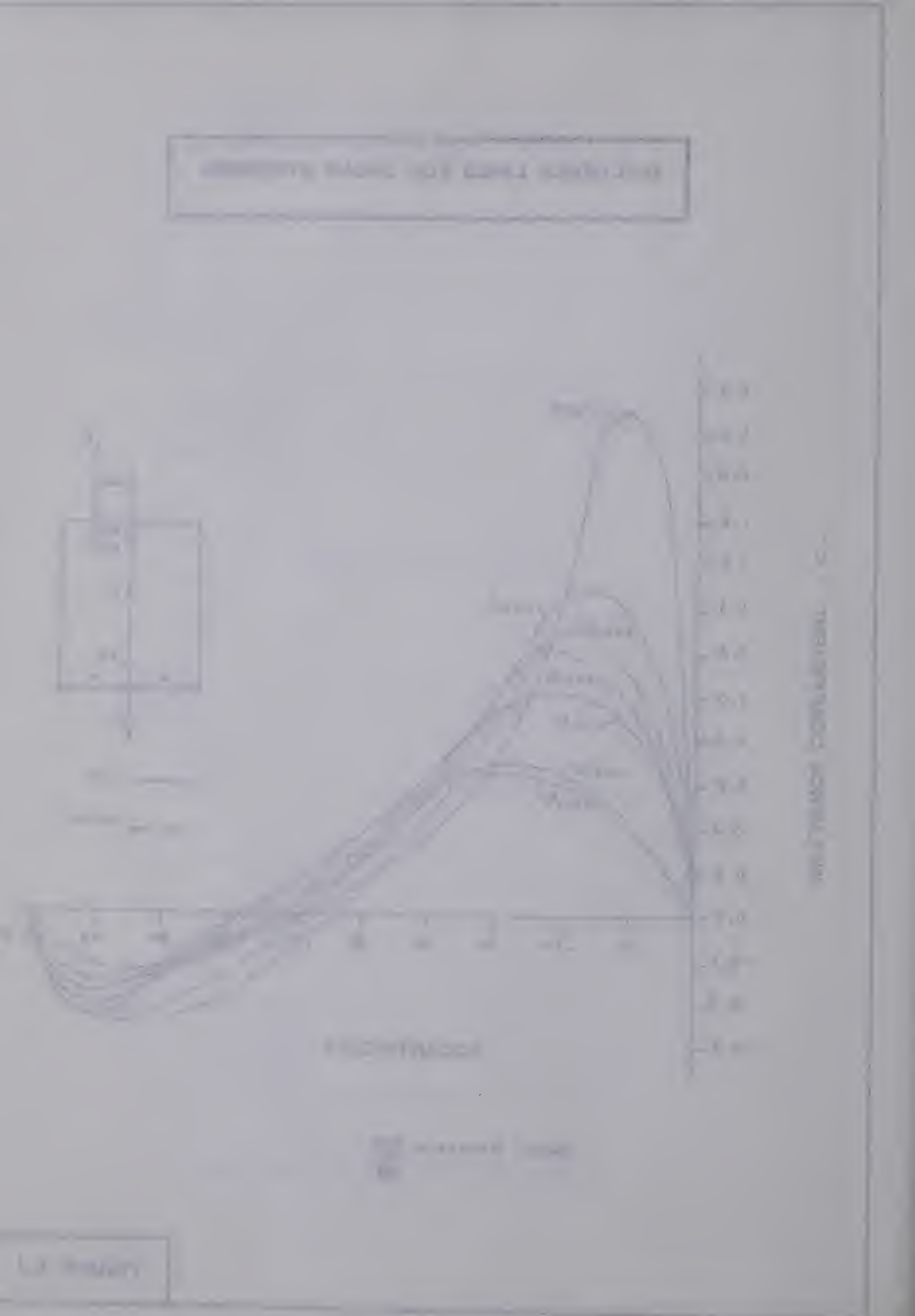

where the delamination occurs at the neutral axis of the beam. Guyon's method, on the other hand, may be applied regardless of the position of the delamination.

1-5 Distribution of Stress and Strain in Douglas Fir Glulam Beams

The elastic beam theory predicts with certain limits the flexural behavior of wood beams. The theory may be applied to wood beams if the tensile strength is reduced by defects, so that tensile failure occurs before the compression stress reaches the proportional limit value. At the critical section of the beam the distribution of stress and strain is linear up to failure. The proportional limit stress in bending for clear wood is much greater than the value determined by the compression test parallel to the grain. In bending it usually exceeds the crushing strength determined from the compression test. As shown below a linear stress-strain relation, on which the elastic theory is based, is not valid for these beams when the failure load is approached.

When a clear wood beam is subjected to bending deformation, within the elastic limit, the strain distribution and corresponding stress distribution across the depth of the beam are as shown in FIGURE 1.5A. With progressive bending deformation the compressive strain increases beyond the proportional limit strain. As a result the extreme compression fibers begin to deform in a non-linear elastic manner. (FIGURE 1.5B). Further bending causes the compression fibers to reach their elastic limit and deform plastically while the tension fibers continue to deform elastically. Consequently a stress redistribution occurs and the neutral axis shifts down toward the tension face as in FIGURE 1.5C. This stress redistribution continues with increasing applied moment until a tension

GLULAM STRESS - STRAIN DISTRIBUTIONS FOR PROGRESSIVE BENDING DEFORMATIONS

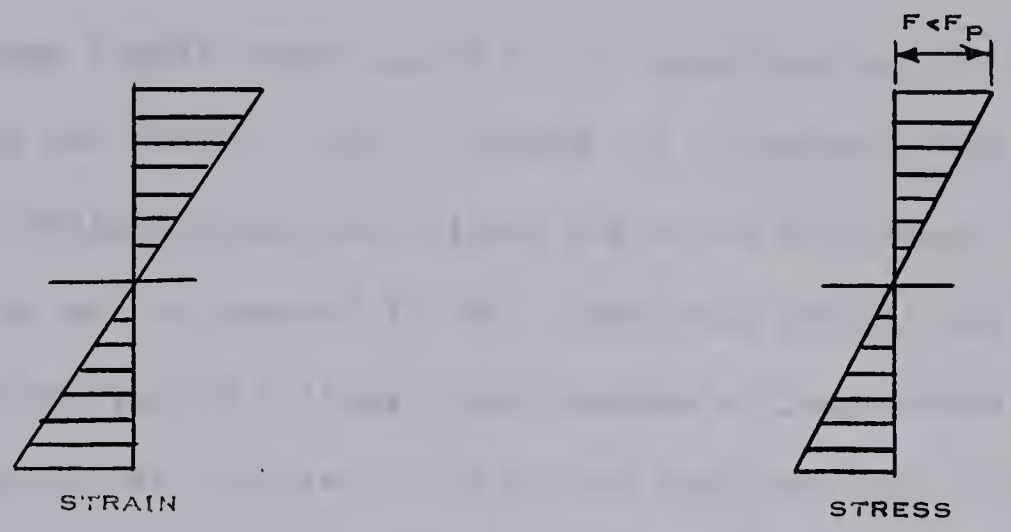

[A] BENDING WITHIN THE PROPORTIONAL LIMIT

[B] BENDING AT THE PROPORTIONAL LIMIT

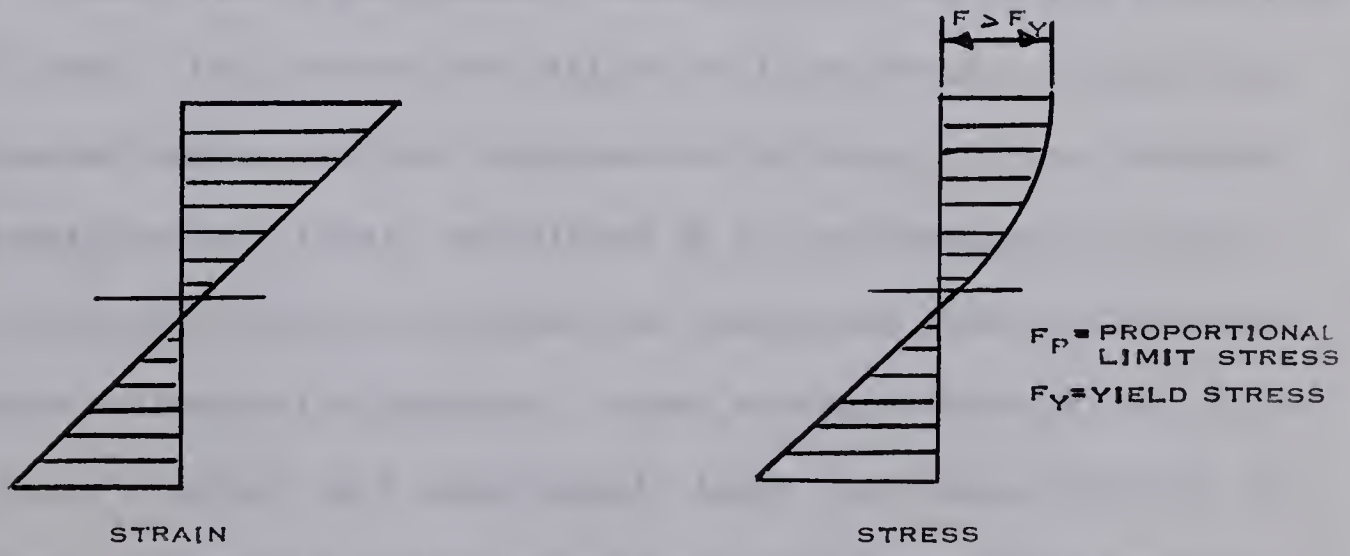

[A] BENDING IN THE PLASTIC REGION

FIGURE 1.5

failure occurs.

Ramos (1961) investigated strain distribution in Douglas Fir beams within the plastic range. FIGURE 1.6 illustrates the strain distributions obtained preceding failure for three test beams 2" x 6" in cross section with a span of 12'-0". From this work it was concluded that the assumption of a linear distribution of longitudinal strain is valid for practical purposes. The strain distributions in FIGURE 1.6 clearly illustrate the gradual shift of the neutral axis towards the tension face of the beam.

1-6 Previous Experimental Investigations

One of the major problems in the area of timber engineering lies in the evaluation of the strength characteristics of beams. This is very evident when studies on the horizontal shear strength of glulam beams are examined for conclusive results. Furthermore, there are a limited number of published investigations concerning horizontal shear stresses in delaminated glulam beams.

Huggins, Aplin and Palmer (1964) tested 175 beams, 3 1/4" x 6" x 9'-0", under static and dynamic concentrated loads at the centerline of a 8'-0" span. One hundred and fifteen of these beams contained full width delaminations at various locations in the beam. It was observed that an average shear stress, calculated on the undelaminated surface, did not explain the relative incidence of horizontal shear failures for the different delamination patterns. Shear stress concentrations calculated by Guyon's method were considerably lower than those obtained by Lee's method. Using this latter method very good correlation was ob-

LONGITUDINAL STRAIN DISTRIBUTIONS
[AFTER RAMOS]

BEAM 1

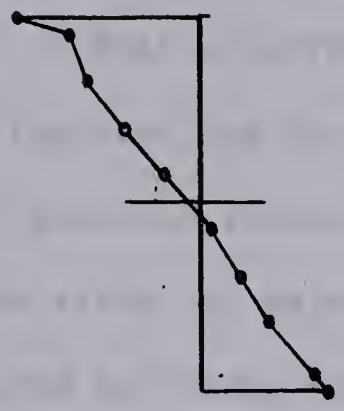

PLANE 1

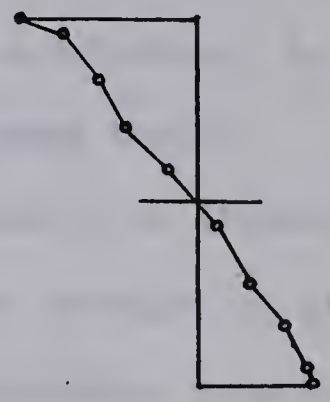

PLANE 2

BEAM 2

PLANE 1

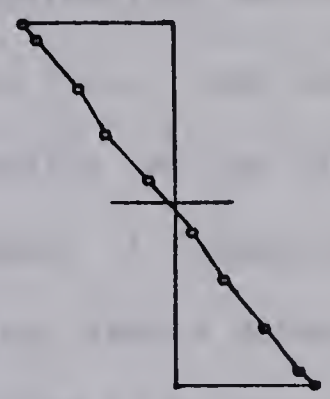

PLANE 2

BEAM 3

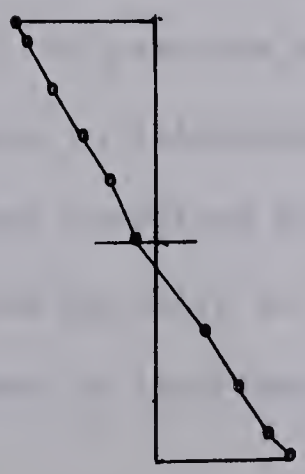

PLANE 1

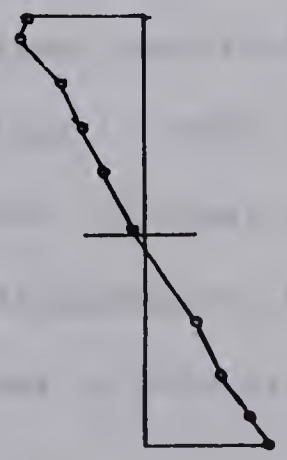

PLANE 2

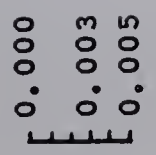

STRAIN SCALE
[IN. / IN.]

NOTE

PLANES 1 AND 2 REFER TO TRANSVERSE SECTIONS IN THE CONSTANT MOMENT REGION OF THE BEAMS

FIGURE 1.6

tained between the shear strength of glulam beams, indicated by shear block tests, and the occurrence of horizontal shear failures. The reducation of strength under repeated loading was confirmed. However, the extent of this occurrence was impossible to determine, due to the manner of the test and the limited number of beams tested.

A previous investigation at the University of Alberta, concerning the effect of delamination on the shear strength of glulam beams, was conducted by Strong (1964). In this comprehensive program, 239 Douglas Fir beams and 110 shear block specimens were tested. Length of delamination and position of delamination were the major variables in the 3" x 6" x 6'-2" long beams. Artificial delaminations were introduced by inserting two layers of wax paper at the glue line. Test results indicated that an increase in length of delamination had the effect of decreasing the load carrying capacity of the beams. A delamination located at mid-depth was shown to be more critical than a delamination at 1/4 depth or 3/4 depth. End delamination proved to be more critical than centerline delamination. As in previous investigations no correlation was found to exist between shear block and beam tests.

In the previous experimental investigations described horizontal shear stresses in delaminated glulam beams have been in terms of the average stress sustained prior to failure. However, if shear stress concentrations do exist at the termination of a delamination, they must have an effect on longitudinal strain distributions in this vicinity.

1-7 Scope of Present Investigation

The investigation described in this thesis was conducted primarily for the purpose of studying the effect of delamination on the longitudinal strain distribution in glue laminated Douglas Fir beams. Secondly, the feasibility of calculating the actual horizontal shear stress distribution from the strain distribution was examined.

Thirteen rectangular simply supported beams were tested to failure under the application of a single concentrated load at midspan. Ten of the beams contained artificial delaminations in which the type of delamination and length of delamination were major variables. In these beams the location of the delamination was at mid-depth of the section and symmetrical with respect to the centerline of the span.

CHAPTER II

HORIZONTAL SHEAR STRESS DISTRIBUTION

2-1 Introduction

In the development of the expression for flexural stresses in beams of homogeneous material it is assumed that transverse sections which are plane before bending remain plane during bending. For a material which obeys Hooke's Law this results in the familiar equation:

$$f = \frac{My}{I}$$

Since horizontal shearing stresses are related to the distribution of flexural stresses, it follows that the same assumption of plane sections remaining plane is made in deriving expressions for shear in beams of homogeneous material. In other words the equation for shearing stress in a rectangular beam

$$v = \frac{VQ}{Ib}$$

is based on the assumption that sections do not warp due to bending. However, if warping of the section occurs, the horizontal shear stresses cannot be expressed as $\frac{VQ}{Ib}$.

2-2 Warped Transverse Sections

Consider a simple span rectangular beam with a single concentrated load at midspan, as shown in FIGURE 2.1. If we assume that due to bending transverse sections of the beam are warped, we may express the longitudinal strains by the equation:

$$e = a y^{\frac{1}{n}}$$

where y = the distance from the neutral axis to a longitudinal fiber

e = the longitudinal strain at this fiber

a = a constant

n = an index which determines the degree of the equation defining the strain distribution

Assuming stress is proportional to strain, the change in flexural stress on any fiber between section 1 and 2 (FIGURE 2.1C) is:

$$\Delta f = E(a_1 - a_2) y^{\frac{1}{n}}$$

$$= E a_{12} y^{\frac{1}{n}}$$

Considering the horizontal equilibrium of the element ABCD, we can derive the expression for horizontal shear stresses v_{yo}.

$$v_{yo}\, b\Delta X = \int_{y_o}^{c} \Delta f b\, dy$$

STRESSES AND STRAINS AT WARPED SECTIONS

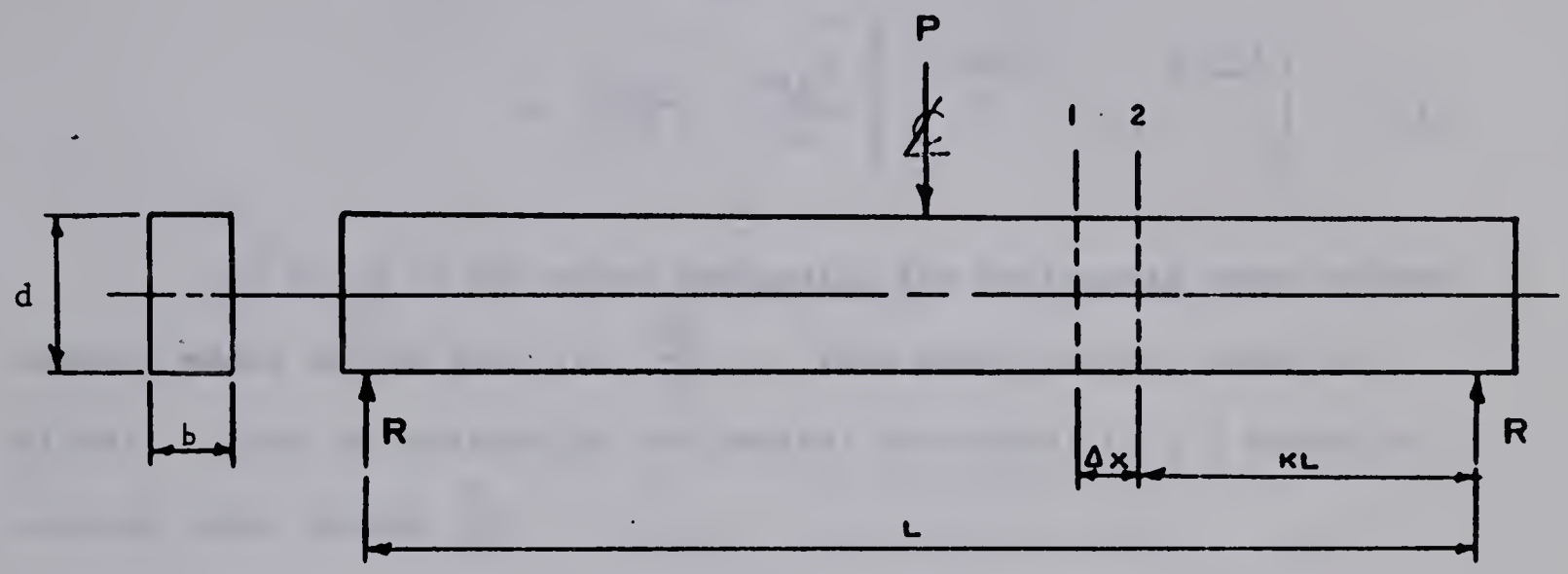

[A] RECTANGULAR BEAM

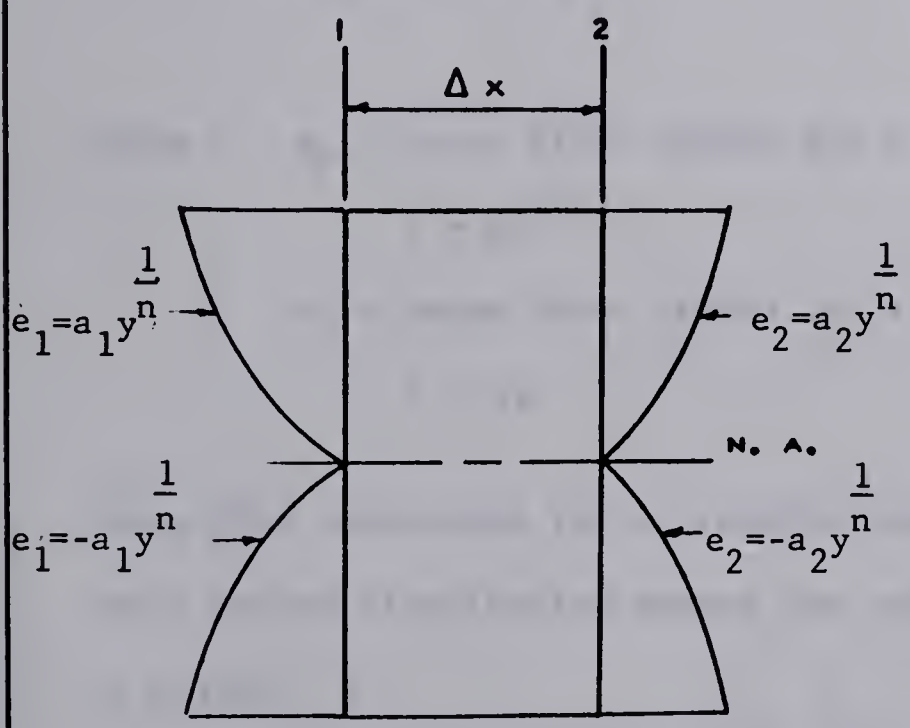

[B] NON - LINEAR STRAIN DISTRIBUTIONS

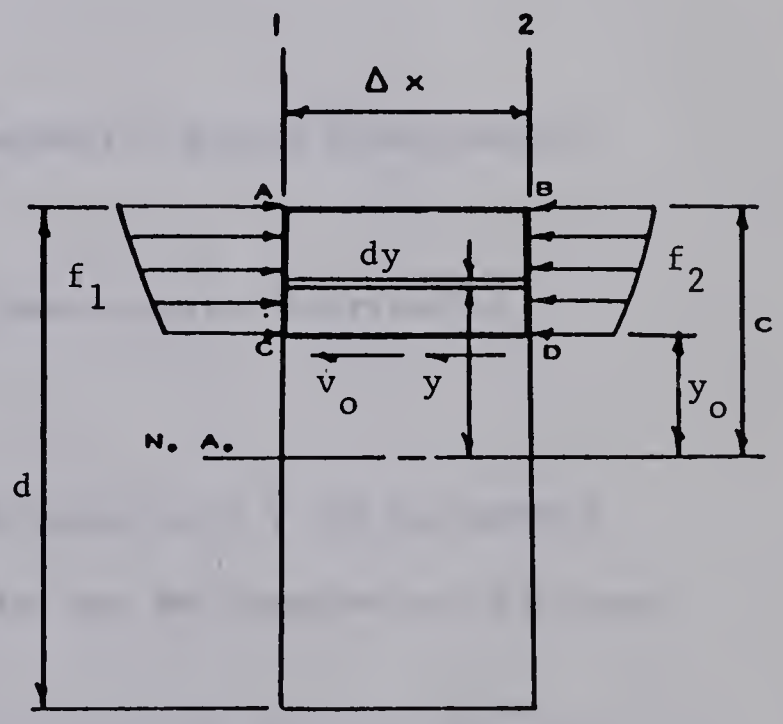

[C] ELEMENT STRESSES

FIGURE 2.1

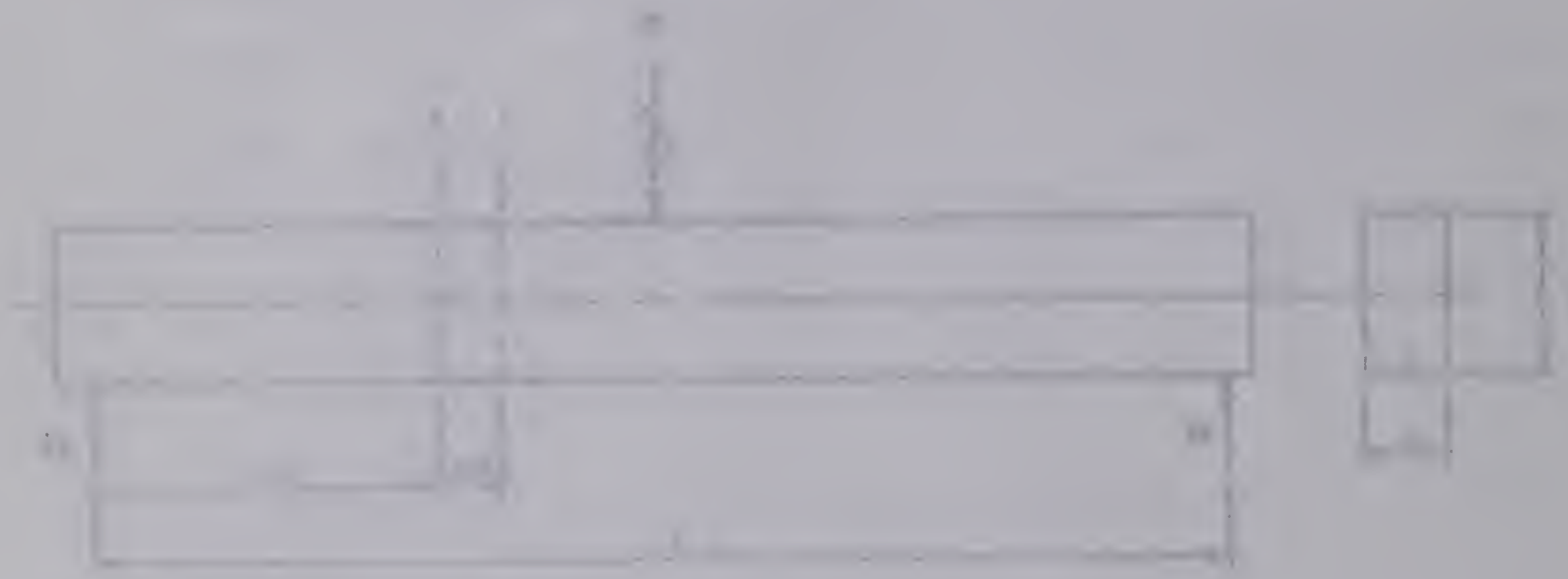

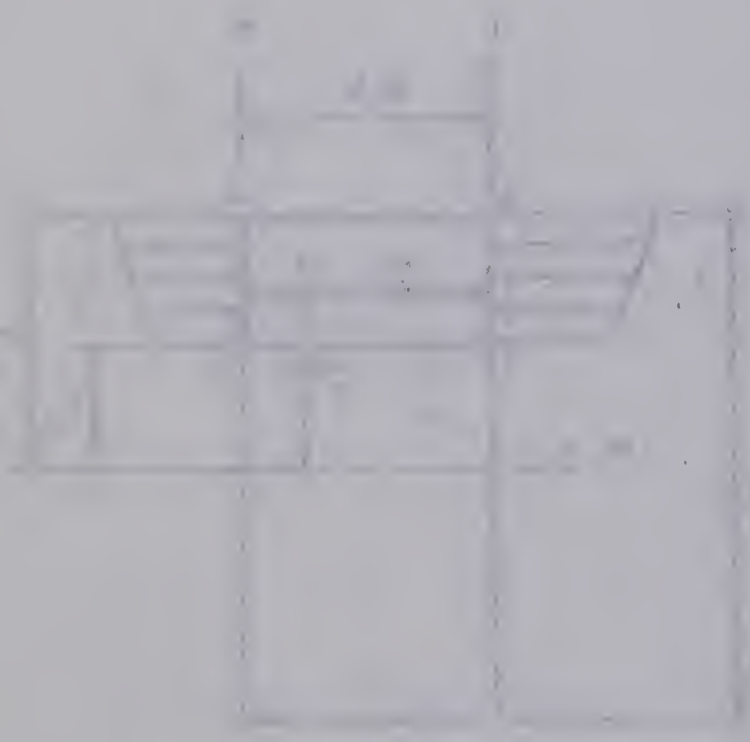

$$v_{y_o} = \frac{a_{12}E}{\Delta X} \int_{yo}^{c} y^{\frac{1}{n}}\, dy$$

$$= \frac{n}{n+1} \frac{a_{12}E}{\Delta X} \left[c^{\frac{n+1}{n}} - y_o^{\frac{n+1}{n}} \right] \qquad (2.1)$$

If $n = 1$ in the above expression the horizontal shear stress becomes equal to the familiar $\frac{VQ}{Ib}$. This distribution, shown in FIGURE 2.2 has an ordinate at the neutral axis equal to 1.5 times the average shear stress $\frac{V}{bd}$.

To illustrate the effect of warping let us now take $n = 2$. To satisfy the equilibrium of internal and external moments:

$$e_p = \frac{5}{6} e_L$$

where e_p = outer fiber strain for a parabolic strain distribution

$e = ay^{1/2}$

e_L = outer fiber strain for a linear strain distribution

$e = ay$

Using this expression for e_p together with equation 2.1 the horizontal shear stress distribution across the section can be computed and is shown in FIGURE 2.2.

FIGURE 2.2 indicates that warping of cross sections increases the magnitude of the maximum horizontal shear stress. Therefore, if longitudinal strains can be measured and the strain distribution

HORIZONTAL SHEAR STRESS DISTRIBUTIONS

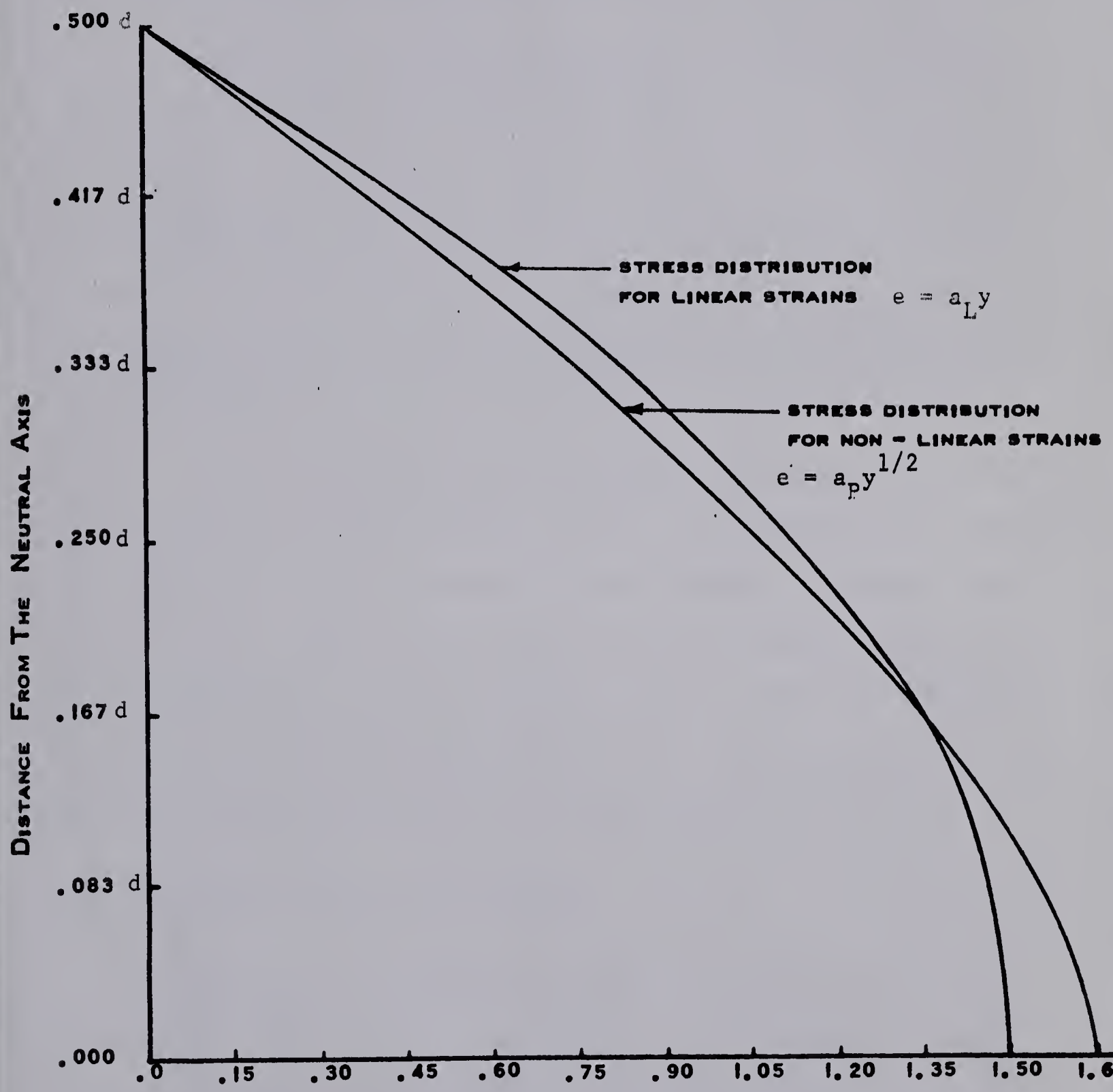

FIGURE 2.2

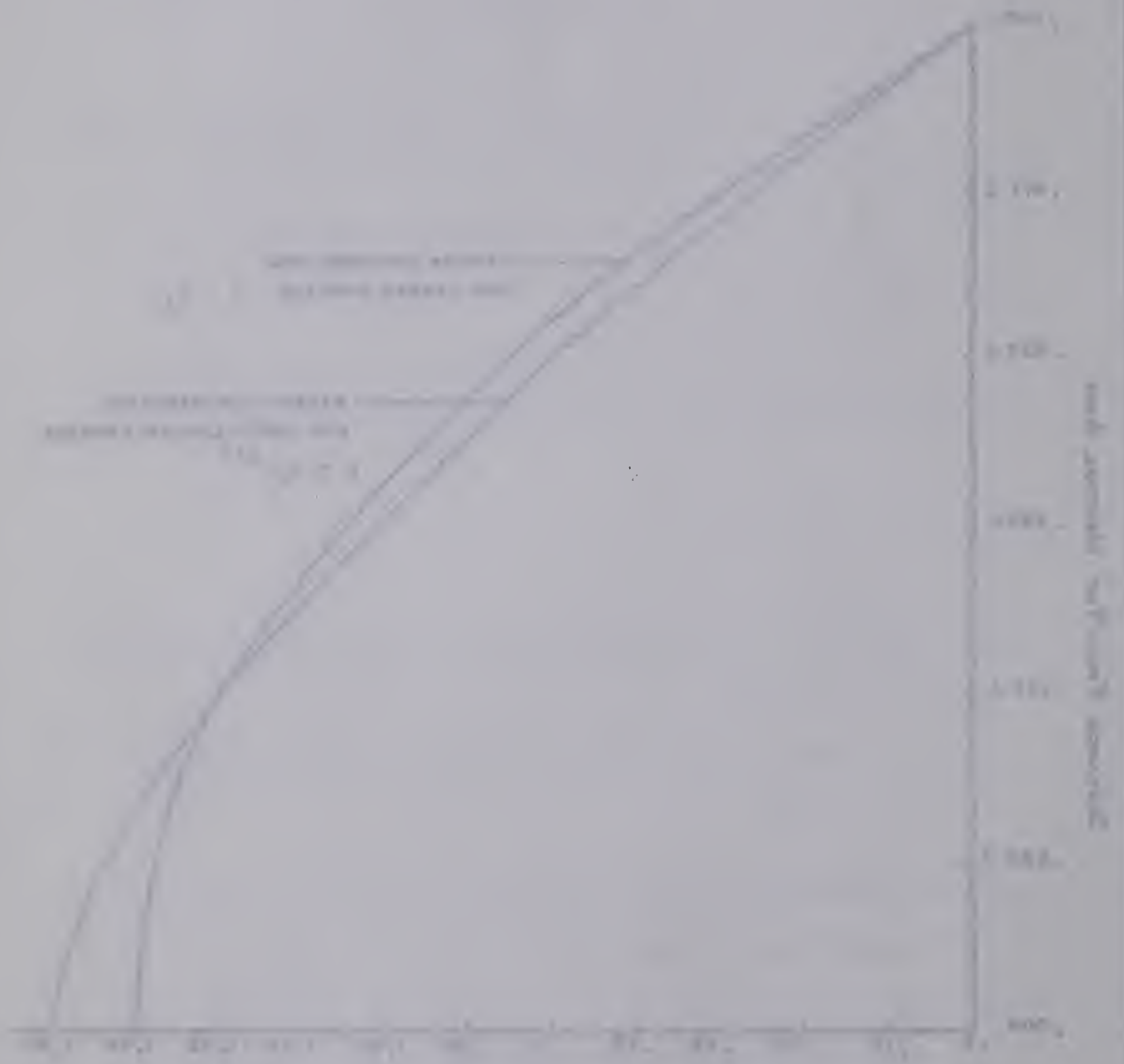

established, it should be possible to compute the actual shear stress distributions.

CHAPTER III

MATERIAL PROPERTIES

3-1 Moisture Content and Specific Gravity

Prior to the fabrication of the beam specimens and tension and compression test specimens all laminating stock was checked for excessive variations in moisture content by means of an electrical resistance moisture indicator. The "Moore Moisture Meter Model MN-1" used for this purpose is shown in PLATE 3.1A. The moisture content of the laminating stock used in this program was controlled between 10% and 12% with an average of 11.5%.

After fabrication the beam specimens were wrapped in polyethylene to maintain the beam moisture content. On completion of a beam test one moisture content and specific gravity sample , measuring about 3/4" x 3" x 3" , was cut from each lamination through the depth of the beam. The samples were taken from the region of the beam in which failure was initiated. The moisture content and specific gravity of each sample were determined by methods outlined in APPENDIX A.

3-2 Modulus of Elasticity in Tension

A total of five tension test specimens, selected from flat grained fabricating stock, were tested to determine the modulus of elasticity parallel to the grain in tension. FIGURE 3.1 indicates

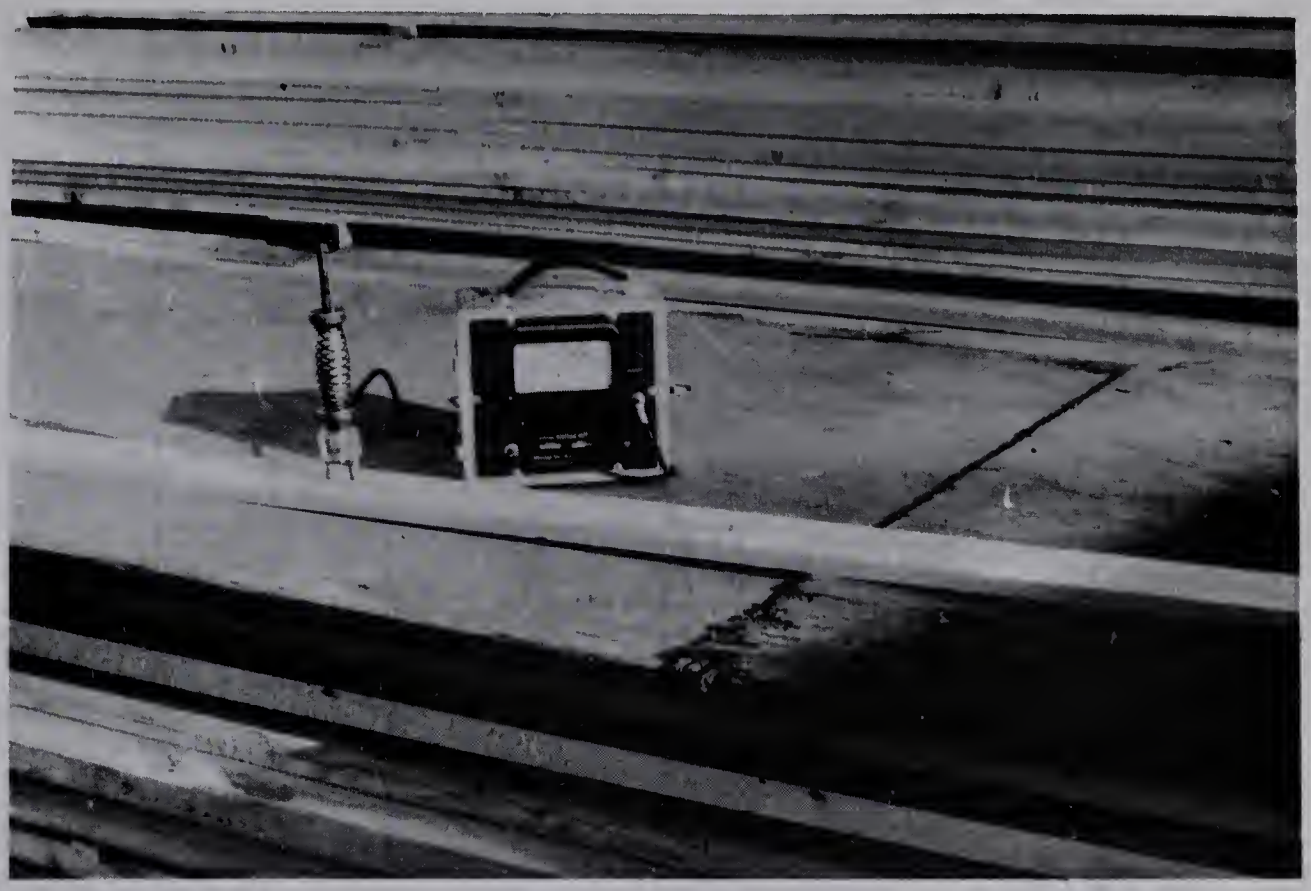

[A] MOORE MOISTURE METER

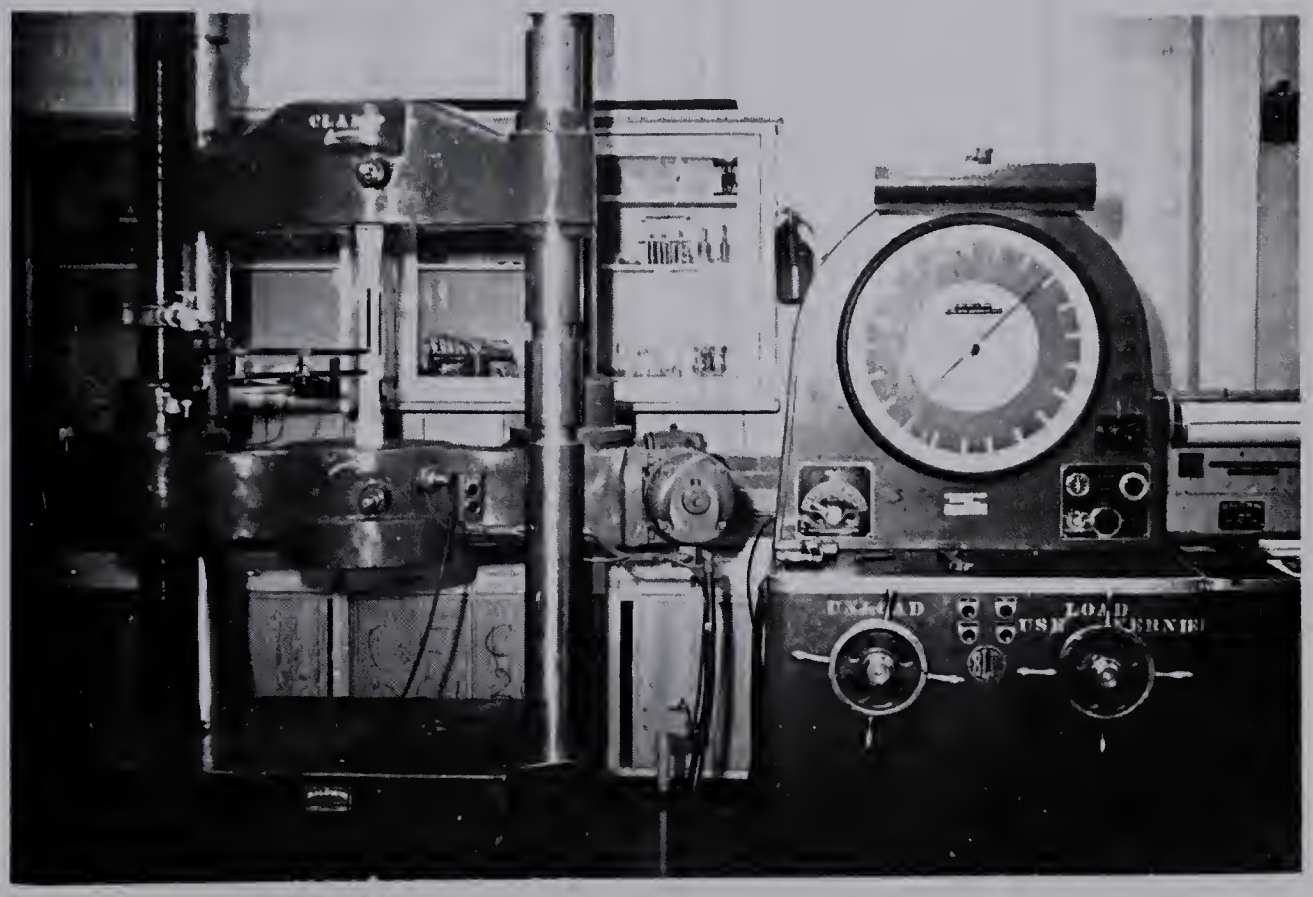

[B] TENSION SPECIMEN TEST

PLATE 3.1

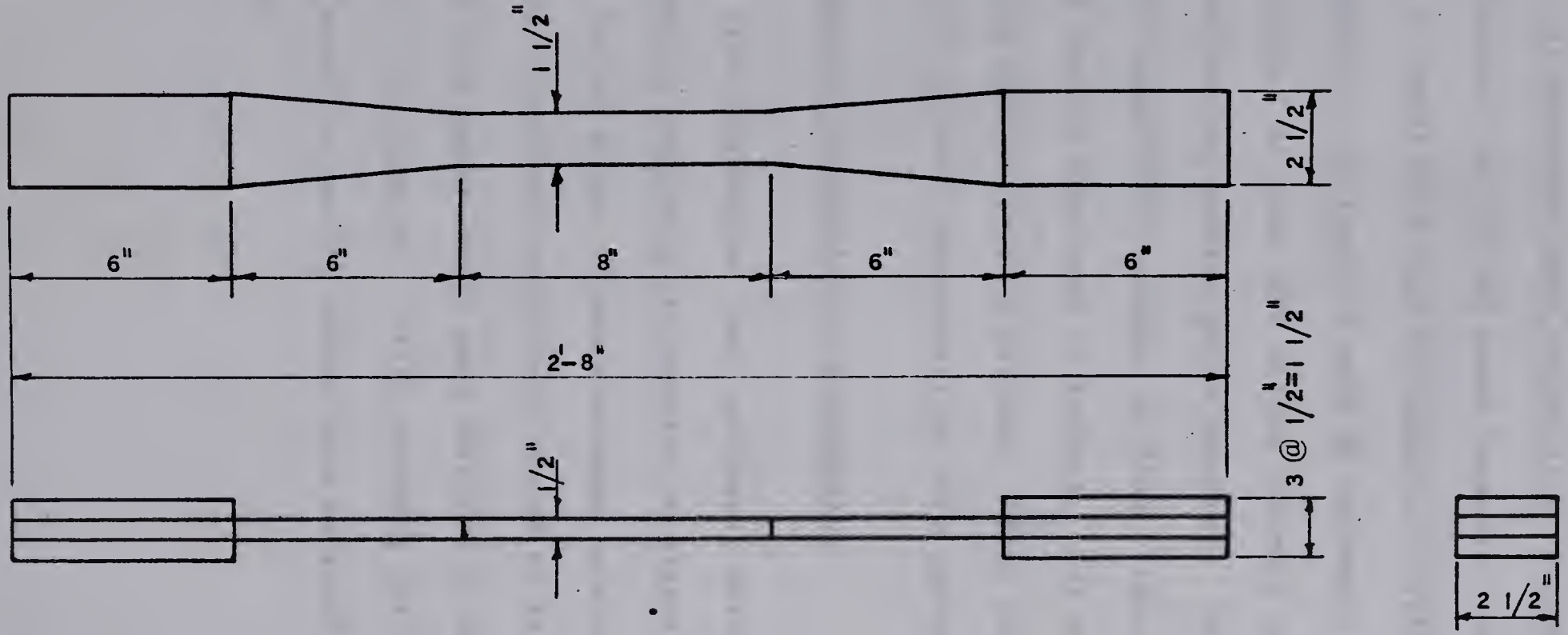

TENSION TEST SPECIMEN DIMENSIONS

FIGURE 3.1

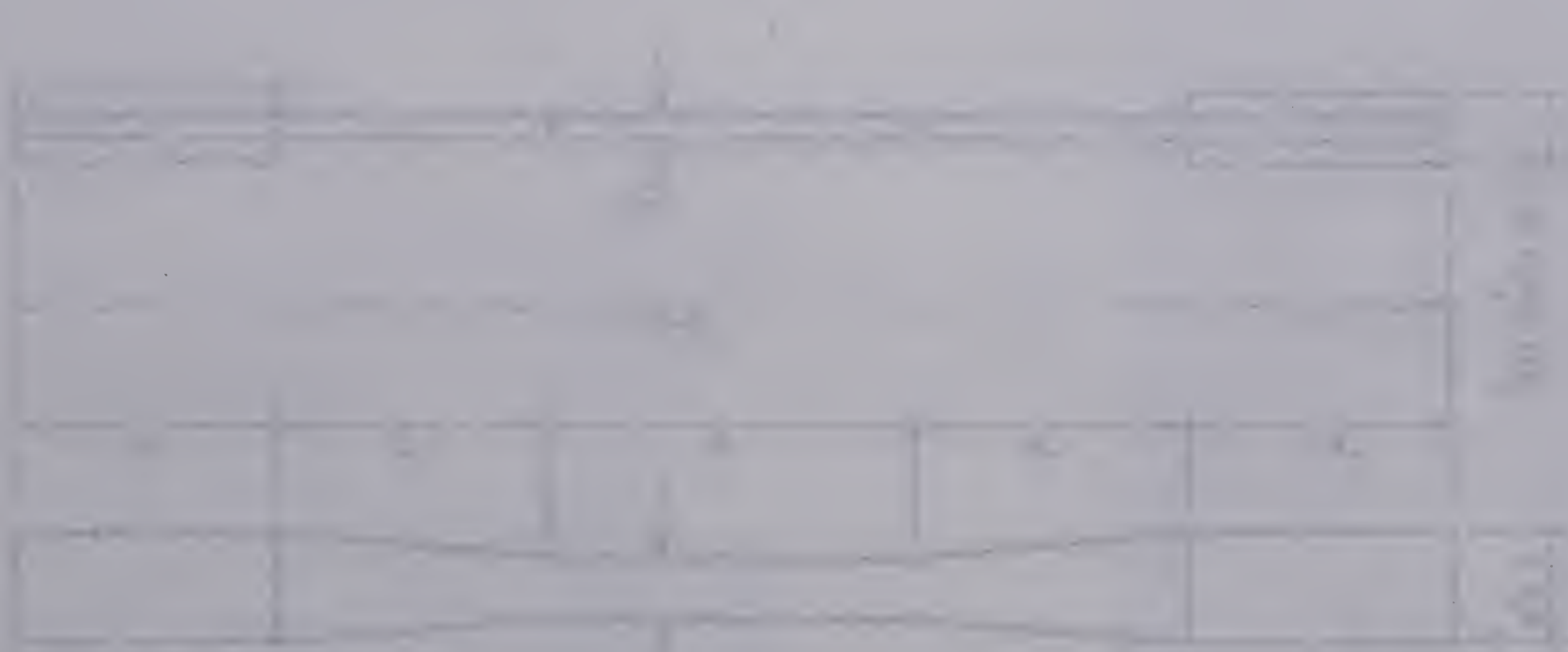

the nominal dimensions for these tension test specimens.

All specimens were tested in a "Baldwin-Tate-Emery Universal Testing Machine" of 200,000 pound capacity. Strains were measured by means of a "Model TS-M Dual Extensometer" (PLATE 3.1B), with an 8-inch gauge length, in conjunction with an automatic electrical load-deformation recorder. At about 80% of the ultimate load slippage of the specimen in the testing machine grips occurred. As valid load deformation plots were impossible to obtain at this stage, the extensometer was removed and loading continued to failure. All specimens exhibited a splintering tension type of failure. After failure, moisture content and specific gravity determinations were performed.

3-3 Modulus of Elasticity in Compression

Five compression test specimens, measuring 2" x 2" x 1'-2", were tested to determine the modulus of elasticity in compression parallel to the grain. These specimens were cut from the end regions of XY-4 beam specimens previously tested to failure. Longitudinal strains over an 8-inch gauge length were obtained by means of an "H.F. Moore Mechanical Extensometer". After crushing failure occured, moisture content and specific gravity values were obtained for all compression test specimens.

CHAPTER IV

BEAM SPECIMENS AND FABRICATION

4-1 Beam Specimen Types

Thirteen beams, 3" x 6" in cross section and 6'-2" long, were tested in this program. These beams were sub-divided into three groups as described in TABLE 4-1. The first group, consisting of three control beams, contained no delaminations. The ten delaminated beams were divided into two groups each comprising five different types. In one group of delaminated beams, the wood surfaces at the delaminated section were in contact; whereas in the other group the surfaces were not in contact. Details are shown in FIGURE 4.1.

4-2 Beam Fabrication Procedures

Prior to beam fabrication the laminating stock was examined and sorted with respect to moisture content, approximate specific gravity, grain orientation and occurrence or knots and checks. The resulting beams consisted of eight 3/4" clear, check free laminations of Grade B Douglas Fir laminating stock. These laminations were generally flat grained. The moisture content was controlled to a tolerance of $\pm$ 1% and the specific gravity varied from a maximum at beam mid-depth to a minimum at the outer fibers.

In order to facilitate convenient manufacture of the delaminated

TABLE IV-1

BEAM TEST SPECIMENS

Beam Mark	Number of Specimens	Delamination Length (ft.)	D/L Ratio*	Type of Delamination
X-001	1	Control Beam	N.A.	N.A.
X-002	1	Control Beam	N.A.	N.A.
X-003	1	Control Beam	N.A.	N.A.
XZ-41	1	1'-0	0.162	
XZ-42	1	2'-0	0.324	
XZ-425	1	2'-6	0.405	Clearance between laminations
XZ-43	1	3'-0	0.485	at delaminated section
XZ-44	1	4'-0	0.648	
XY-41	1	1'-0	0.162	
XY-42	1	2'-0	0.324	Wood contact between laminations
XY-425	1	2'-6	0.405	at delaminated section
XY-43	1	3'-0	0.486	
XY-44	1	4'-0	0.648	

* $\frac{\text{Delamination Length}}{\text{Beam Length}}$ Ratio

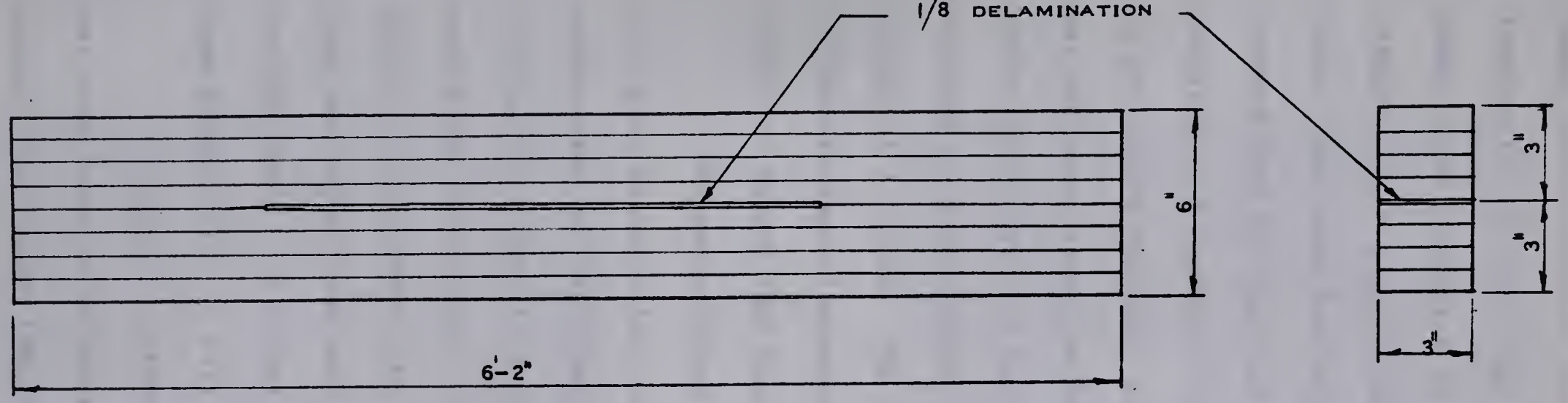

BEAM SERIES XZ-4

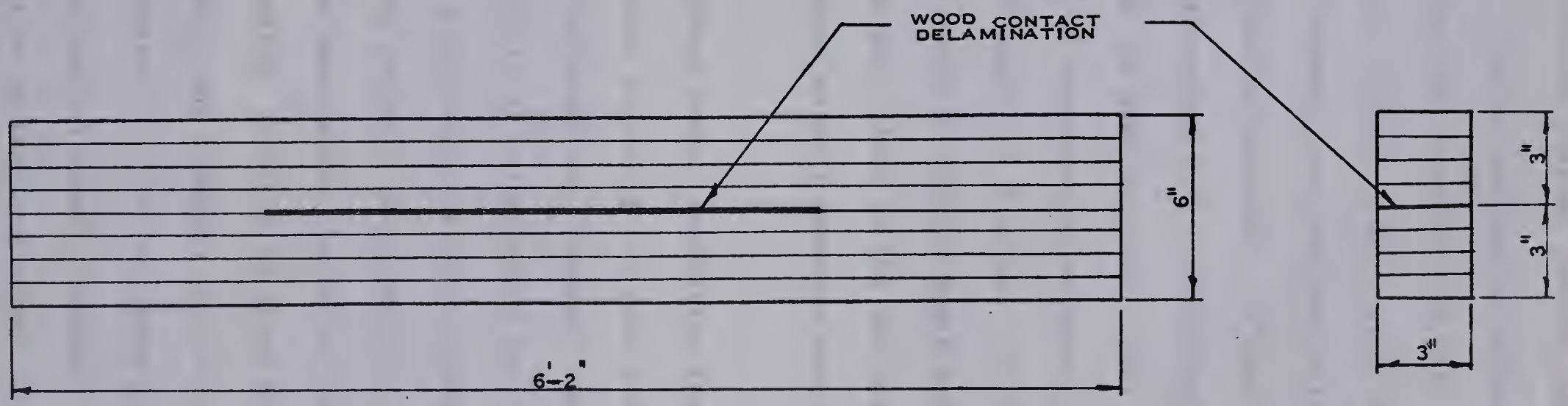

BEAM SERIES XY-4

DELAMINATED BEAM DIMENSIONS

VERTICAL SCALE 1" 6"
HORIZONTAL SCALE 1" 1'-0"

FIGURE 4.1

beams, which contained an actual clearance between laminations, a special fabrication procedure was followed. The top and bottom halves of these beams, each consisting of four laminations, were individually glued and clamped in the jigs as separate units. (PLATE 4.1A). After allowing twenty four hours for curing of the casein glue, the beam halves were removed from the jigs and the delamination prepared. On each beam half, material to a depth of 1/16 inch was removed from the lamination adjacent to the future mid-depth glue line of the beam specimen. This operation was performed along the full length of the required delamination by a power router having a cutting head diameter of 6 inches. This preparation resulted in a very clean full width gouge of uniform depth having an end radius of 3 inches. The beam halves were glued on the unrouted surfaces of the mid-depth laminations, assembled as full beams in the jigs and cured for twenty four hours.

The second group of delaminated beams, containing the wood contact type delamination, were fabricated following the same basic procedure used for the clearance type delamination. However, instead of routing out material to form the artificial delamination the following method was substituted. Initially 3 inch square double layers of wax paper were stapled at the ends of the required delamination. After glue was spread from each end of the beam halves, up to and not including the wax paper, the halves were assembled. PLATE 4.1B shows the glued beam halves prior to full beam assembly and clamping in the jigs.

To ensure uniformity of fabrication, the two stage gluing process was also employed in fabricating the control beams. However, at the second gluing stage the entire surfaces of the beam halves were glued resulting in a continuous glue joint at mid-depth of the control beams.

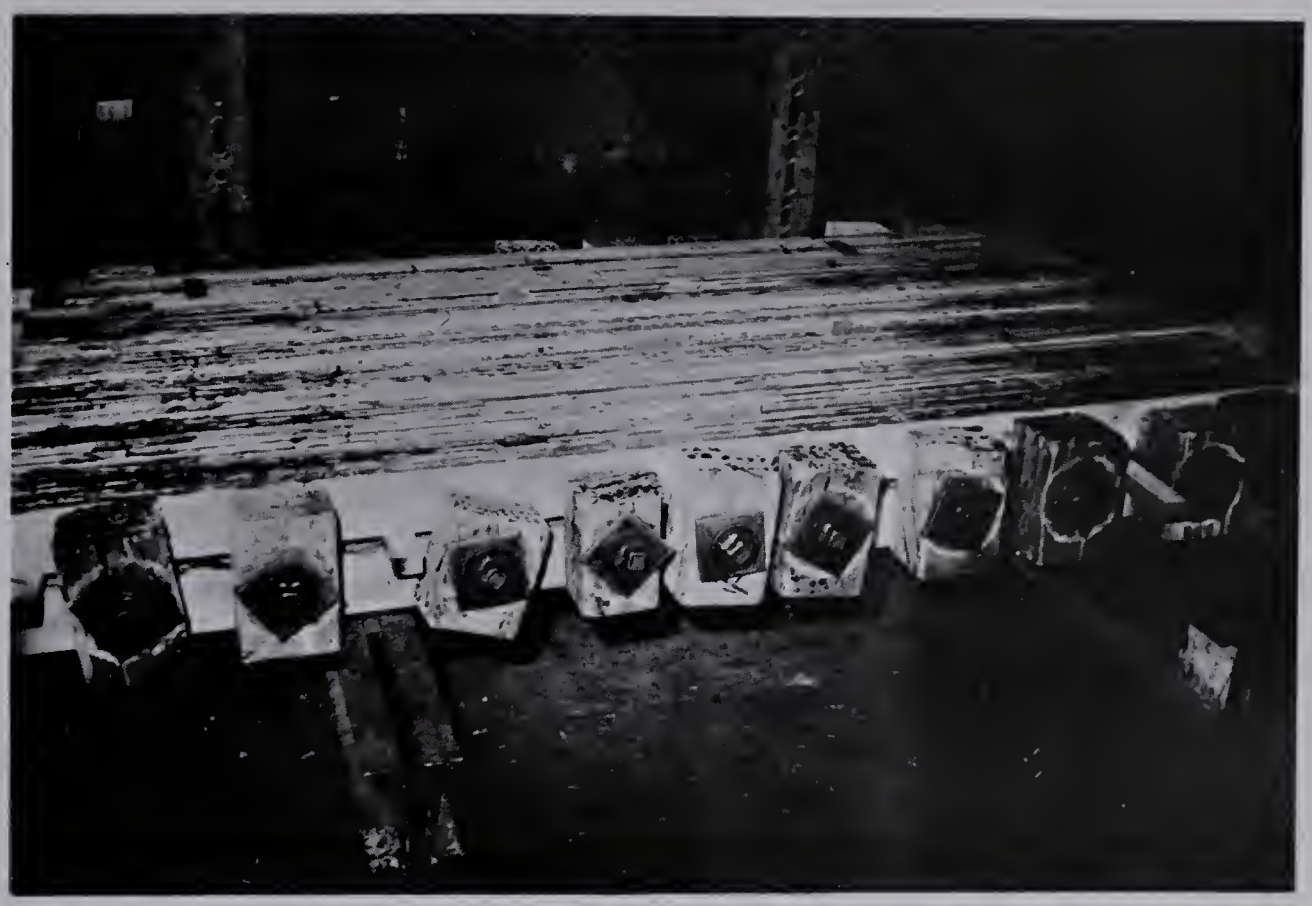

[A] BEAMS IN CLAMPING JIGS

[B] HALF BEAMS AFTER GLUING

PLATE 4.1

CHAPTER V

BEAM TESTS

5-1 Loading System

The beam testing program was conducted using a standard testing frame and the "Amsler Hydraulic Jack Plant" in the Graduate Structures Laboratory. FIGURE 5.1 illustrates the test equipment arrangement.

Load was applied at the midspan through a 3" x 4" x 3/8" distribution plate. When testing the delaminated beams, containing the clearance type delamination, 3" x 4" lubricated sheet metal shims were snugly fitted in the delamination at midspan. This prevented local bending in the top half of the beam and assured equal load distribution to both halves of the beam.

Strong, in the previous investigation at the University of Alberta, encountered difficulties in testing a number of beams to failure because of lateral instability. In the present project reaction blocks, as shown in PLATE 5.1A, were provided to prevent lateral buckling. These blocks, one hinged and one mounted on a roller, satisfied fully the conditions of simple supports while still providing lateral support to the beam. The reactions were transferred through these reaction blocks to the beam through 2" x 3" x 3/8" bearing plates.

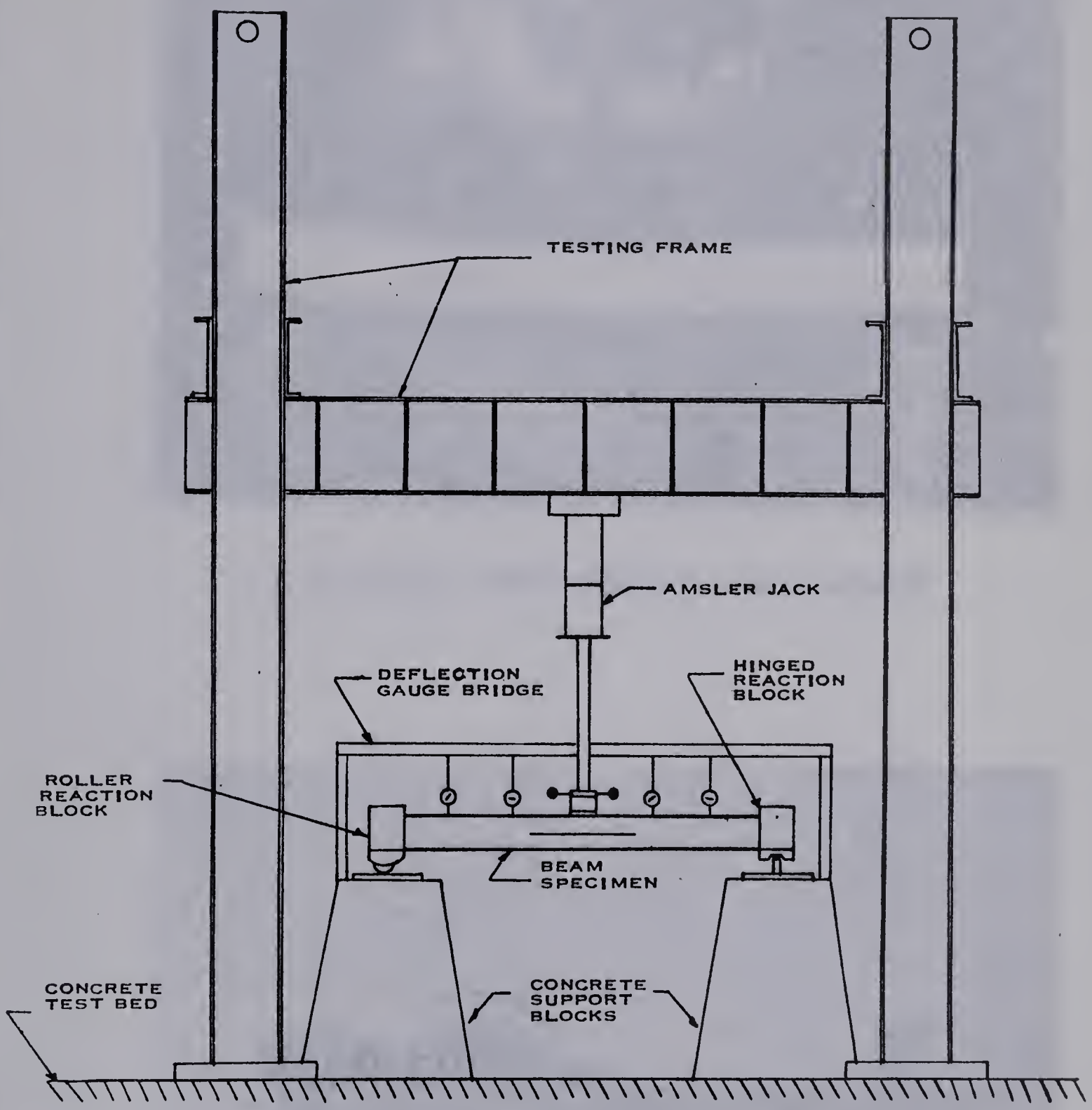

BEAM TESTING ARRANGEMENT

FIGURE 5.1

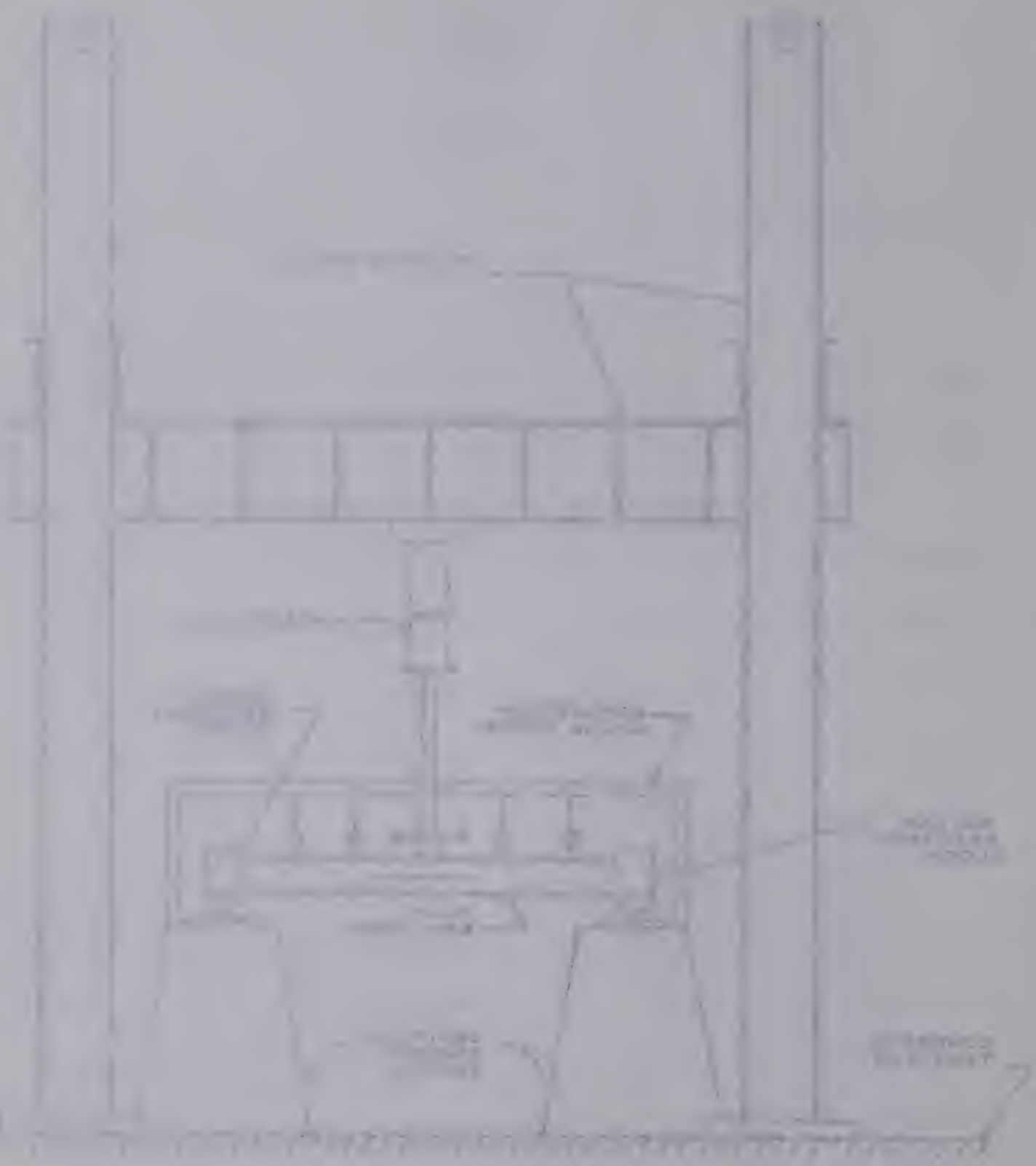

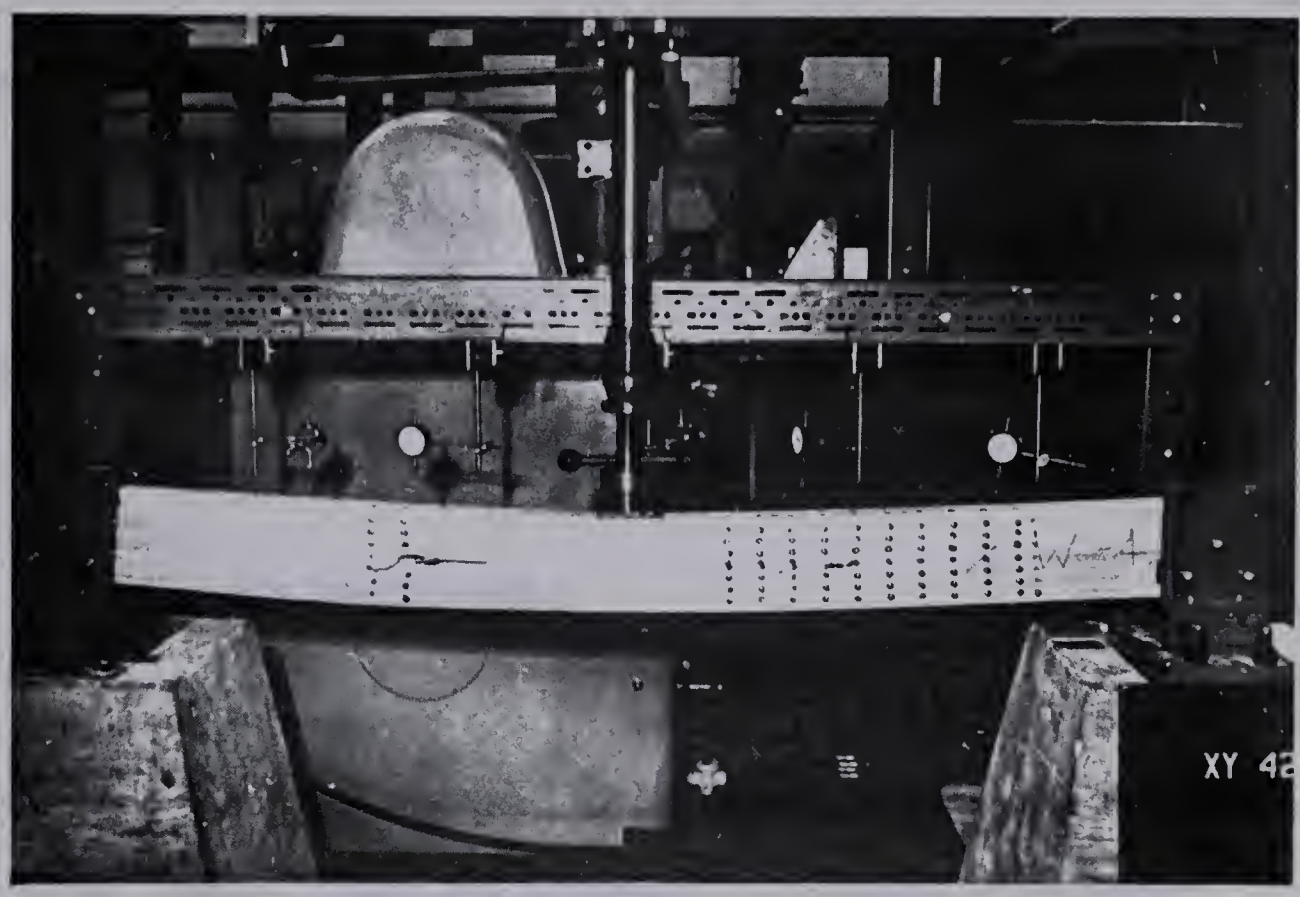

[A] TYPICAL BEAM TESTING ARRANGEMENT

[B] CONVERTED DEMEC GAUGE

PLATE 5.1

5-2 Beam Instrumentation

i. Deflection Measurement

Vertical deflections were measured at one foot intervals along the beam by dial gauges having a one-inch travel and reading to 0.001 inch.

ii. Demec Strain Measurements

In order to measure strains over a small gauge length it was necessary to modify an 8-inch Demec strain gauge to obtain readings on a 2-inch gauge length. This was achieved by clamping a removable conversion bar securely to the Demec gauge as shown in PLATE 5.1B. This bar contained a machined hole at one end which fitted over the fixed Demec gauge point, assuring no relative movement between the gauge and conversion bar. At 6-inches from the fixed Demec gauge point, another fixed gauge point was located on the conversion bar. This modification made it possible to record deformations over a 2-inch gauge length with an accuracy of $\pm$ 0.000004 in./in. A calibration factor for the 2-inch Demec strain gauge was obtained from a tension test of a 1/2 inch diameter steel rod. This rod was instrumented with two electrical resistance SR-4 Type A-3 strain gauges and two sets of Demec gauge points, providing the necessary data for the computation of a calibration factor.

Demec gauge points were bonded with sealing wax to the delaminated beams and control beam X-003 in locations as shown in FIGURE 5.2 and 5.3 respectively.

PLAN

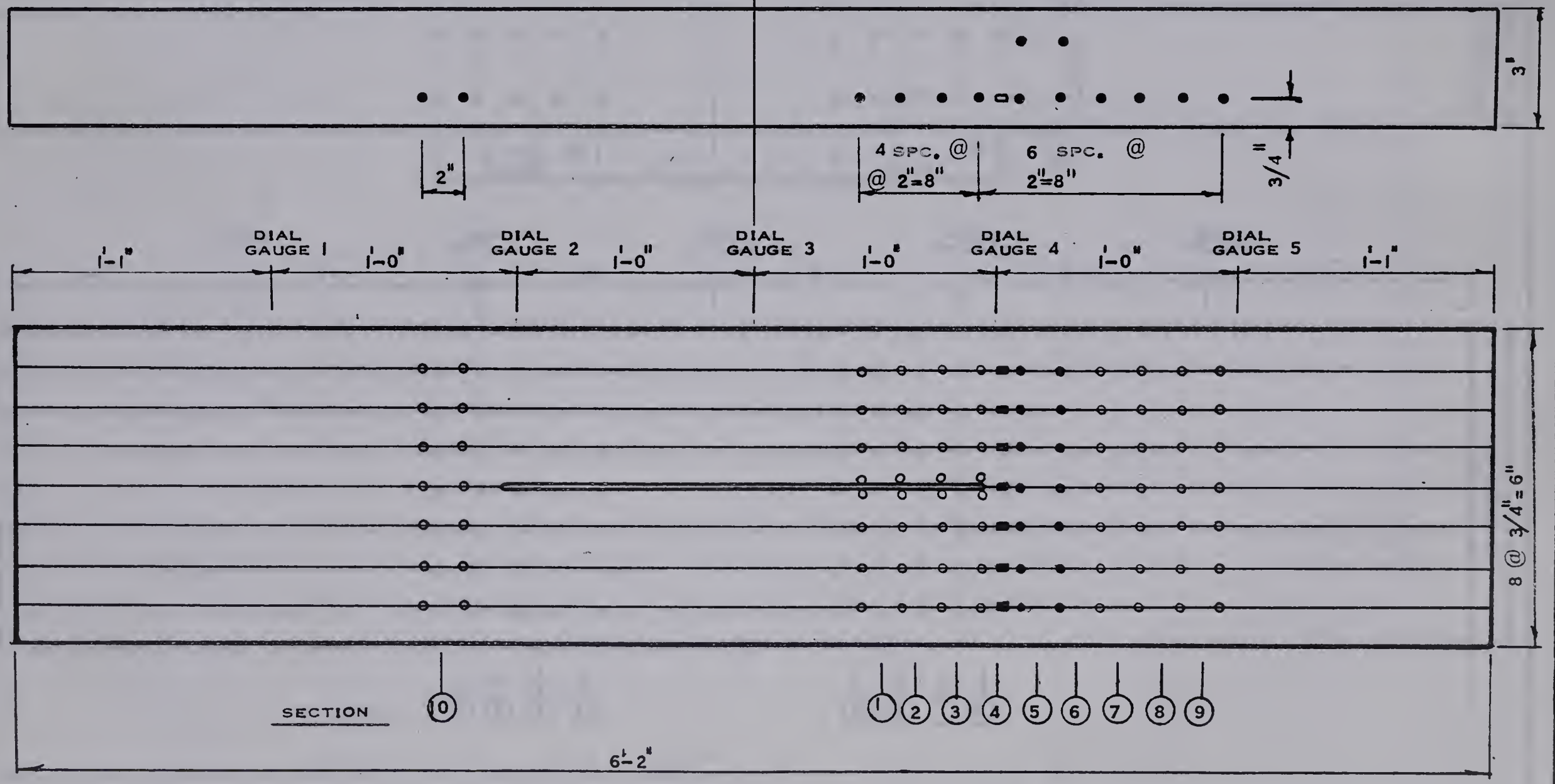

ELEVATION

Horiz. scale 1/8"=1"
Vert. scale 1"=3"

DELAMINATED BEAM INSTRUMENTATION

o DEMEC POINT NEAR SIDE
● DEMEC POINT BOTH SIDES
▭ SR-4 GAUGE BOTH SIDES
▬ SR-4 GAUGE NEAR SIDE

FIGURE 5.2

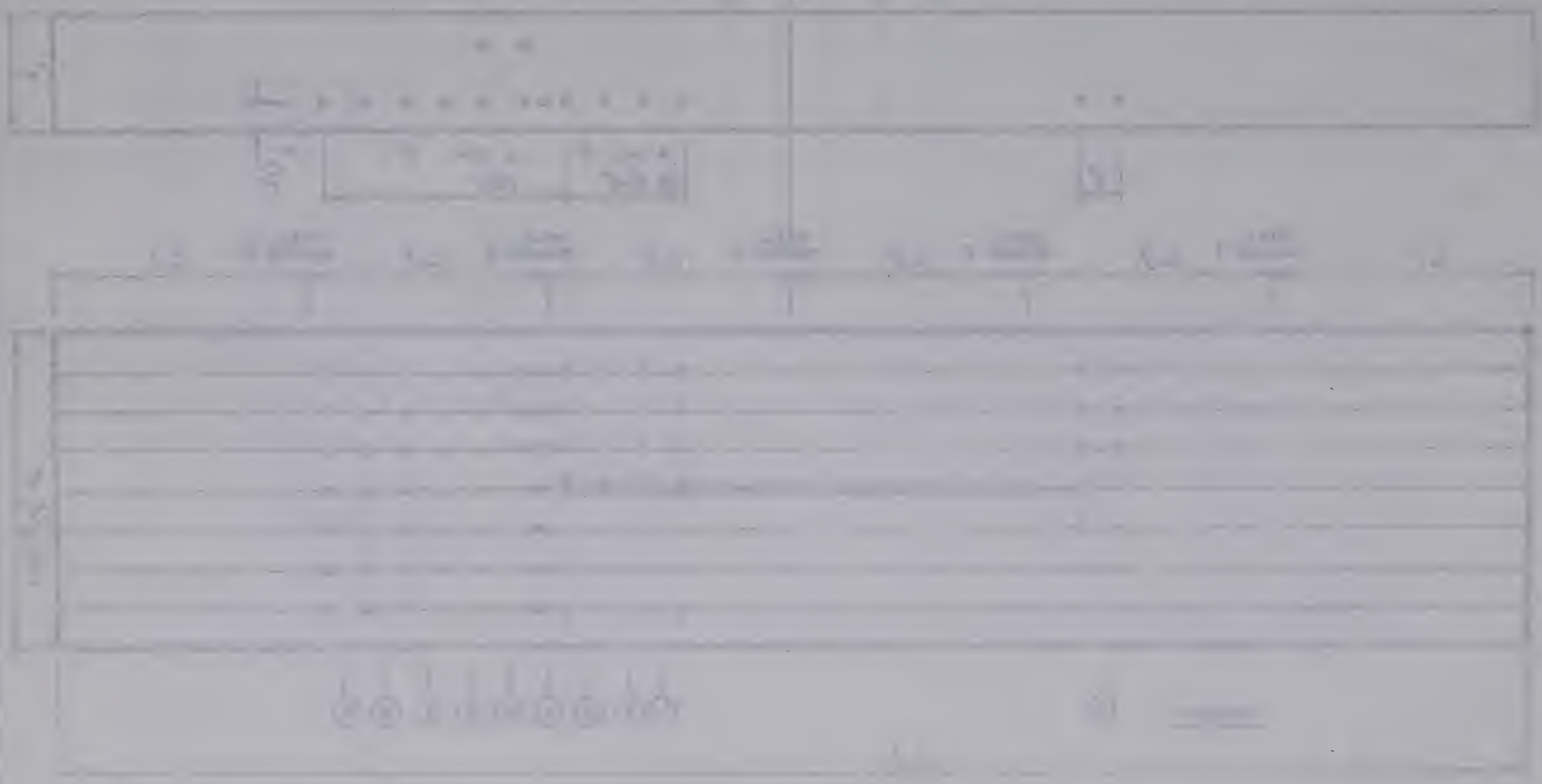

PLAN

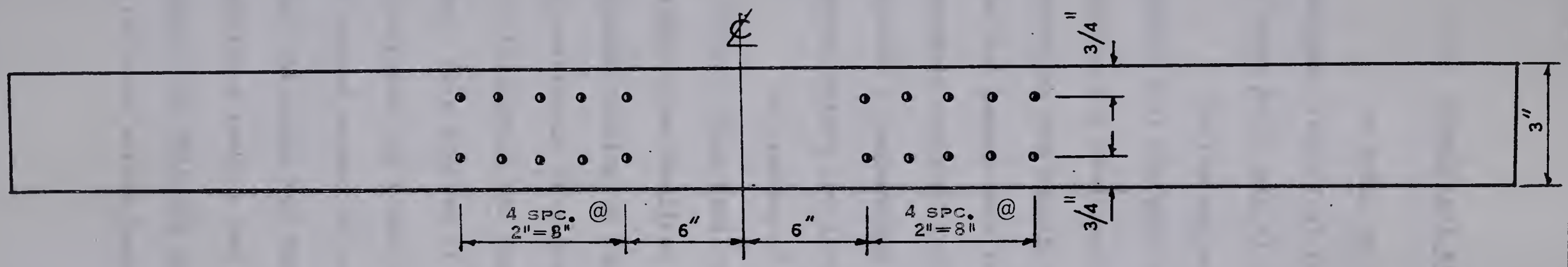

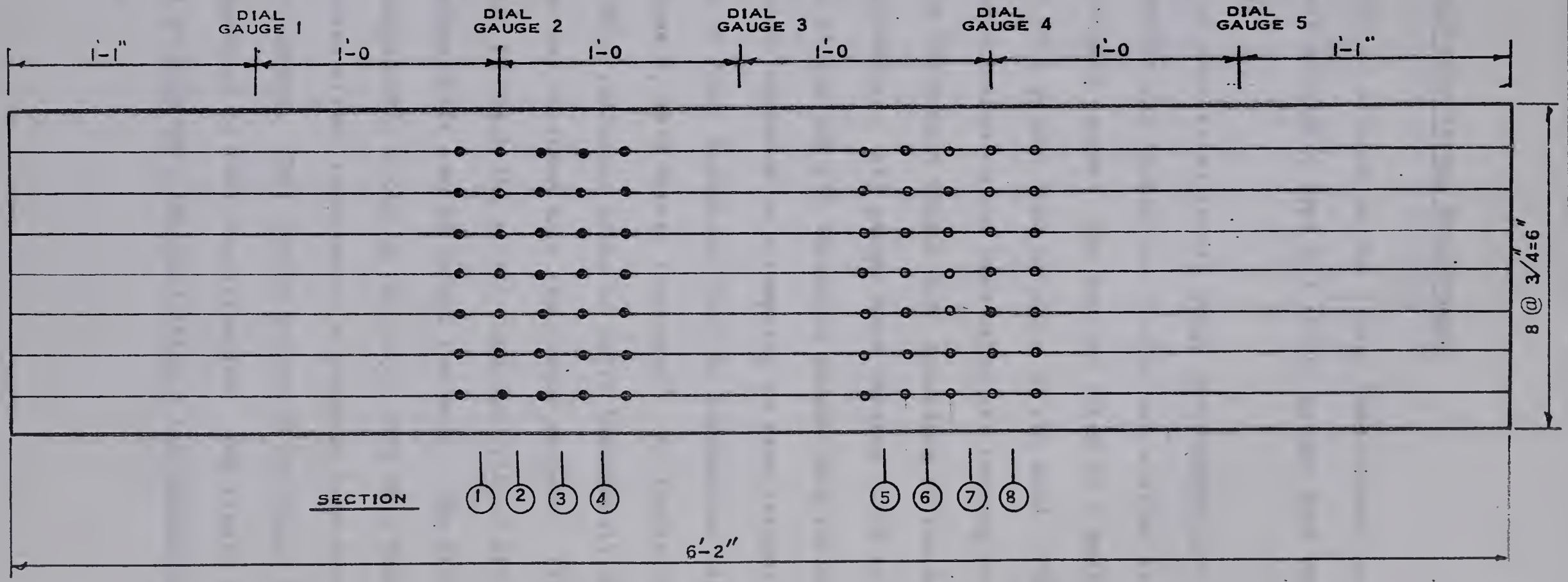

ELEVATION

- DEMEC POINT NEAR SIDE
- DEMEC POINT FAR SIDE
- DEMEC POINT BOTH SIDES

HORIZ. SCALE 1/8"=1"
VERT. SCALE 1"=3"

CONTROL BEAM X-003
INSTRUMENTATION

FIGURE 5.3

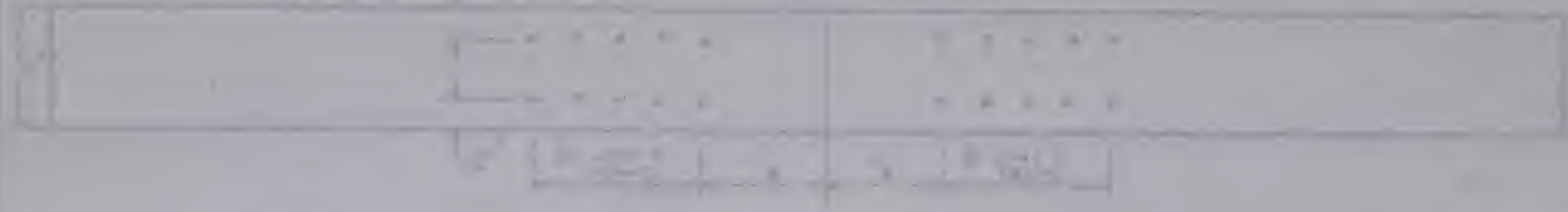

iii. Electrical Resistance Strain Measurement

In order to provide a check on the 2-inch Demec strain gauge readings, electrical resistance SR-4 Type A-3 strain gauges were employed on beams X2-41 and X2-42.

In the region of electrical strain gauge instrumentation (FIGURE 5.2) the beam surface was sanded and shellac was applied in preparation for mounting the SR-4 gauges. The shellac acted as a sealer in protecting the sensitive SR-4 gauges from moisture in the wood. The SR-4 Type A-3 gauges were then attached to the beam using the bonding and curing compounds supplied in the "Budd GA-1 Cement Kit" according to the manufacturer's recommended procedure. All gauges were checked with an ohmeter before and after wiring and all defective gauges were replaced.

A problem of drift appeared on attempting to read strains using a "Baldwin-Lima-Hamilton 20 Point Switching Unit" in conjunction with a "Baldwin-Lima-Hamilton Type N, SR-4 Strain Indicator". An initially balanced reading on the SR-4 indicator began to drift immediately after the particular SR-4 gauge was switched into the bridge circuit. FIGURE 5.4 illustrates the manner in which the strain readings drifted with time. This problem of gauge drift can be solved two ways. The first is to power the gauge continuously avoiding the drift with each reading. The second method is to take strain readings at a constant time interval after the gauge has been powered. This latter method of obtaining a stabilized reading was employed in this investigation. The strain indicator was balanced and strains were recorded after a two minute warm up for each strain gauge.

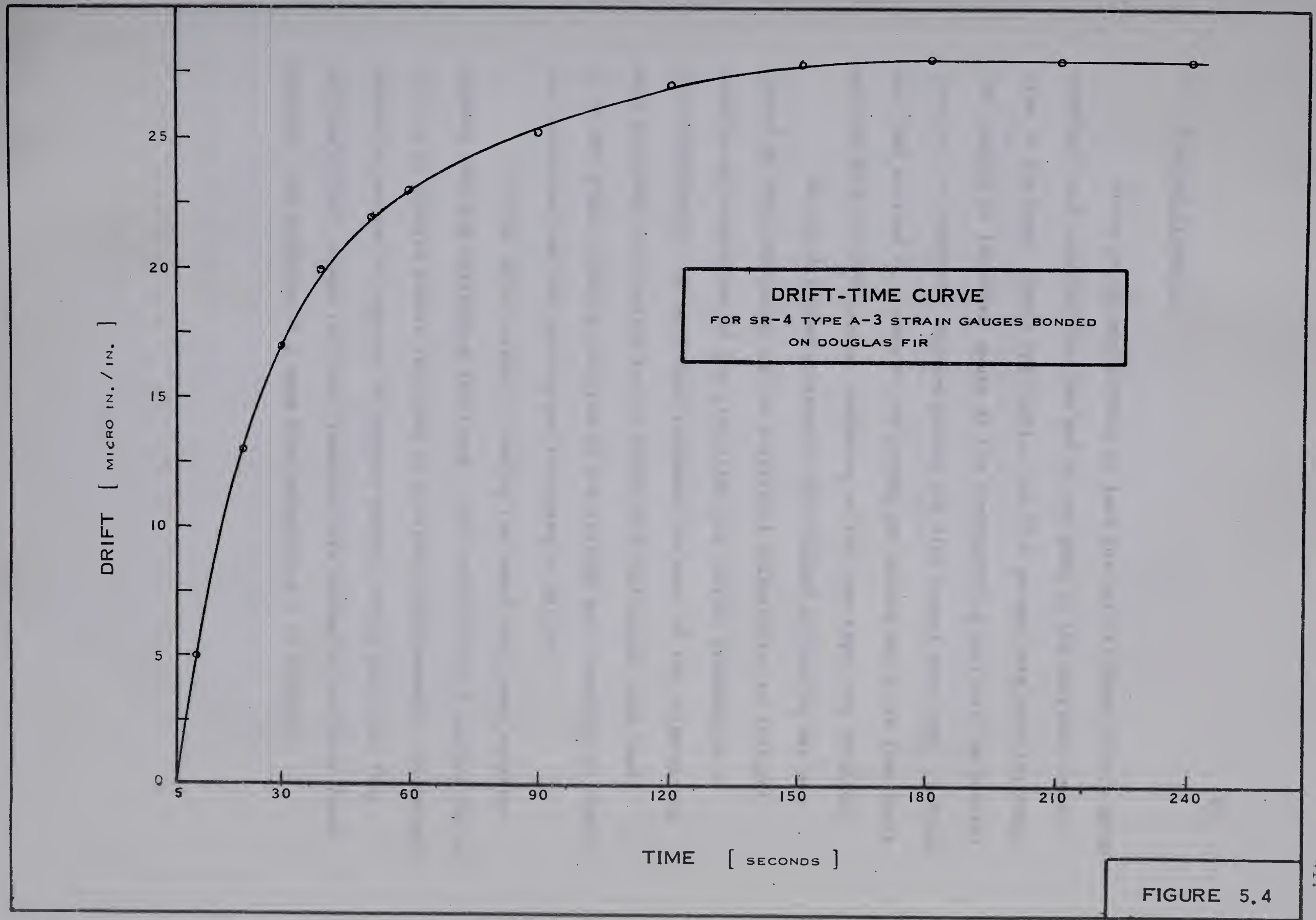
DRIFT-TIME CURVE
FOR SR-4 TYPE A-3 STRAIN GAUGES BONDED ON DOUGLAS FIR
DRIFT [MICRO IN. / IN.]
0
5
10
15
20
25
5
30
60
90
120
150
180
210
240
TIME [SECONDS]

FIGURE 5.4

5-3 Testing Procedure

Prior to the application of load the initial Demec strain gauge readings were recorded from the end of the beam to the vertical centerline of the beam. Where applicable, the SR-4 gauges were read following the reading of the Demec gauge at the corresponding section. An initial load of 150 pounds was applied before the dial gauges were read. Loading was then applied at a rate of 250 pounds per minute until the load increment of 1000 or 1500 pounds, depending on the beam type, was obtained.

On the delaminated beams a small amount of sealing wax was placed at the termination of the artificial delamination to indicate readily any separation of the glue joint and further propagation of the delamination. At each load increment the ends of the delamination were examined for cracking before strain and dial gauges were read. If at any stage cracking occurred in the sealing wax, recording of strain was terminated and the loading was increased to failure.

In the later stages of loading the usual non-linear relation between load and deflection developed. This necessitated a waiting period of 5 to 10 minutes before recording of strains could commence. Occasional checks on strains in regions of maximum moment, before and after this waiting period, showed an almost imperceptible change in the outer fiber strains. The duration of a beam test varied from 4 to 6 hours.

CHAPTER VI

PRESENTATION OF TEST RESULTS

6-1 Tension and Compression Test Results

The test results of the laminating stock tension and compression test specimens are presented in FIGURES 6.1, 6.2 and TABLE VI-1.

6-2 Beam Test Results

Beam test results are presented in tabular form as follows:

1. Control beam test data (TABLES VI-2 and VI-3)
2. Delaminated beam test data (TABLES VI-4 and VI-5)
3. Computed shear stresses (TABLE VI-6)

Further test results are presented in graphical form as follows:

1. Control beam strain distributions (FIGURE 6.3)
2. Delaminated beam strain distributions (FIGURES 6.4 to 6.20)
3. Load-deflection curves (FIGURES 6.21 to 6.24)
4. Horizontal shear stress distributions (FIGURES 6.25 and 6.26).

PLATE 6.1A shows the typical horizontal shear failure which occurred in all the delaminated beams and in one control beam. PLATE 6.1B shows the typical occurrence of the horizontal shear failure beginning at the glue line near the end of the delamination. Proceedings towards the reaction the failure surface propagates into the lamination rather than continuing along the glue line.

A computer program (APPENDIX B) was written in order to obtain shear stresses from horizontal equilibrium considerations, using the strain distributions obtained in the tests.

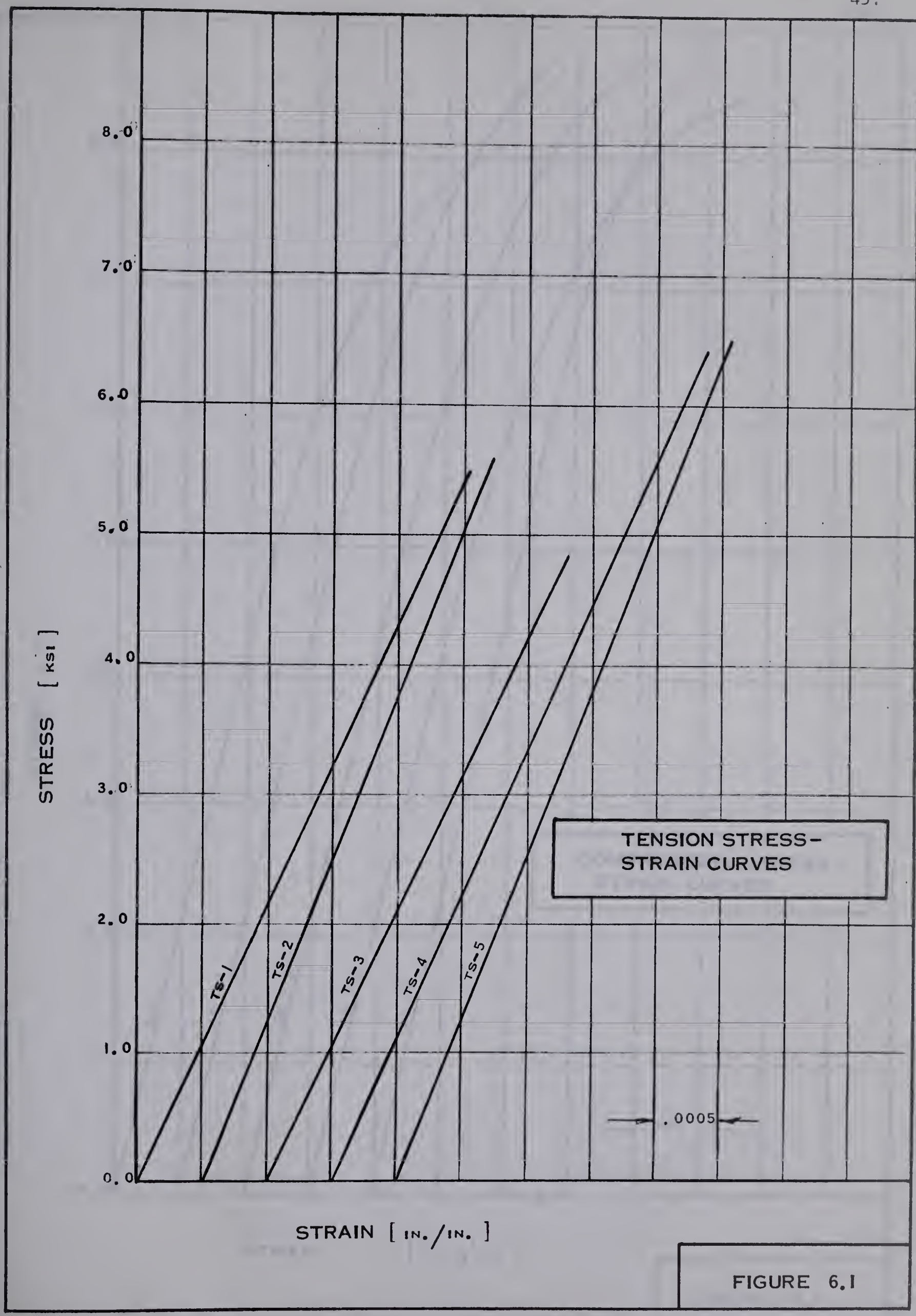
8.0
7.0
6.0
5.0
4.0
3.0
2.0
1.0
0.0
STRESS [KSI]
TS-1
TS-2
TS-3
TS-4
TS-5
TENSION STRESS-
STRAIN CURVES
.0005
STRAIN [IN./IN.]

FIGURE 6.1

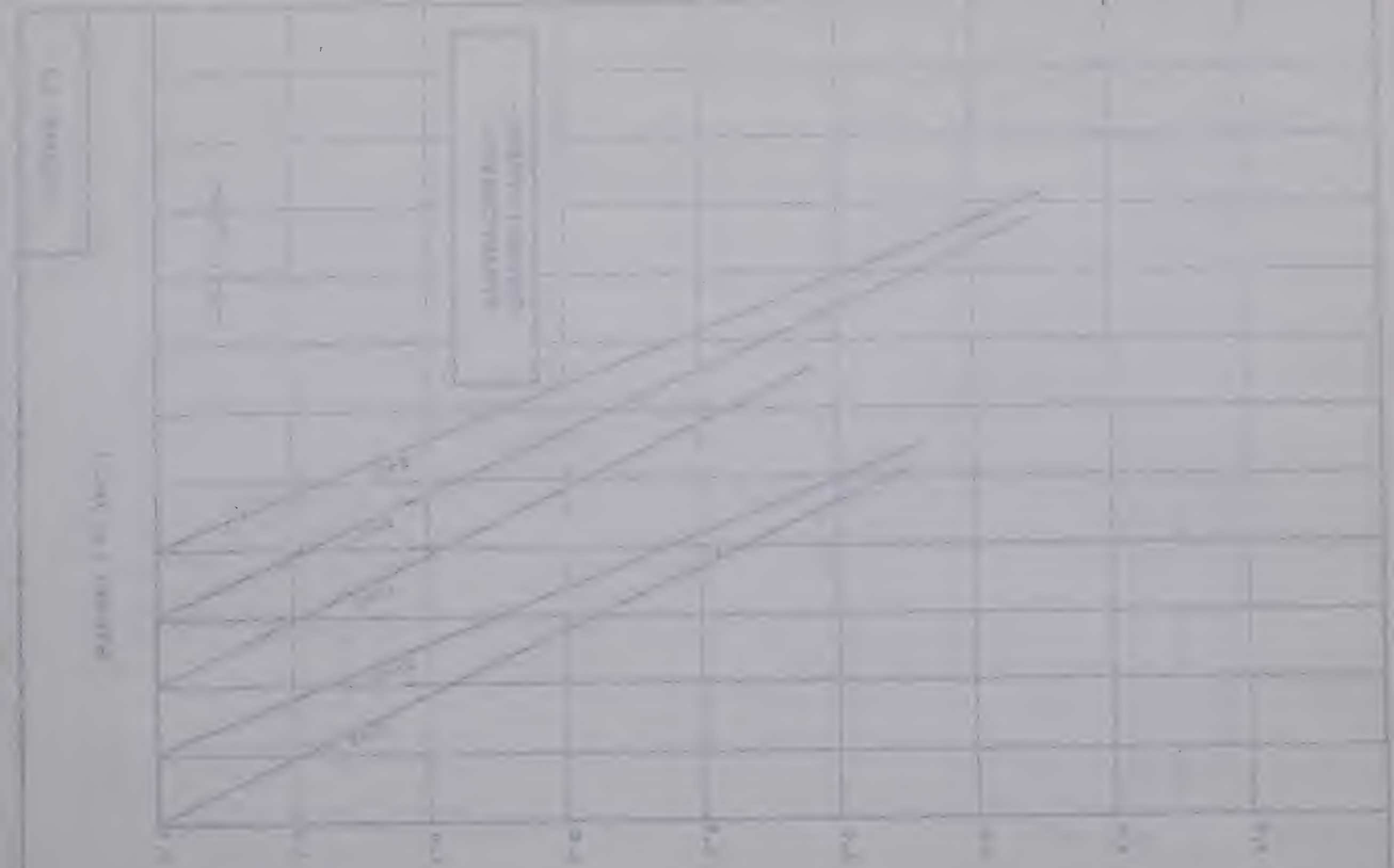

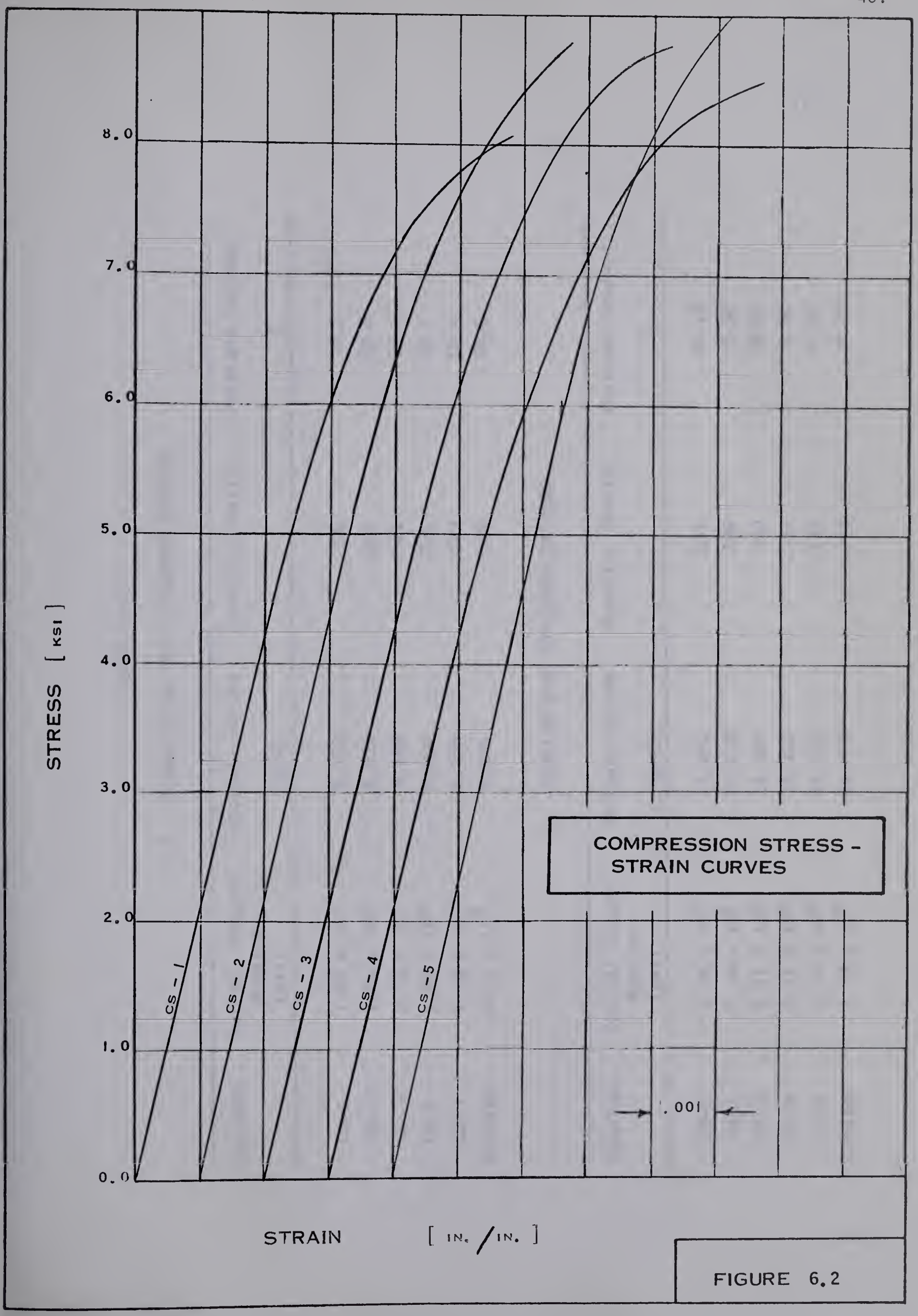

COMPRESSION STRESS - STRAIN CURVES

FIGURE 6.2

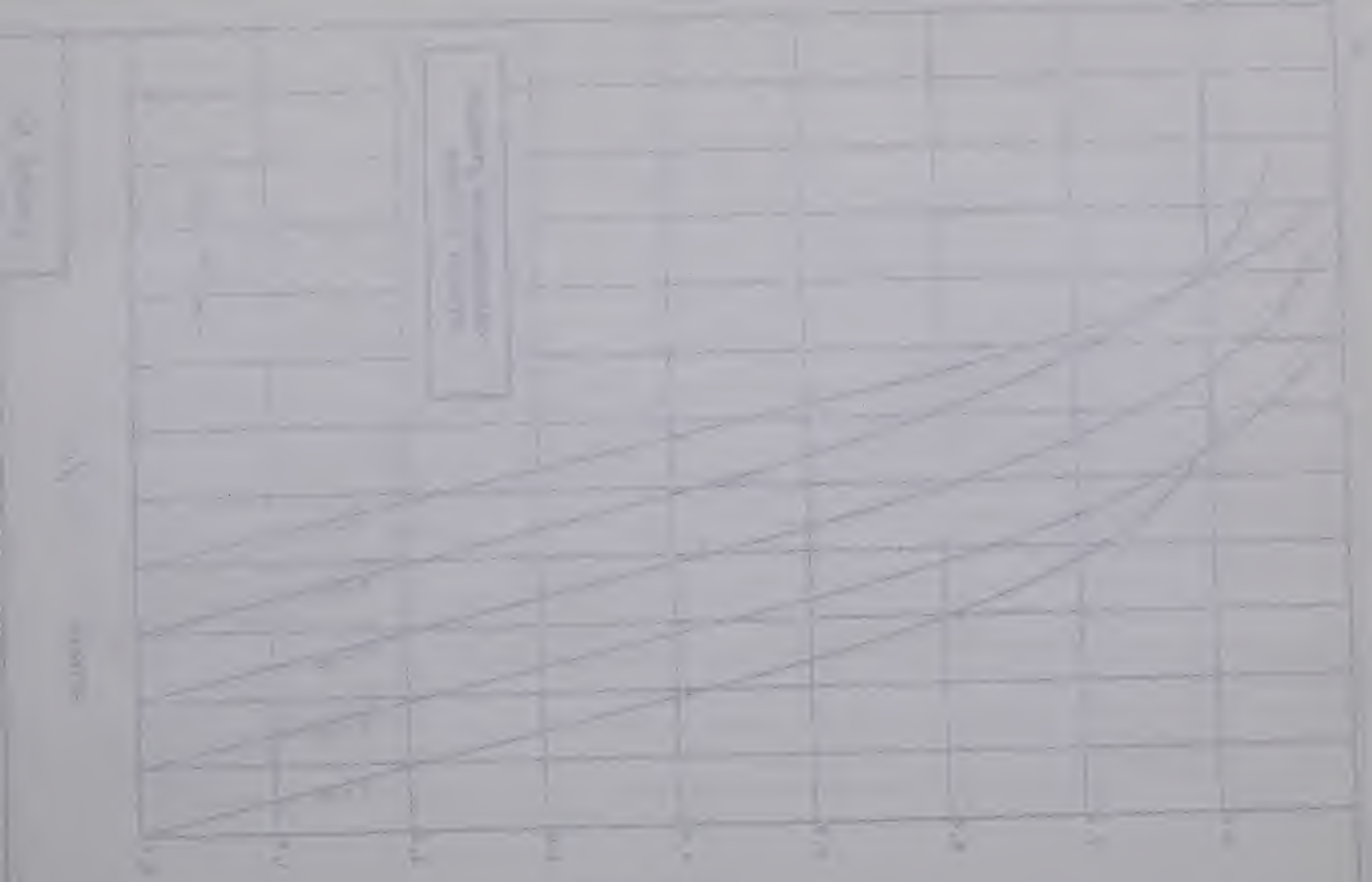

TABLE VI-1

A. COMPRESSION TEST SPECIMEN RESULTS

Specimen	Initial Tangent Modulus (psi)	Ultimate Stress (psi)	Specific Gravity	Moisture Content %
CS-1	2.08×10^6	8,140	.530	9.2
CS-2	2.24×10^6	8,950	.567	10.2
CS-3	2.14×10^6	8,890	.522	10.8
CS-4	2.04×10^6	8,800	.530	10.7
CS-5	2.38×10^6	9,450	.533	10.4
Average	2.17×10^6	8,846	.536	10.2

B. TENSION TEST SPECIMEN RESULTS

Specimen	Initial Tangent Modulus (psi)	Ultimate Stress (psi)	Specific Gravity	Moisture Content %
TS-1	2.16×10^6	11,100	.657	9.13
TS-2	2.34×10^6	17,750	.590	8.52
TS-3	2.51×10^6	12,100	.540	8.26
TS-4	2.11×10^6	15,100	.557	8.68
TS-5	2.54×10^6	16,550	.537	9.24
Average	2.33×10^6	14,520	.576	8.77

TABLE VI-2

CONTROL BEAM TEST DATA

Beam	Failure Load (kips)	Horizontal Shear Stress (psi)	Modulus of Rupture (psi)	Average Specific Gravity	Average Moisture Content %	Failure Mode*
X-001	8.76	365	8,760	.561	11.8	B.T.
X-002	10.50	437	10,600	.576	11.3	S.T.
X-003	9.00	375	9,000	.547	11.5	H.S.

*Failure Code

B.T. Brash Tension
S.T. Splintering Tension
H.S. Horizontal Shear

TABLE VI-3

CONTROL BEAM MOISTURE CONTENT AND SPECIFIC GRAVITY

Beam Lamination	X-001		X-002		X-003	
	S.G.	M.G.	S.G.	M.G.	S.G.	M.G.
1	.477	11.6	.571	11.2	.545	11.0
2	.538	11.5	.587	11.6	.642	11.5
3	.608	11.1	.580	10.9	.560	11.5
4	.561	11.9	.615	11.0	.539	11.4
5	.592	11.8	.557	11.2	.619	11.6
6	.543	11.2	.552	11.3	.452	10.7
7	.607	11.1	.482	12.2	.482	11.5
8	.569	14.0	.563	11.1	.537	11.6

Table 4-19 (cont'd)

TYPICAL CYCLONE AND TAILING ADDITIVE DATA (cont'd)

TABLE VI-4

BEAM TEST DATA

Beam	Failure Load (kips)	Average Specific Gravity	Average Moisture Content	Failure Mode*
XZ-41	10.17	.519	11.8	H.S.
XZ-42	9.00	.509	11.4	H.S.
XZ-425	7.40	.487	11.3	H.S.
XZ-43	5.90	.533	11.4	H.S.
XZ-44	5.90	.507	11.5	H.S.
XY-41	9.00	.529	11.3	H.S.
XY-42	8.42	.541	11.4	H.S.
XY-425	5.20	.512	11.5	H.S.
XY-43	5.60	.515	11.4	H.S.
XY-44	4.97	.502	11.5	H.S.

*Failure Code
H.S. Horizontal Shear

TABLE VI-5

BEAM MOISTURE CONTENT AND SPECIFIC GRAVITY

Beam	XZ-41		XZ-42		XZ-425		XZ-43		XZ-44	
Lamination	S.G.	M.C.	S.G.	M.C.	S.G.	M.C.	S.G.	M.C.	S.G.	M.C.
1	.510	11.8	.435	11.3	.399	12.1	.457	10.7	.469	11.5
2	.487	11.6	.488	11.7	.519	11.5	.559	11.0	.498	10.8
3	.587	11.7	.556	11.9	.475	11.1	.563	12.4	.573	11.7
4	.527	11.2	.562	11.2	.530	11.2	.593	11.5	.509	11.4
5	.513	11.2	.531	10.9	.474	11.5	.575	11.5	.544	11.7
6	.551	11.7	.471	11.6	.572	10.7	.441	11.4	.514	11.8
7	.470	13.1	.523	11.6	.473	11.5	.495	11.9	.508	11.4
8	.503	12.2	.505	11.0	.455	10.8	.581	10.9	.441	11.8

Beam	XY-41		XY-42		XY-425		XY-43		XY-44	
Lamination	S.G.	M.C.	S.G.	M.C.	S.G.	M.C.	S.G.	M.C.	S.G.	M.C.
1	.555	11.5	.499	11.3	.530	10.7	.558	11.2	.398	12.3
2	.436	11.9	.585	11.5	.519	10.9	.594	11.8	.490	11.3
3	.498	10.8	.554	11.7	.509	11.2	.513	11.0	.473	10.8
4	.602	10.9	.612	11.6	.505	11.4	.503	11.5	.563	11.7
5	.589	11.1	.577	11.1	.571	11.7	.483	11.3	.620	11.3
6	.551	11.4	.495	12.1	.522	11.9	.480	11.5	.502	12.0
7	.467	11.6	.497	10.8	.494	12.0	.533	11.6	.490	11.7
8	.531	10.9	.513	11.4	.446	11.9	.443	11.4	.481	10.7

TABLE VI-6

NEUTRAL AXIS SHEAR STRESSES

A. Delaminated Beams

Beam	Load (lbs.)	Horizontal Shear Stress (psi) Section 4.5	Section 5.6	Section 6.7	Section 7.8	Section 8.9
XZ-41	8500	230	908	557	448	442
		170	356	553	228	682
XZ-42	7600	-238	788	447	24	32
		441	769	447	617	153
XZ-425	5000	169	-2132	2783	-1012	1125
		352	247	311	187	473
XZ-43	5000	145	797	230	157	345
		97	406	178	161	240
XZ-44	5000	770	343	22		
		618	296	6818		
XY-41	7600	259	576	-305	544	510
		513	433	100	601	429
XY-42	6000	263	197	456	218	203
		234	545	321	474	358
XY-425	5000	450	117	268	155	386
		448	603	171	371	639
XY-43	5000	-85	545	287	365	
		196	178	506	70	
XY-44	4000	85	389	-80		
		93	-109	680		

TABLE VI-6 (Continued)

B. Control Beam X-003

Load (lbs.	$\frac{1.5V}{bd}$ (psi)	Horizontal Shear Stress (psi) Section 1.2	Section 2.3	Section 3.4	Section 5.6	Section 6.7	Section 7.8
6000	250	95	1041	299	288	184	290
		-797	980	390	57	514	391

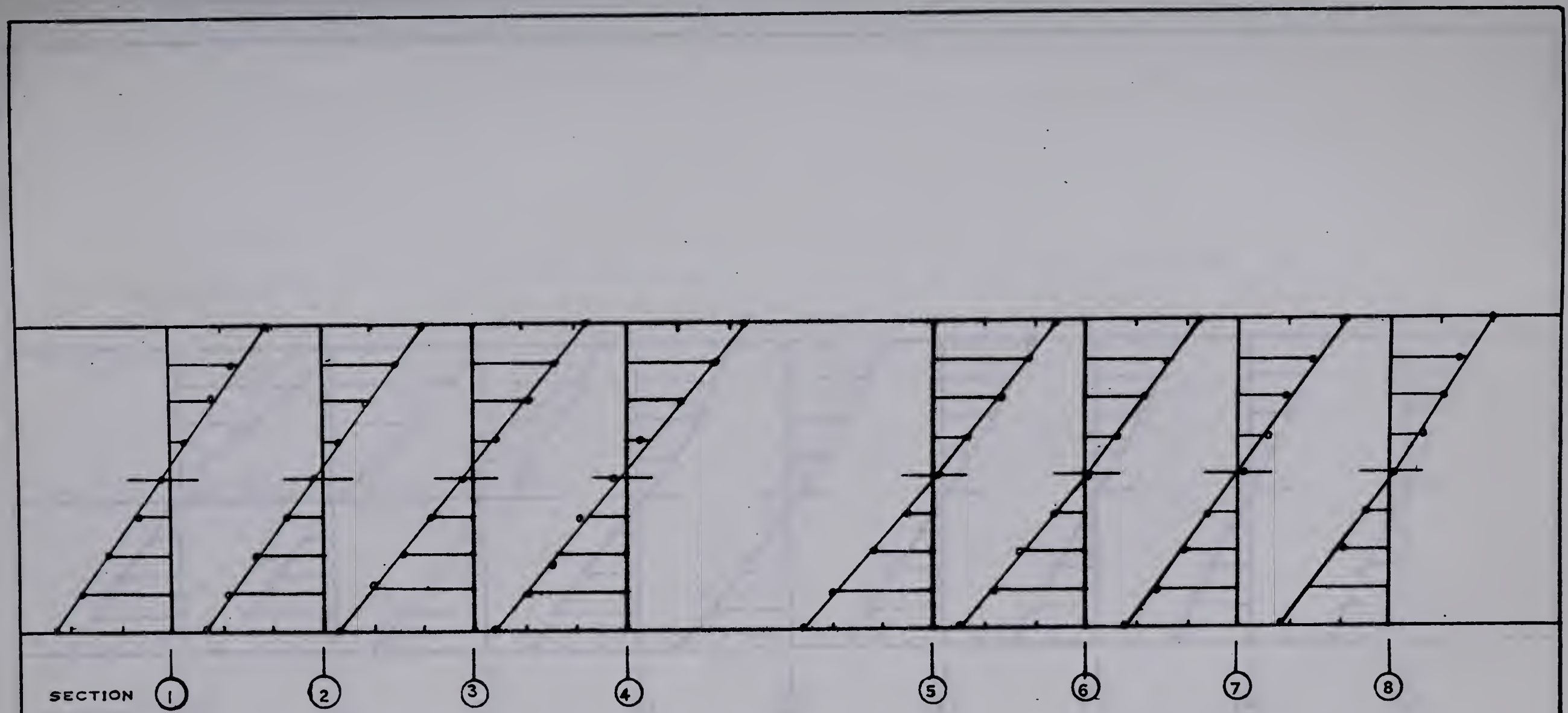

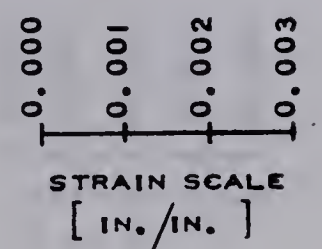

NOTE

1. STRAINS SHOWN FOR P = 6000 LBS
2. ULTIMATE LOAD PU = 9000 LBS.
3. P / PU = 0.67

STRAIN DISTRIBUTIONS
CONTROL BEAM X-003

NOTE

LOCATION OF SECTIONS SHOWN IN THIS FIGURE ARE DEFINED IN FIGURE 5.3

FIGURE 6.3

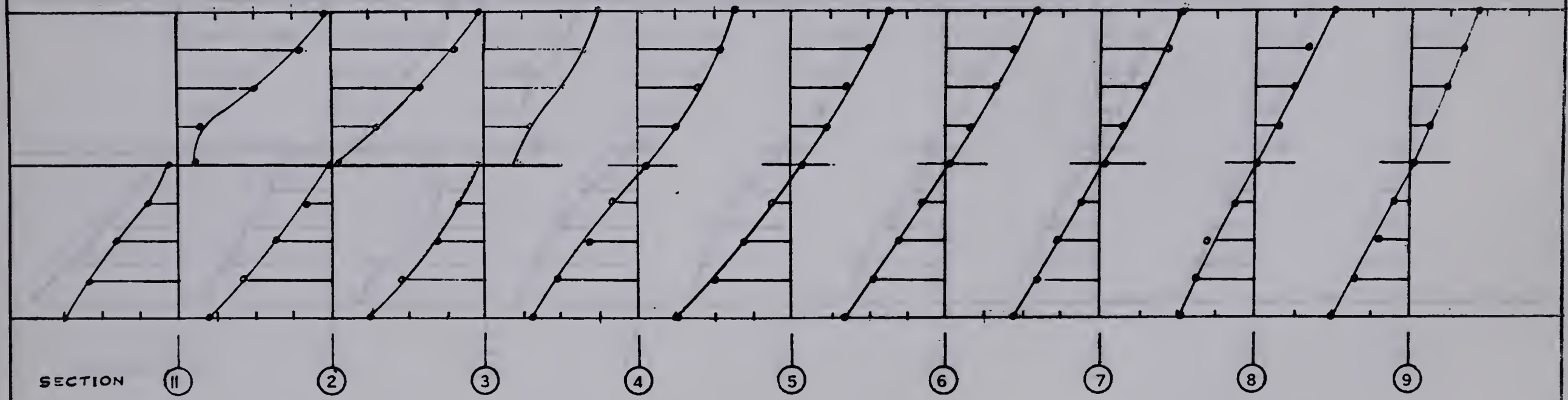

0.000 0.001 0.002 0.003 0.004

STRAIN SCALE
[IN./IN.]

NOTE
1. STRAINS SHOWN FOR P = 7000 LBS.
2. ULTIMATE LOAD PU = 10,170 LBS.
3. P / PU = 0.69
4. DELAMINATION LENGTH = 1'-0
5. D / L RATIO = 0.162

STRAIN DISTRIBUTIONS BEAM XZ-41

NOTE
LOCATION OF SECTIONS SHOWN IN FIGURES 6.4 TO 6.20 ARE DEFINED IN FIGURE 5.2

FIGURE 6.4

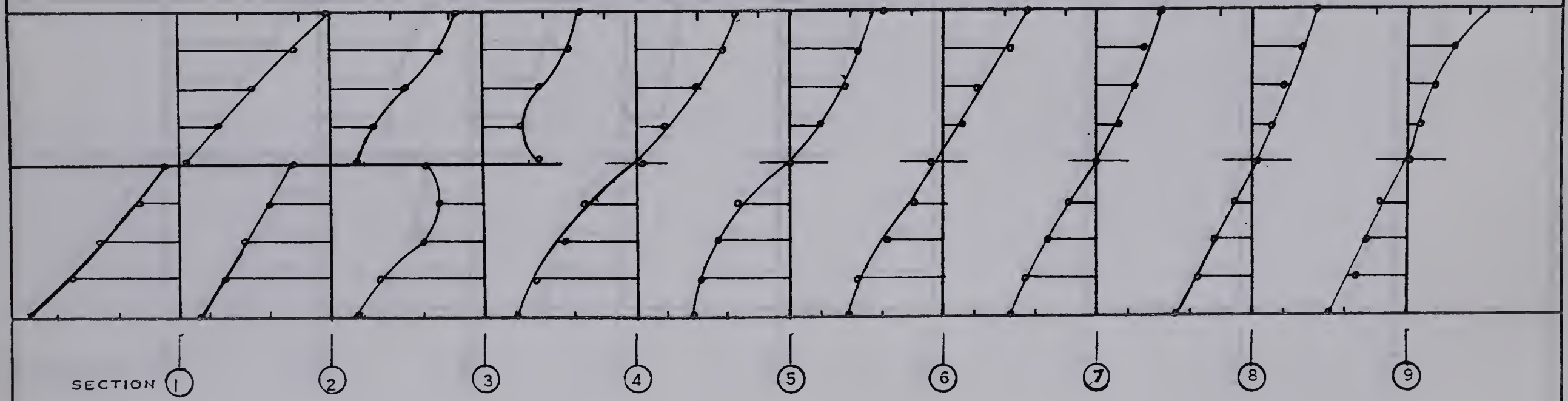

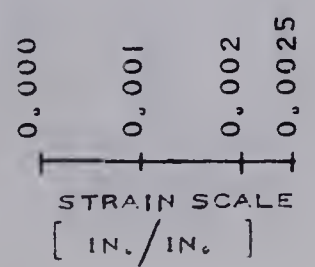

NOTE

1. STRAINS SHOWN FOR P=6000. LBS.
2. ULTIMATE LOAD PU=9000. LBS.
3. P/PU=0.67
4. DELAMINATION LENGTH = 2'-0
5. D / L RATIO = 0.324

STRAIN DISTRIBUTIONS
BEAM XZ-42

FIGURE 6.5

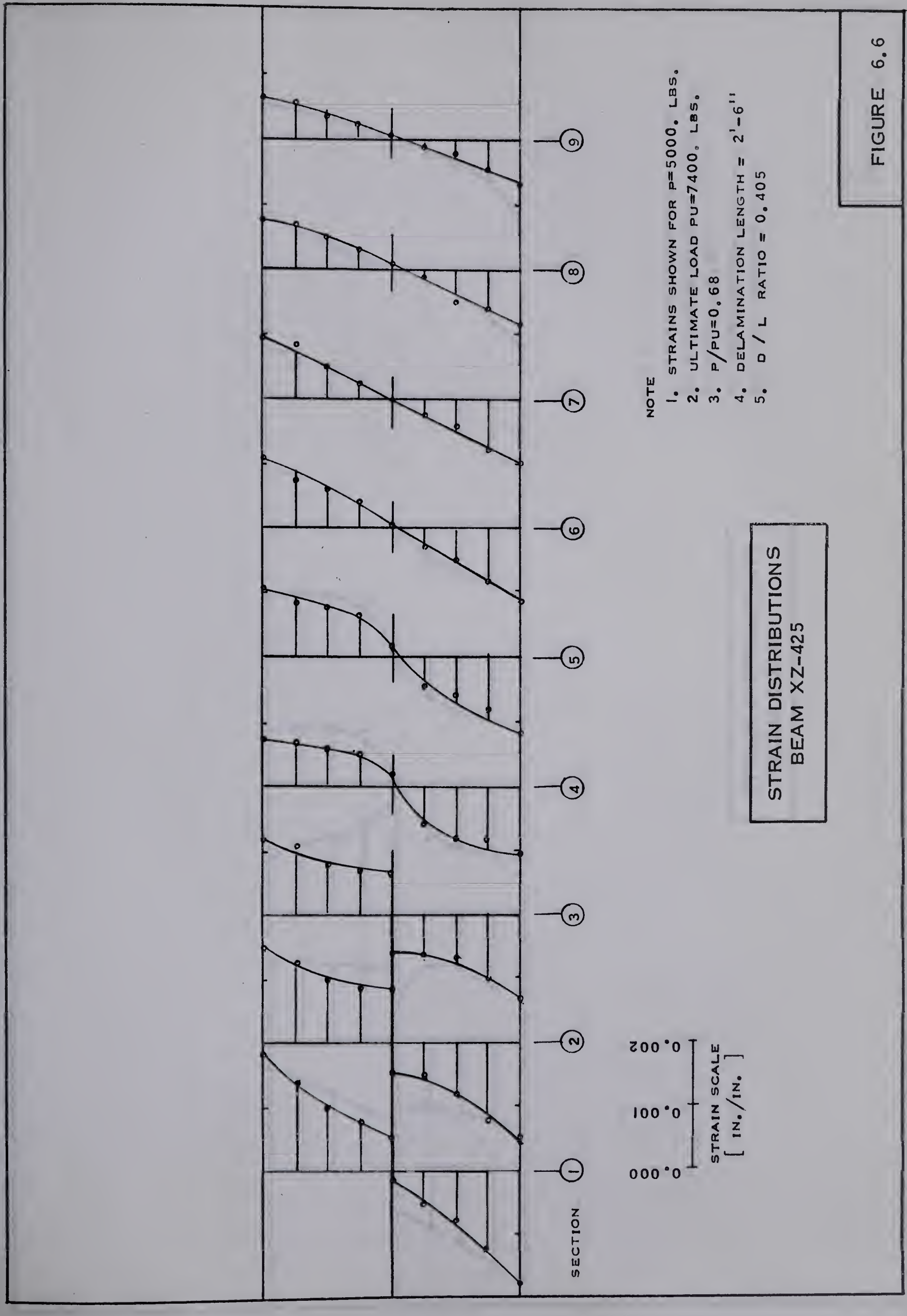
STRAIN DISTRIBUTIONS
BEAM XZ-425
STRAIN SCALE
[IN./IN.]
0.000
0.001
0.002
SECTION
1
2
3
4
5
6
7
8
9
NOTE
1. STRAINS SHOWN FOR P=5000. LBS.
2. ULTIMATE LOAD PU=7400. LBS.
3. P/PU=0.68
4. DELAMINATION LENGTH = 2'-6"
5. D / L RATIO = 0.405

FIGURE 6.6

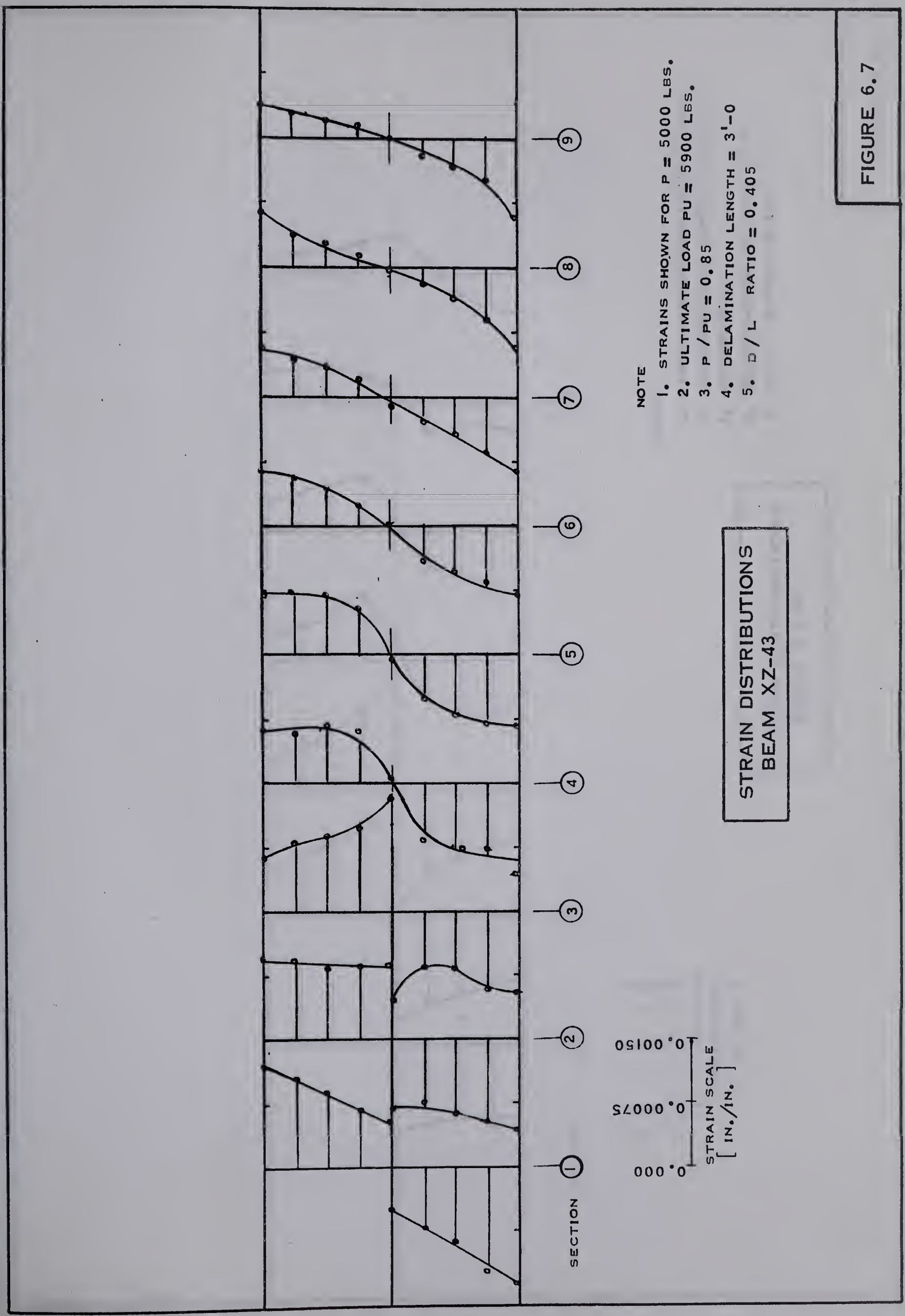
STRAIN DISTRIBUTIONS
BEAM XZ-43
STRAIN SCALE
[IN./IN.]
0.000
0.00075
0.00150
SECTION
1
2
3
4
5
6
7
8
9
NOTE
1. STRAINS SHOWN FOR P = 5000 LBS.
2. ULTIMATE LOAD PU = 5900 LBS.
3. P / PU = 0.85
4. DELAMINATION LENGTH = 3'-0
5. D / L RATIO = 0.405

FIGURE 6.7

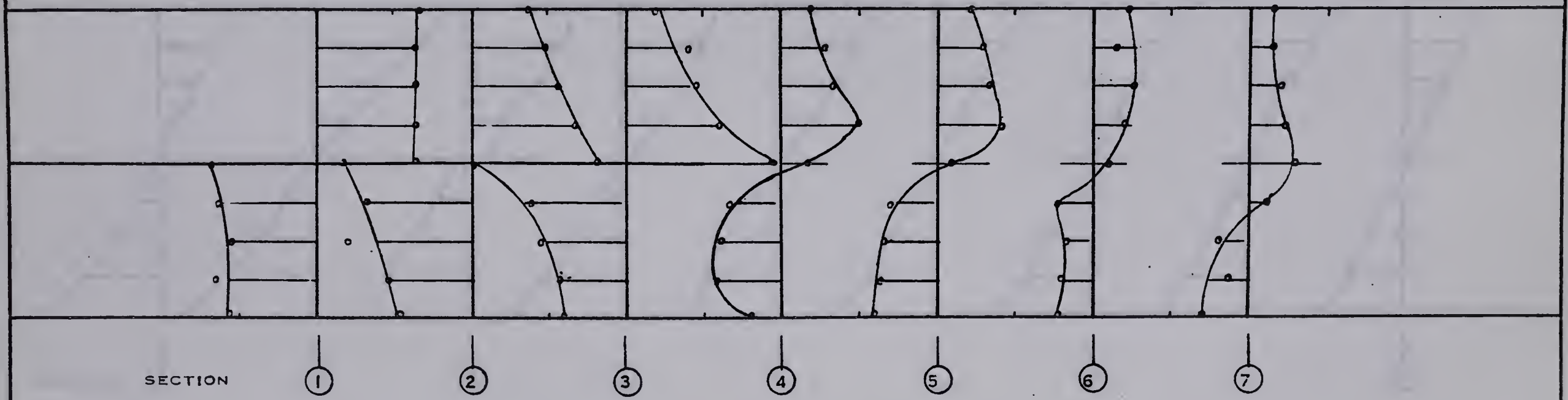

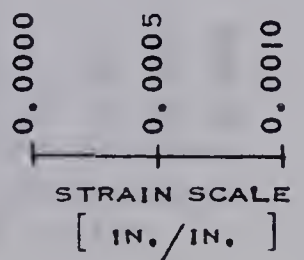

NOTE

1. STRAINS SHOWN FOR P= 4000. LBS.
2. ULTIMATE LOAD PU=4970. LBS.
3. P/PU=0.81
4. DELAMINATION LENGTH = 4'-0
5. D/L RATIO = 0.648

STRAIN DISTRIBUTIONS
BEAM XZ-44

FIGURE 6.8

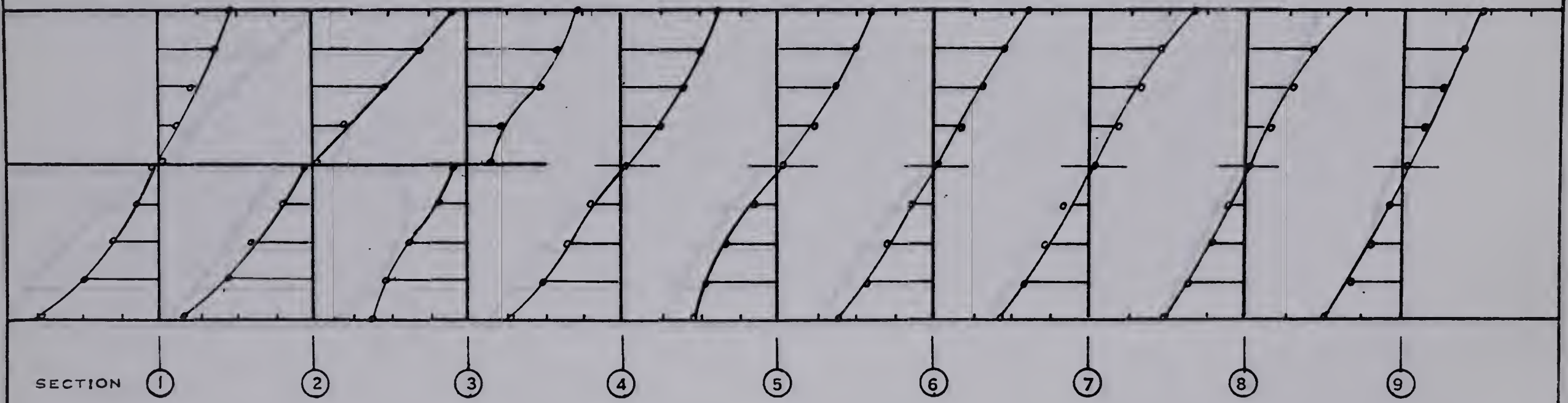

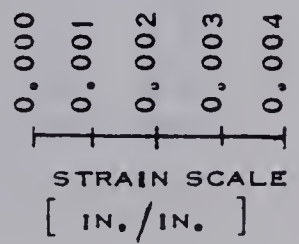

NOTE

1. STRAINS SHOWN FOR P=7500. LBS.
2. ULTIMATE LOAD PU=9000. LBS.
3. P/PU=0.83
4. DELAMINATION LENGTH = 1'-0
5. D / L RATIO = 0.162

STRAIN DISTRIBUTIONS
BEAM XY-41

FIGURE 6.9

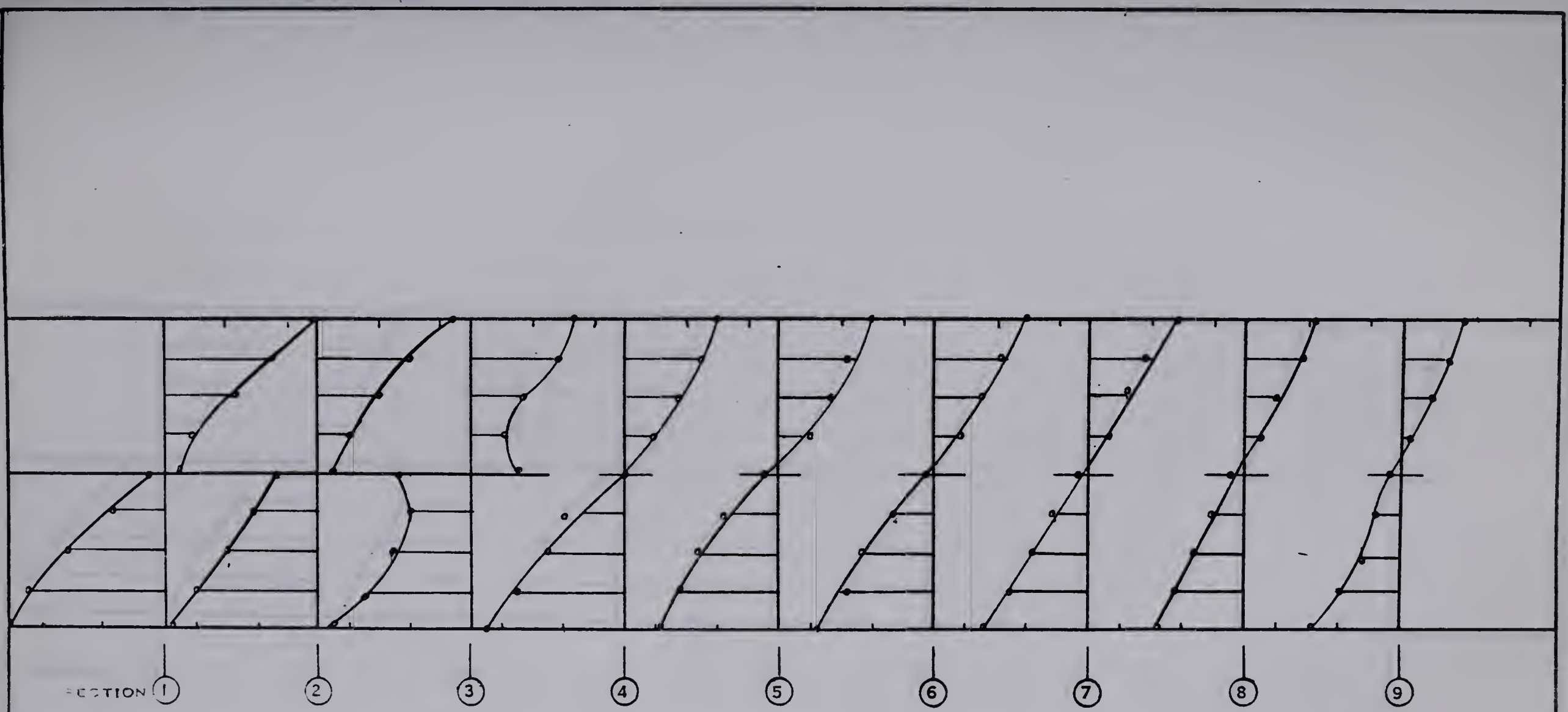

NOTE

1. STRAINS SHOWN FOR P=6000. LBS
2. ULTIMATE LOAD PU=8420. LBS.
3. P/PU=0.72
4. DELAMINATED LENGTH = 2'-0
5. D/L RATIO = 0.324

STRAIN DISTRIBUTIONS
BEAM XY-42

FIGURE 6.10

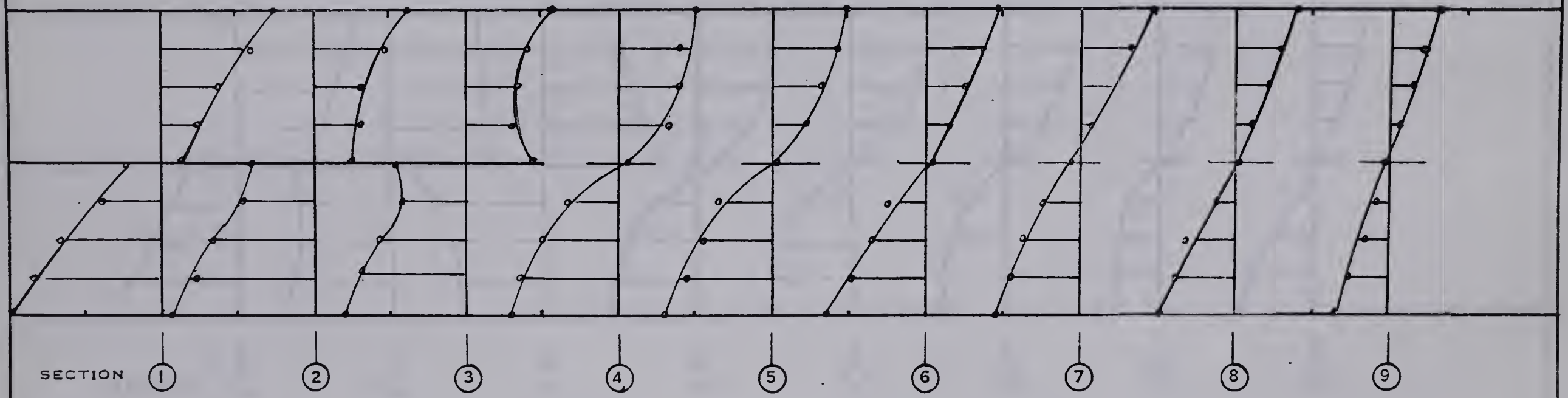

0.000 0.001 0.002

STRAIN SCALE
[IN./IN.]

NOTE

1. STRAINS SHOWN FOR P=5000. LBS
2. ULTIMATE LOAD PU=5200. LBS.
3. P/PU=0.96
4. DELAMINATION LENGTH = 2'-6"
5. D / L RATIO = 0.405

STRAIN DISTRIBUTIONS
BEAM XY-425

FIGURE 6.11

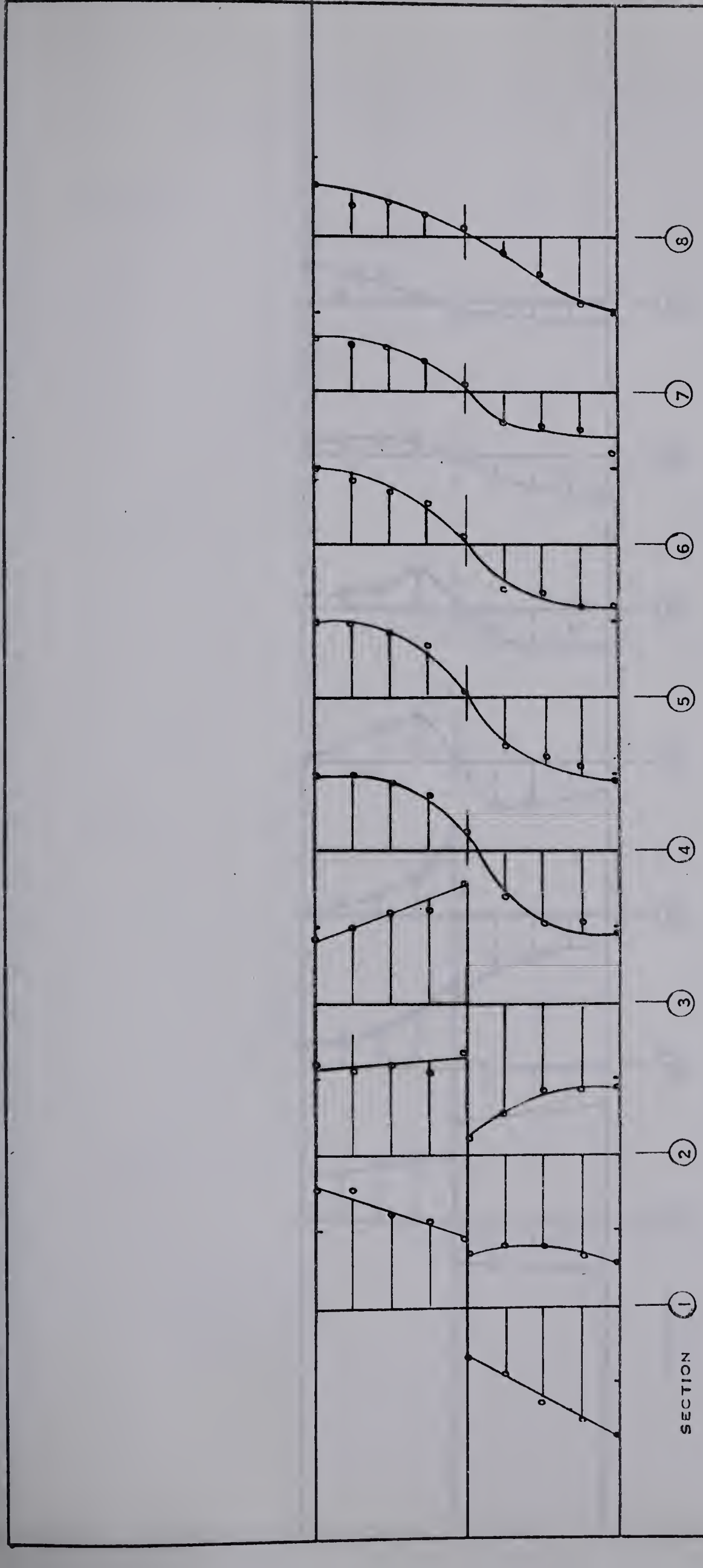
SECTION
1
2
3
4
5
6
7
8
STRAIN SCALE [IN./IN.]
0.0000
0.00075
0.00150
NOTE
1. STRAINS SHOWN FOR P=5000. LBS.
2. ULTIMATE LOAD PU=5600. LBS.
3. P/PU=0.89
4. DELAMINATION LENGTH = 3'-0
5. D /L RATIO = 0.486
STRAIN DISTRIBUTIONS
BEAM XY-43

FIGURE 6.12

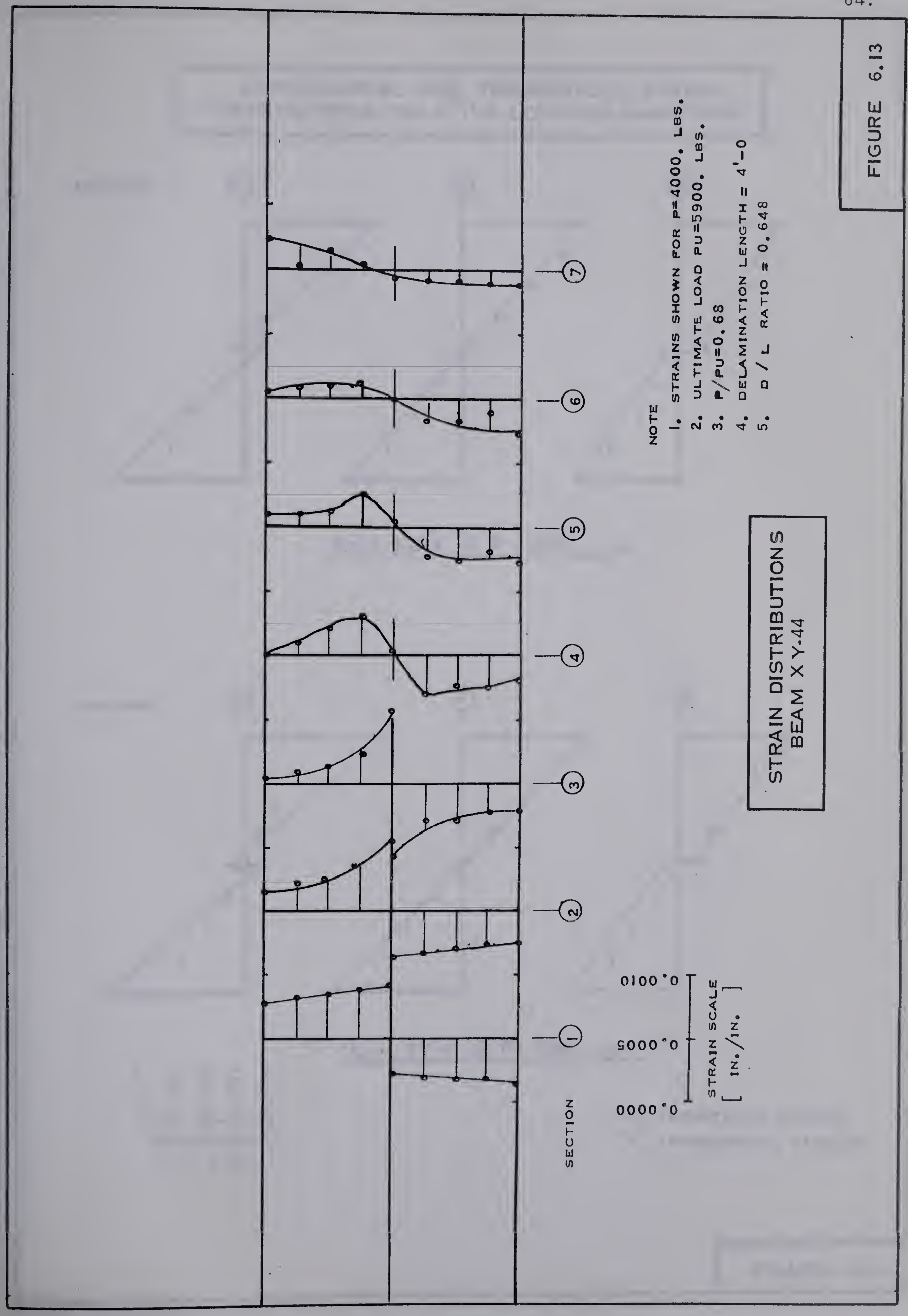
STRAIN DISTRIBUTIONS
BEAM X Y-44
SECTION
1
2
3
4
5
6
7
STRAIN SCALE
[IN./IN.]
0.0000
0.0005
0.0010
NOTE
1. STRAINS SHOWN FOR P=4000. LBS.
2. ULTIMATE LOAD PU=5900. LBS.
3. P/PU=0.68
4. DELAMINATION LENGTH = 4'-0
5. D / L RATIO = 0.648

FIGURE 6.13

EXPERIMENTAL AND THEORETICAL STRAIN DISTRIBUTIONS FOR A 1'-0 LONG DELAMINATION

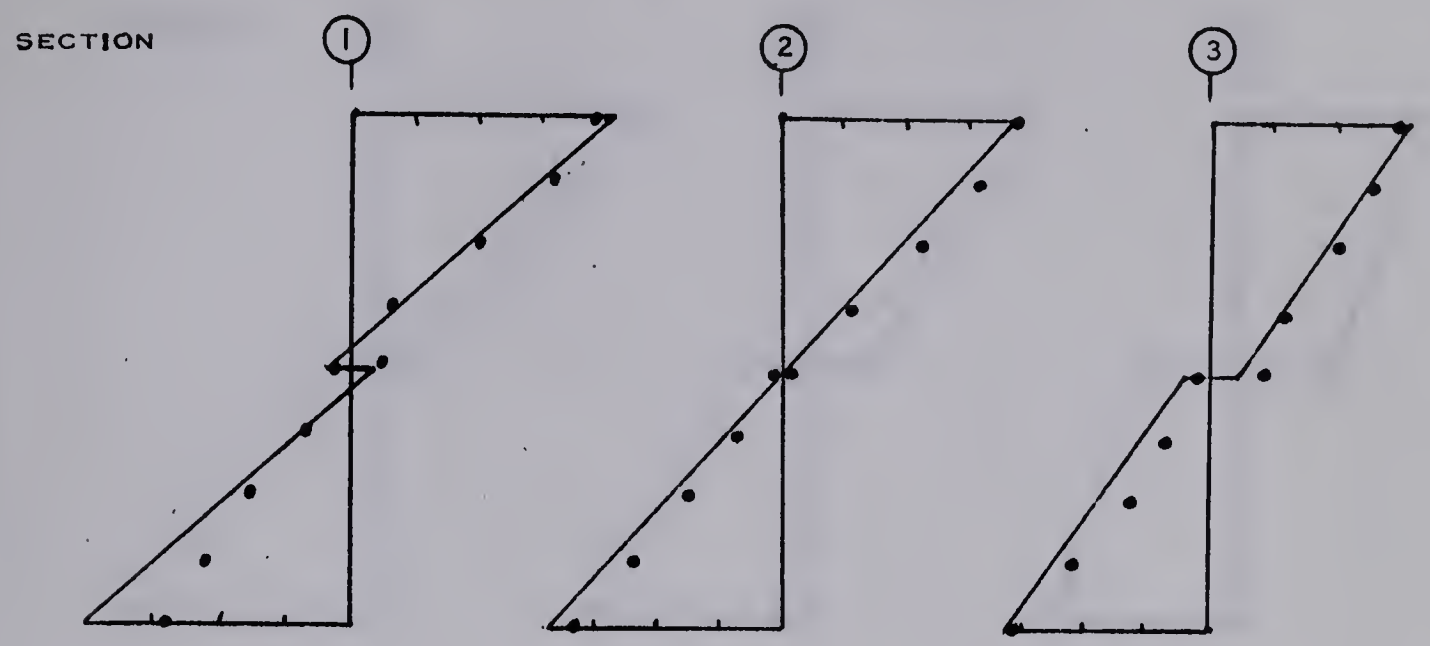

BEAM XZ-4 @ P = 7000. LBS.

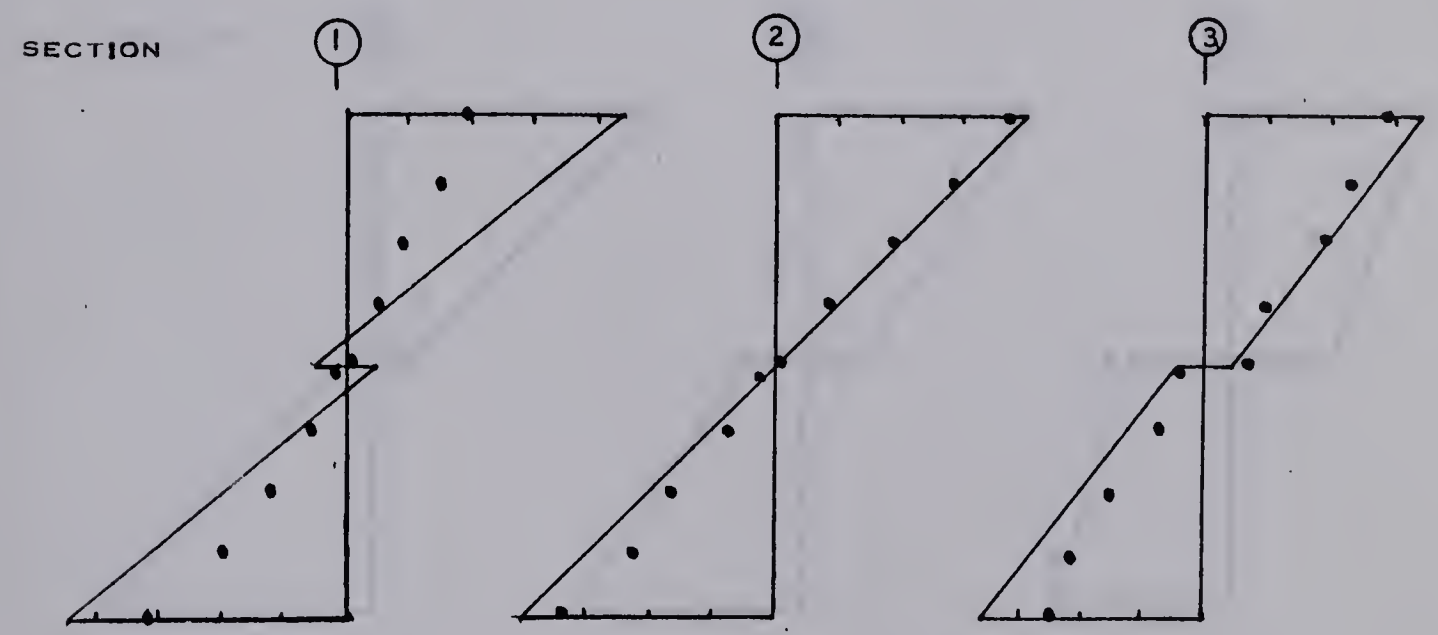

BEAM XY-41 @ P = 7500. LBS.

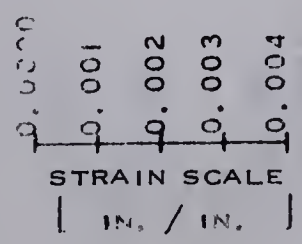

THEORETICAL STRAINS

EXPERIMENTAL STRAINS

FIGURE 6.14

EXPERIMENTAL AND THEORETICAL STRAIN DISTRIBUTIONS FOR A 2'-0 LONG DELAMINATION

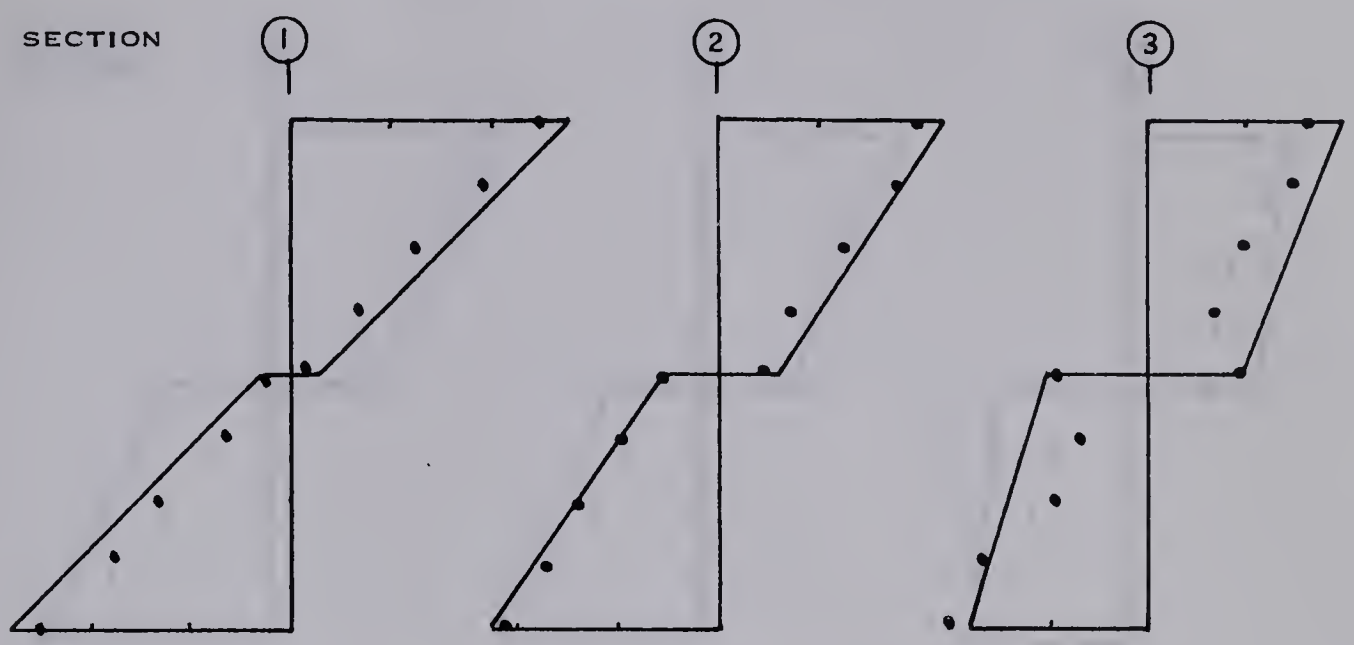

BEAM XZ-42 @ P = 6000. LBS.

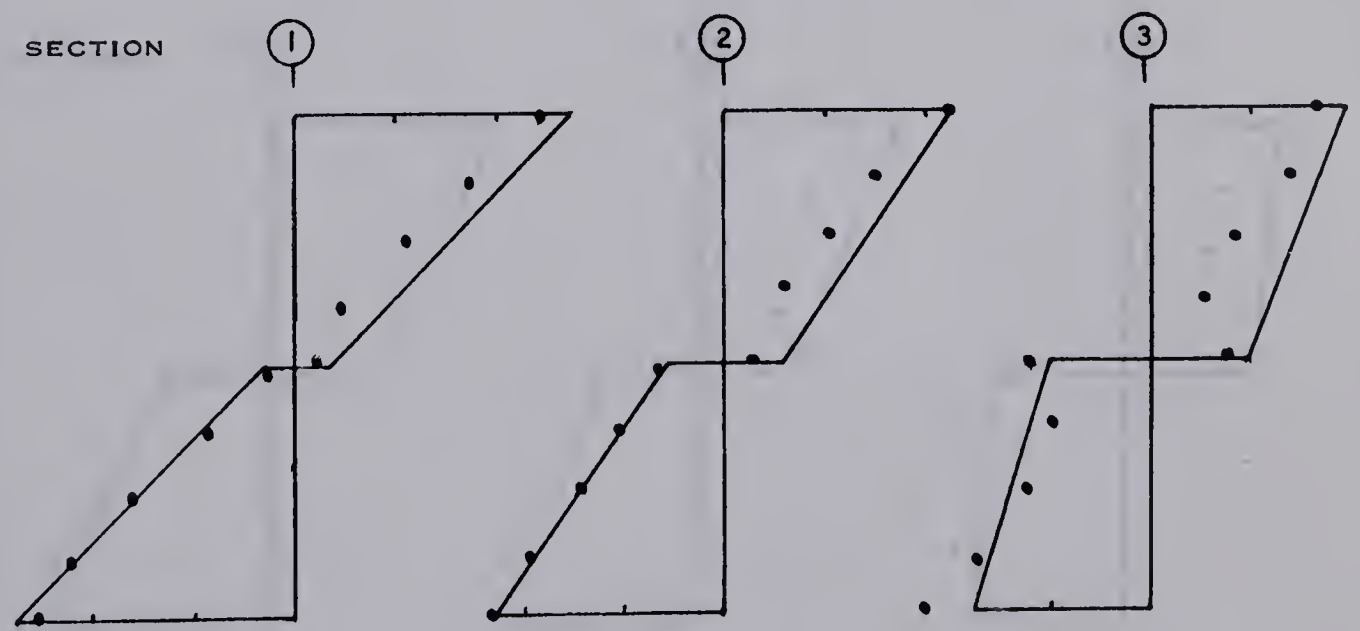

BEAM XY-42 @ P = 6000. LBS.

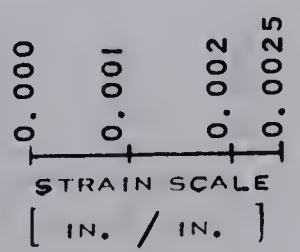

— THEORETICAL STRAINS

• EXPERIMENTAL STRAINS

FIGURE 6.15

EXPERIMENTAL AND THEORETICAL STRAIN DISTRIBUTIONS FOR A 2'-6" LONG DELAMINATION

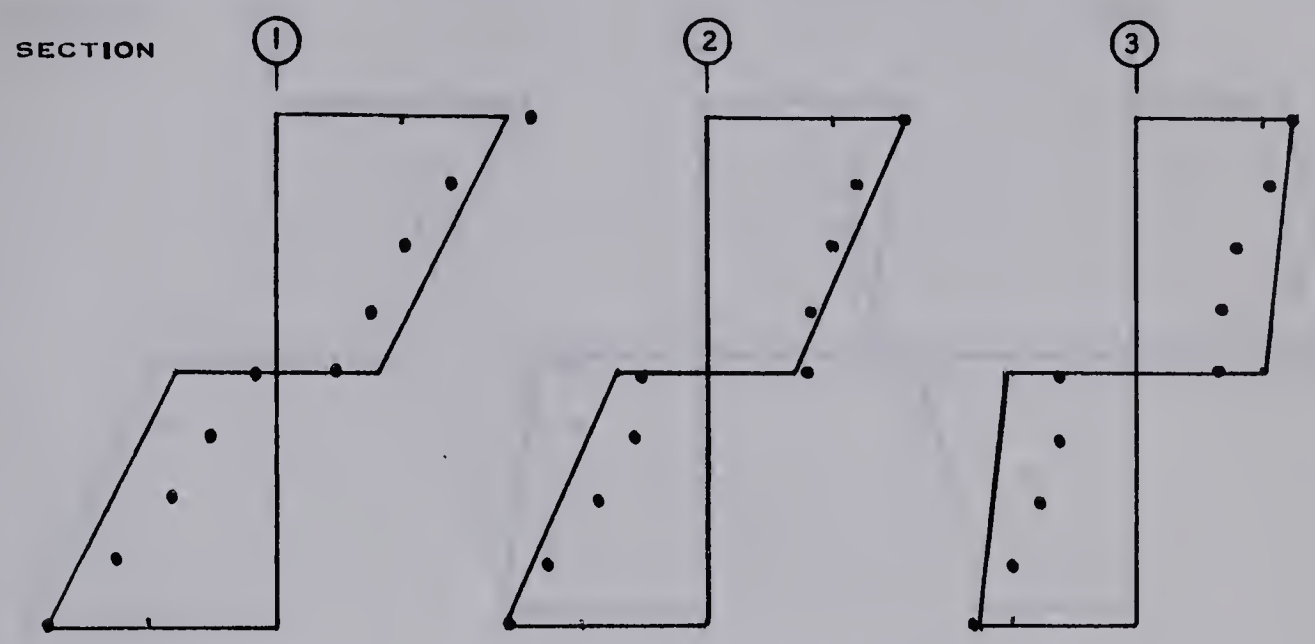

BEAM XZ-425 @ P = 5000. LBS.

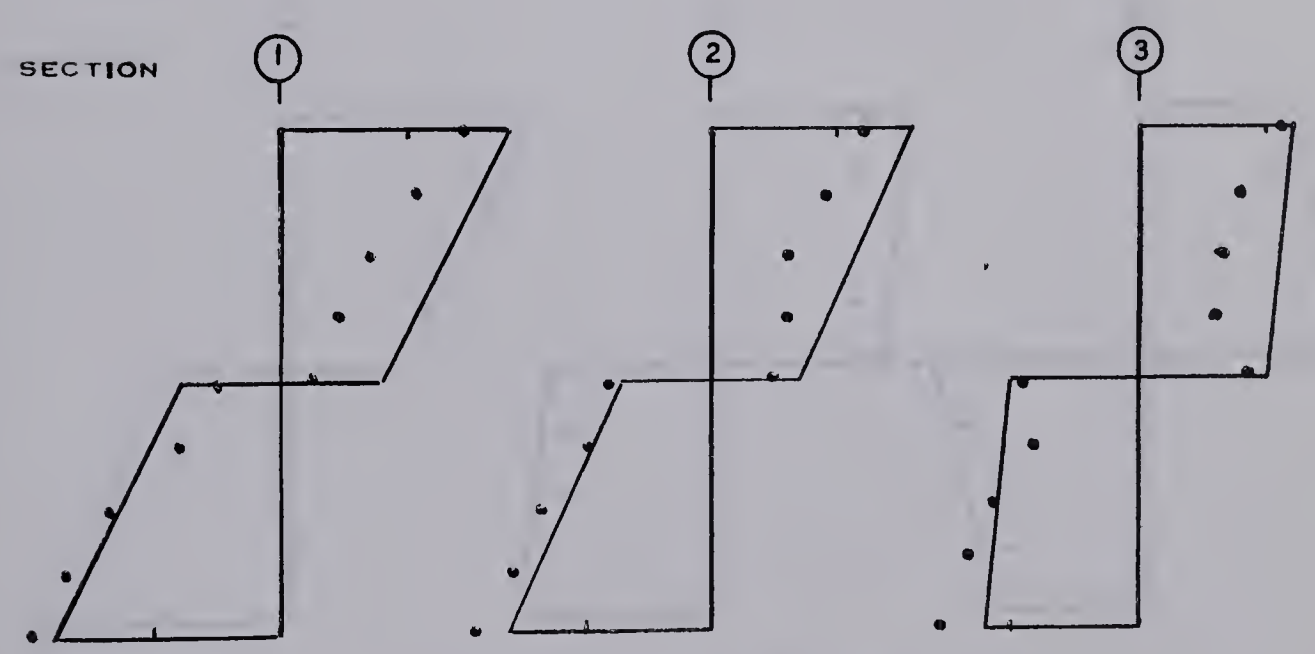

BEAM XY-425 @ P = 5000. LBS.

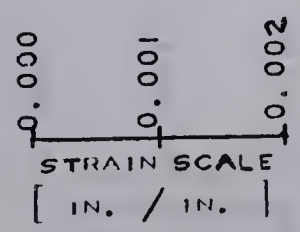

—— THEORETICAL STRAINS

• EXPERIMENTAL STRAINS

FIGURE 6.16

EXPERIMENTAL AND THEORETICAL STRAIN DISTRIBUTIONS FOR A 3'-0 LONG DELAMINATION

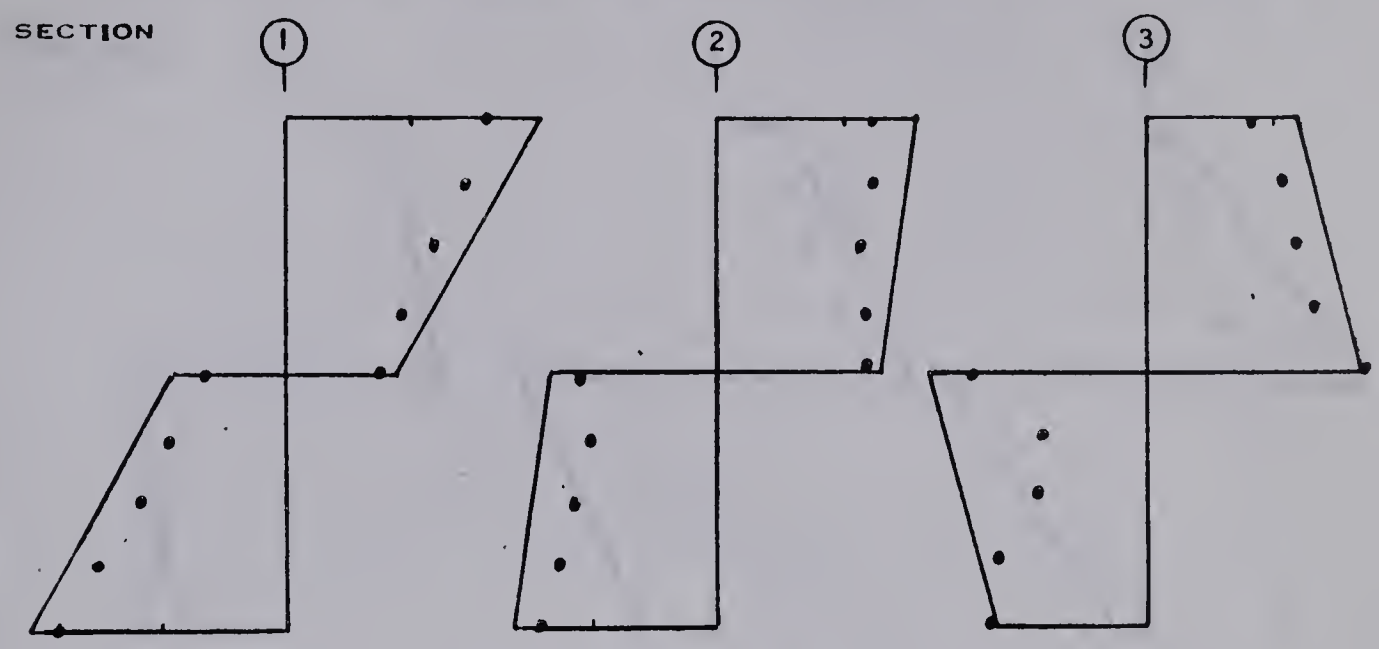

BEAM XZ-43 @ P = 5000. LBS.

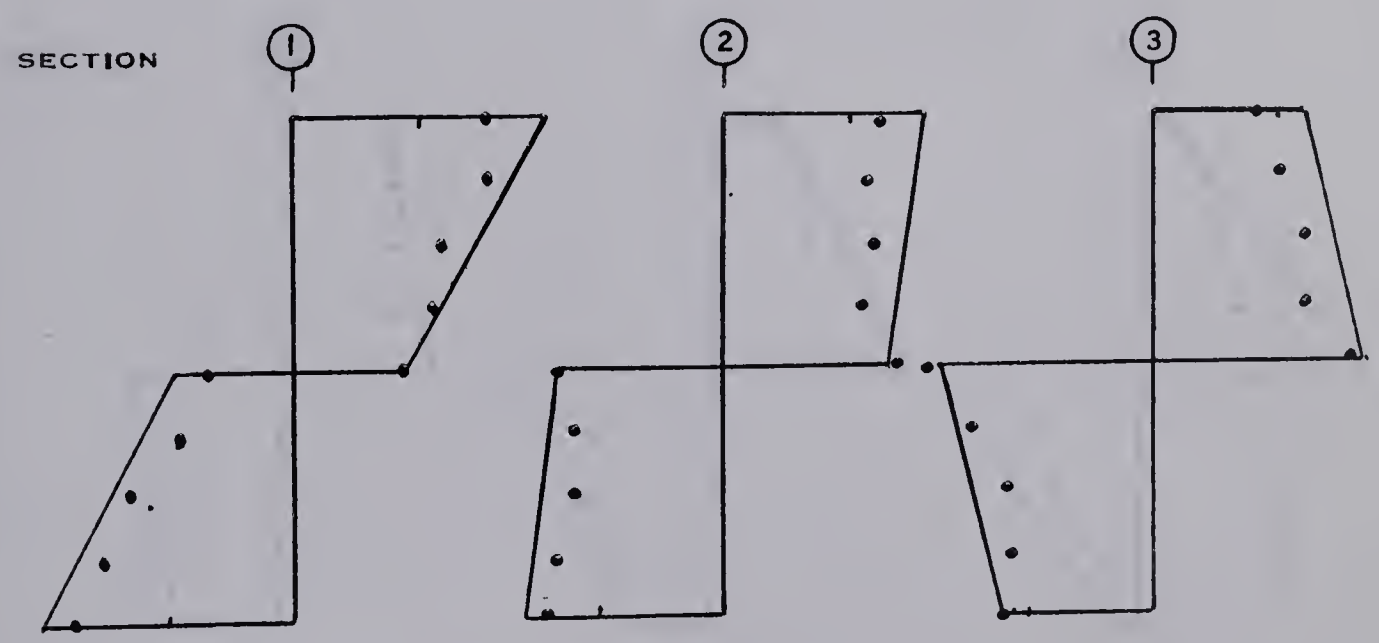

BEAM XY-43 @ P = 5000. LBS.

— THEORETICAL STRAINS

• EXPERIMENTAL STRAINS

FIGURE 6.17

EXPERIMENTAL AND THEORETICAL STRAIN DISTRIBUTIONS FOR A 4'-0 LONG DELAMINATION

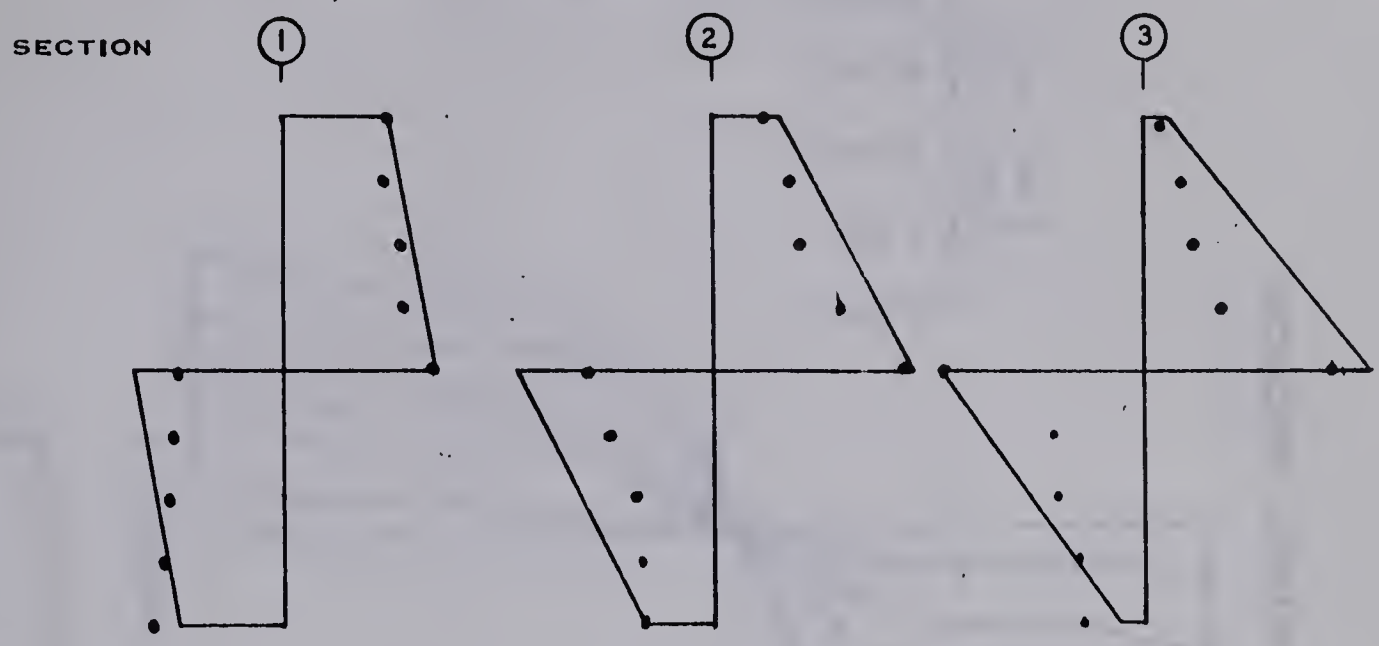

BEAM XZ-44 @ P = 4000. LBS.

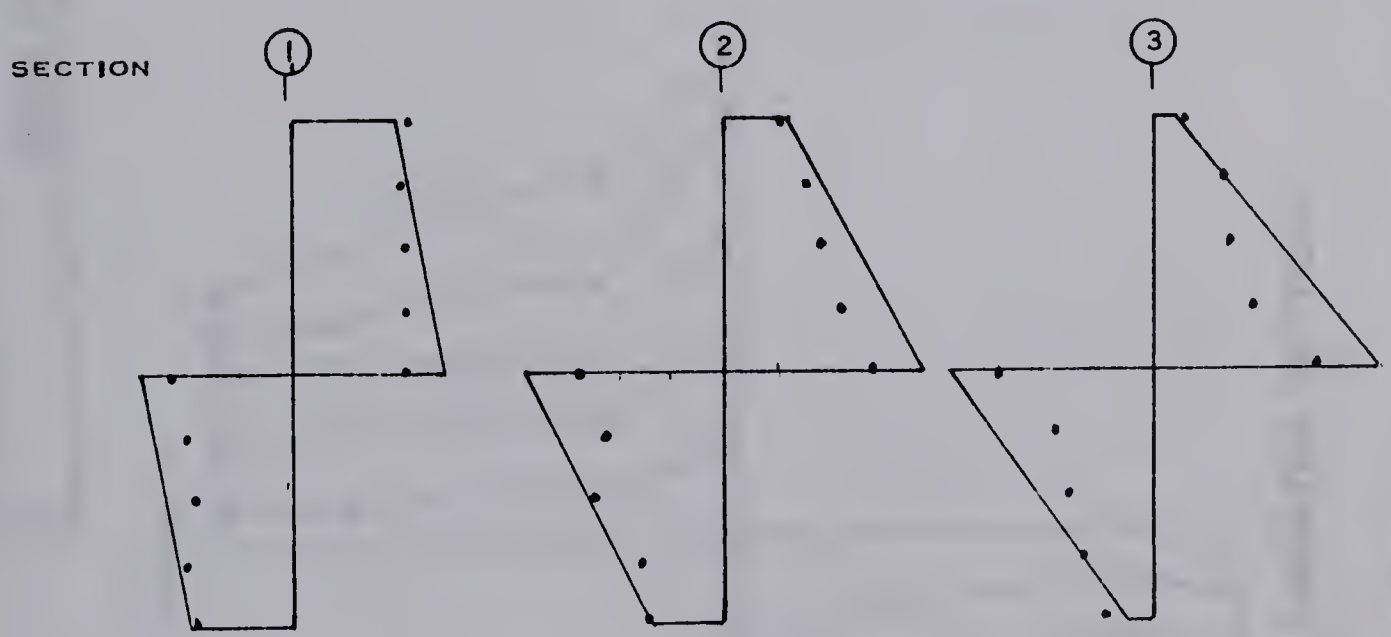

BEAM XY-44 @ P = 4000. LBS.

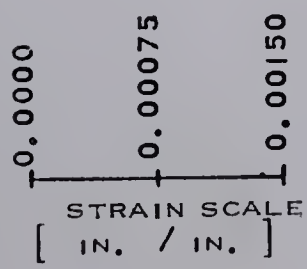

THEORETICAL STRAINS

EXPERIMENTAL STRAINS

FIGURE 6.18

STRAIN DISTRIBUTIONS AT SUCCESSIVE LOADS
BEAM XY - 43

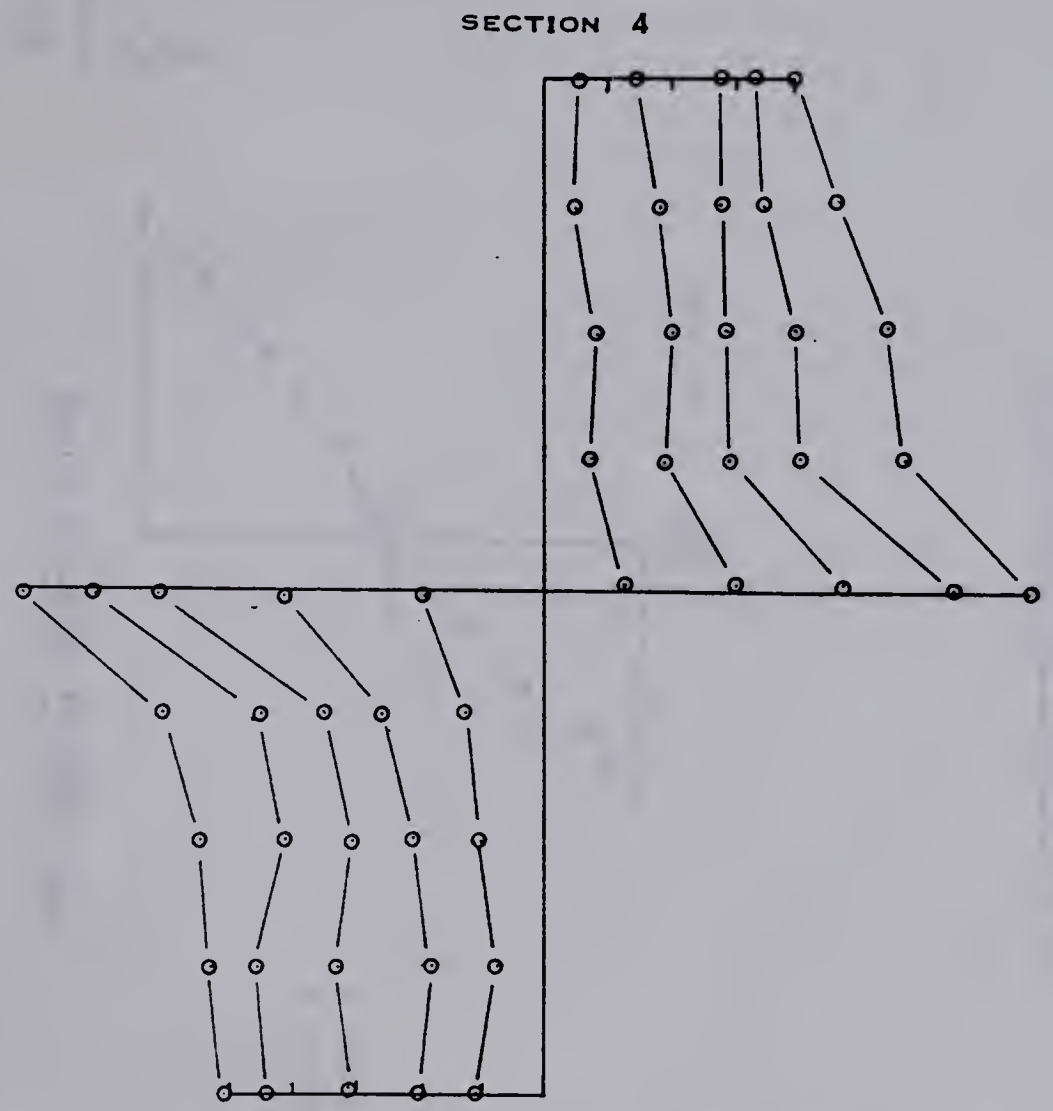

[A] DELAMINATED SECTION

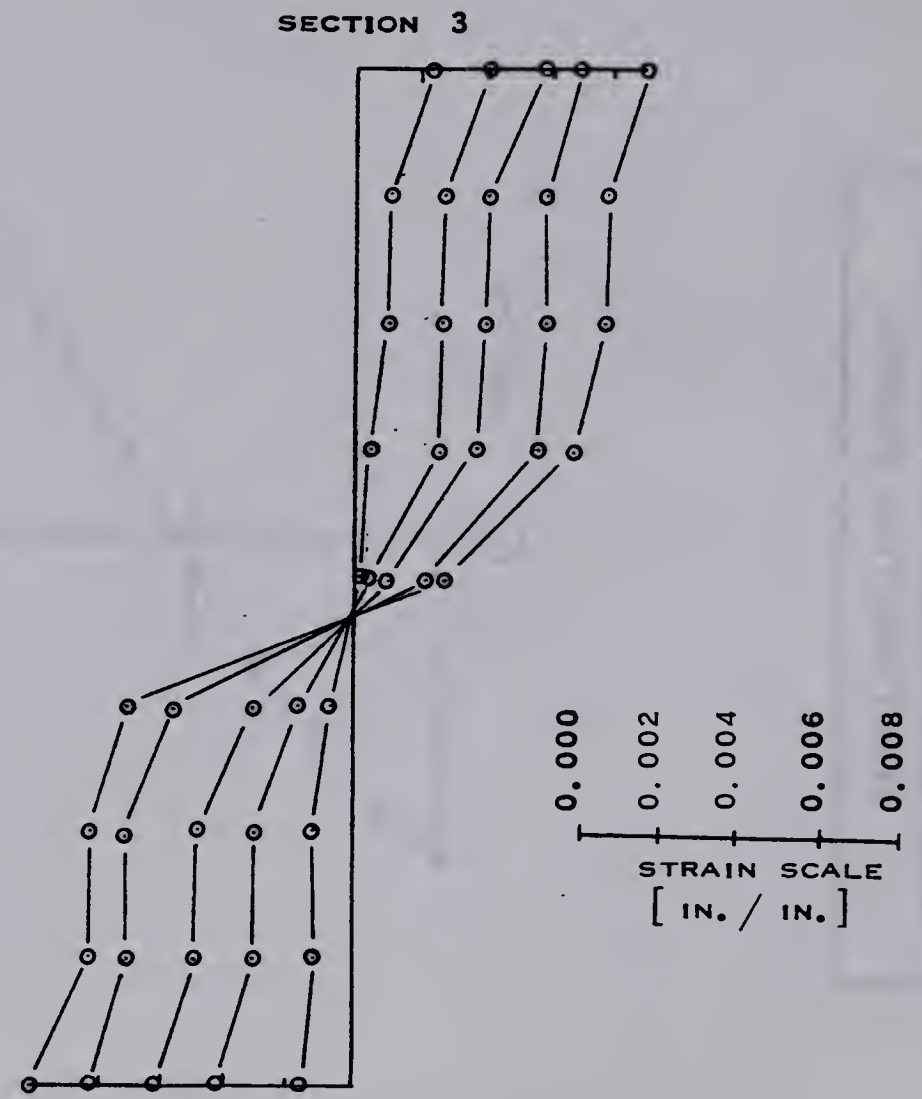

[B] INTACT SECTION

NOTES

1. STRAINS ARE FOR P = 1.0, 2.0, 3.0, 4.0, 5.0 KIPS.
2. DELAMINATION LENGTH = 3' - 0
3. D/L RATIO = 0.486

FIGURE 6.19

COMPARATIVE DEMEC AND SR-4 STRAIN DISTRIBUTIONS

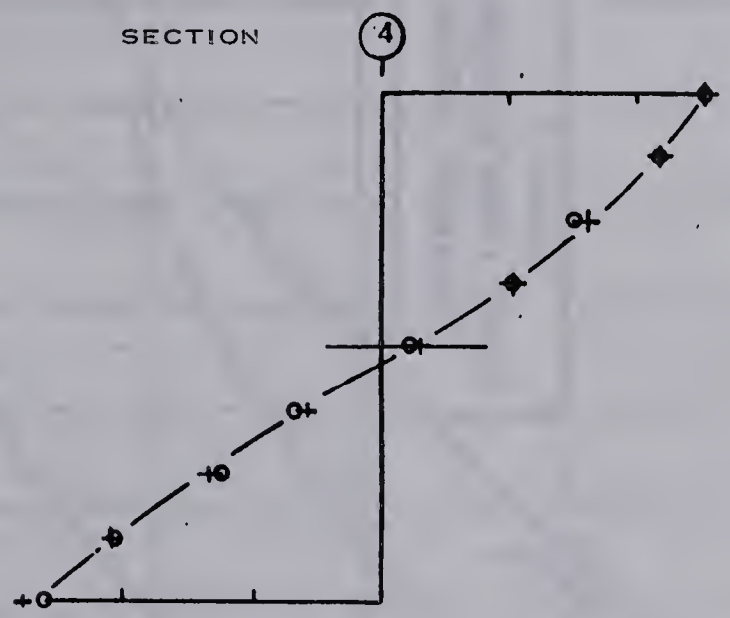

BEAM XZ-41 @ P=7000. LBS.

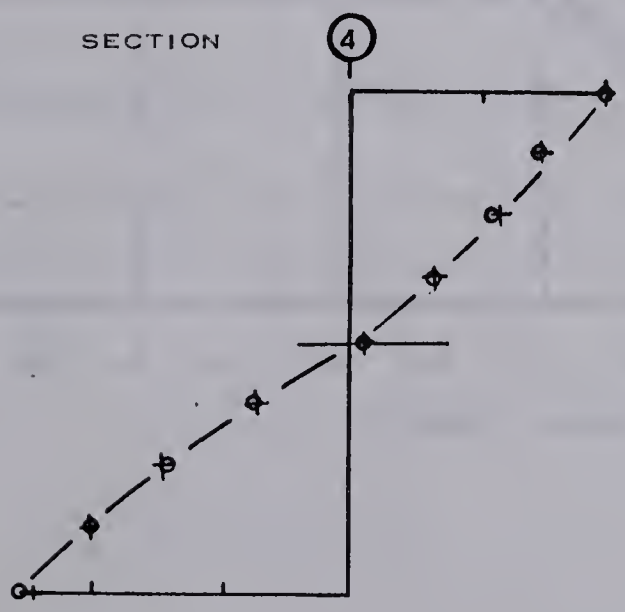

+ SR-4 STRAIN
o DEMEC STRAIN

0.000 0.001 0.002

STRAIN SCALE
[IN./IN.]

BEAM XZ-42@ P=7500. LBS.

FIGURE 6.20

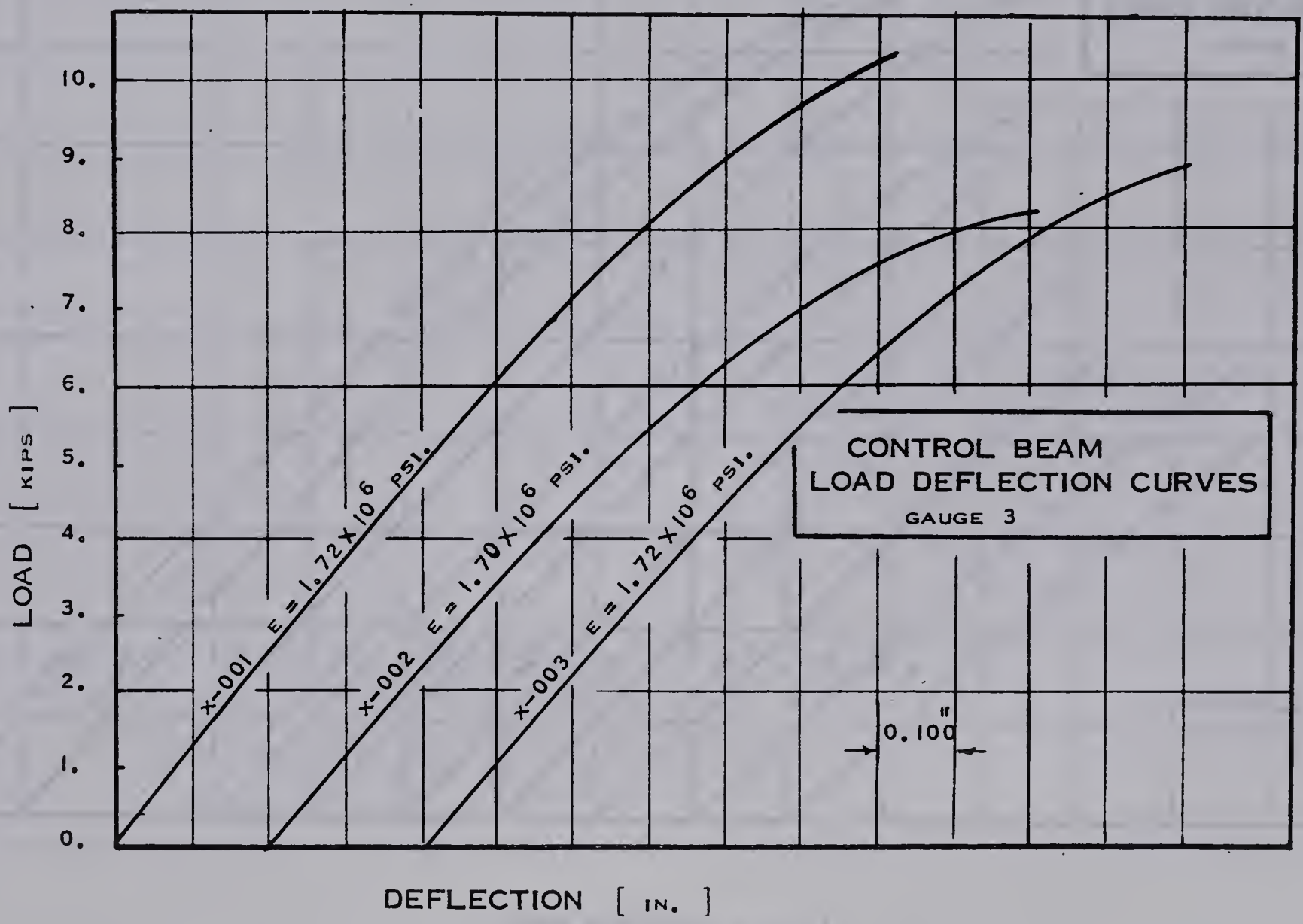
CONTROL BEAM
LOAD DEFLECTION CURVES
GAUGE 3
x-001 E = 1.72 X 10⁶ PSI.
x-002 E = 1.70 X 10⁶ PSI.
x-003 E = 1.72 X 10⁶ PSI.
0.100"
LOAD [KIPS]
DEFLECTION [IN.]
0.
1.
2.
3.
4.
5.
6.
7.
8.
9.
10.

FIGURE 6.21

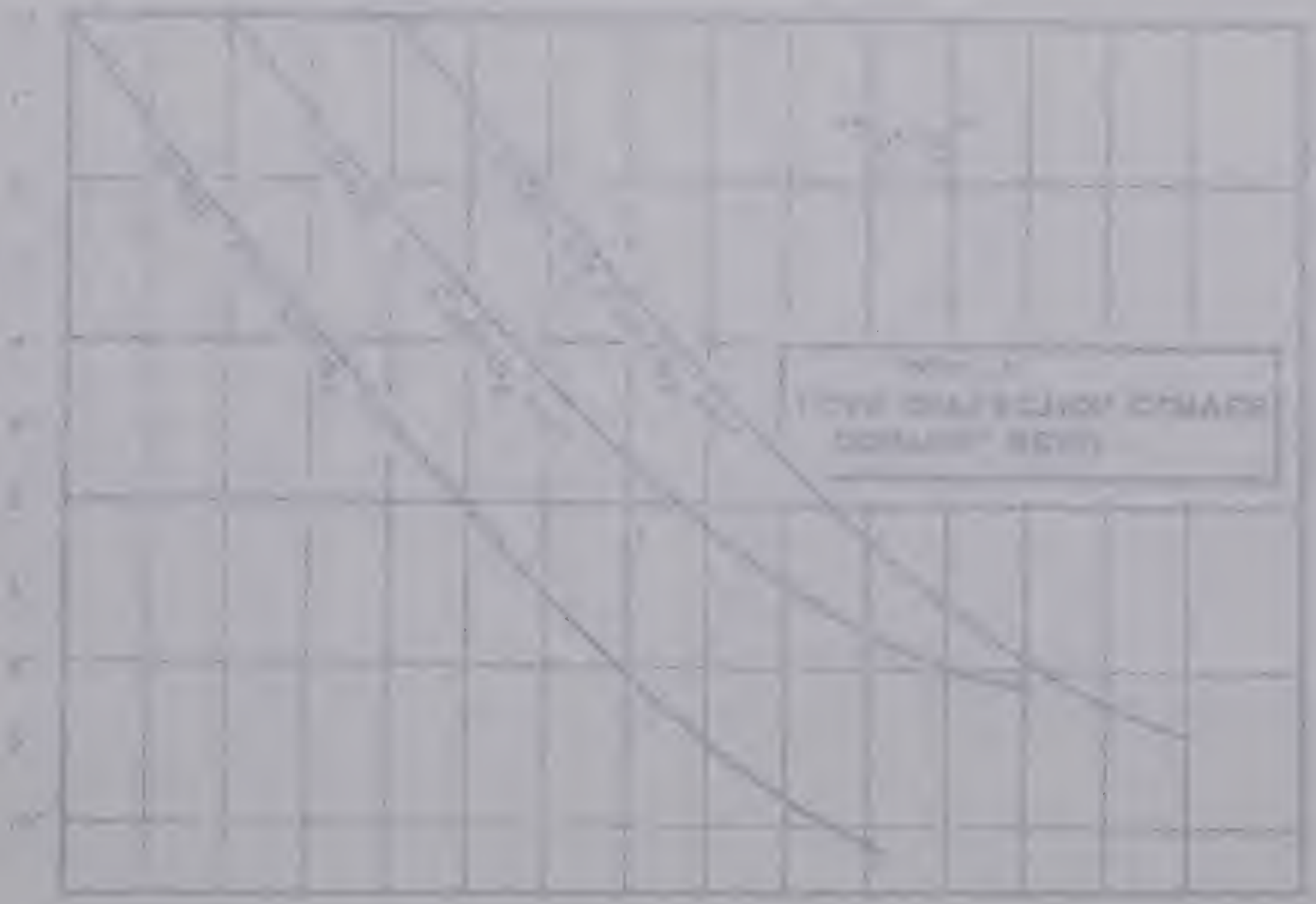

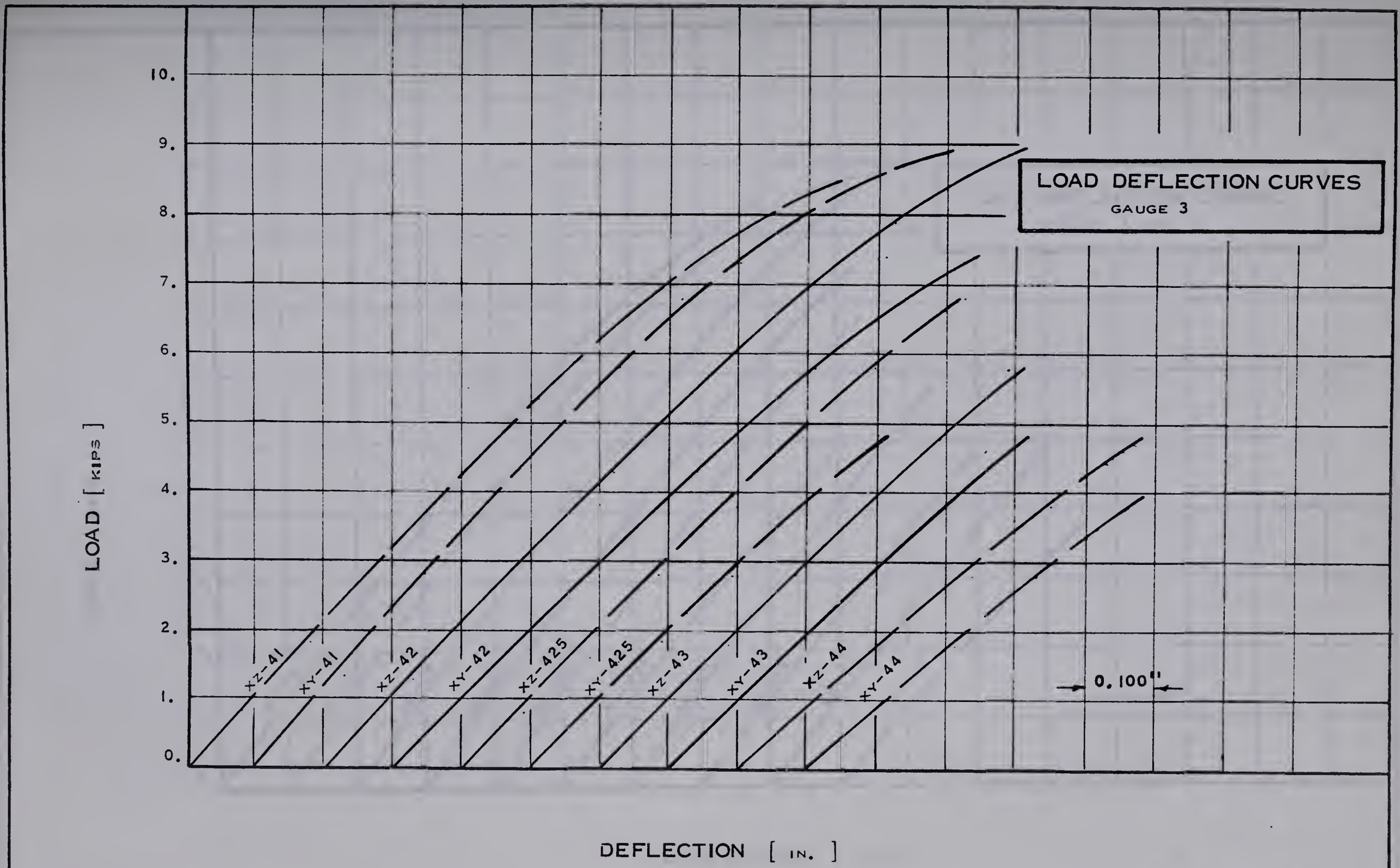
LOAD DEFLECTION CURVES
GAUGE 3
LOAD [KIPS]
10.
9.
8.
7.
6.
5.
4.
3.
2.
1.
0.
XZ-41
XY-41
XZ-42
XY-42
XZ-425
XY-425
XZ-43
XY-43
XZ-44
XY-44
0.100"
DEFLECTION [IN.]

FIGURE 6.22

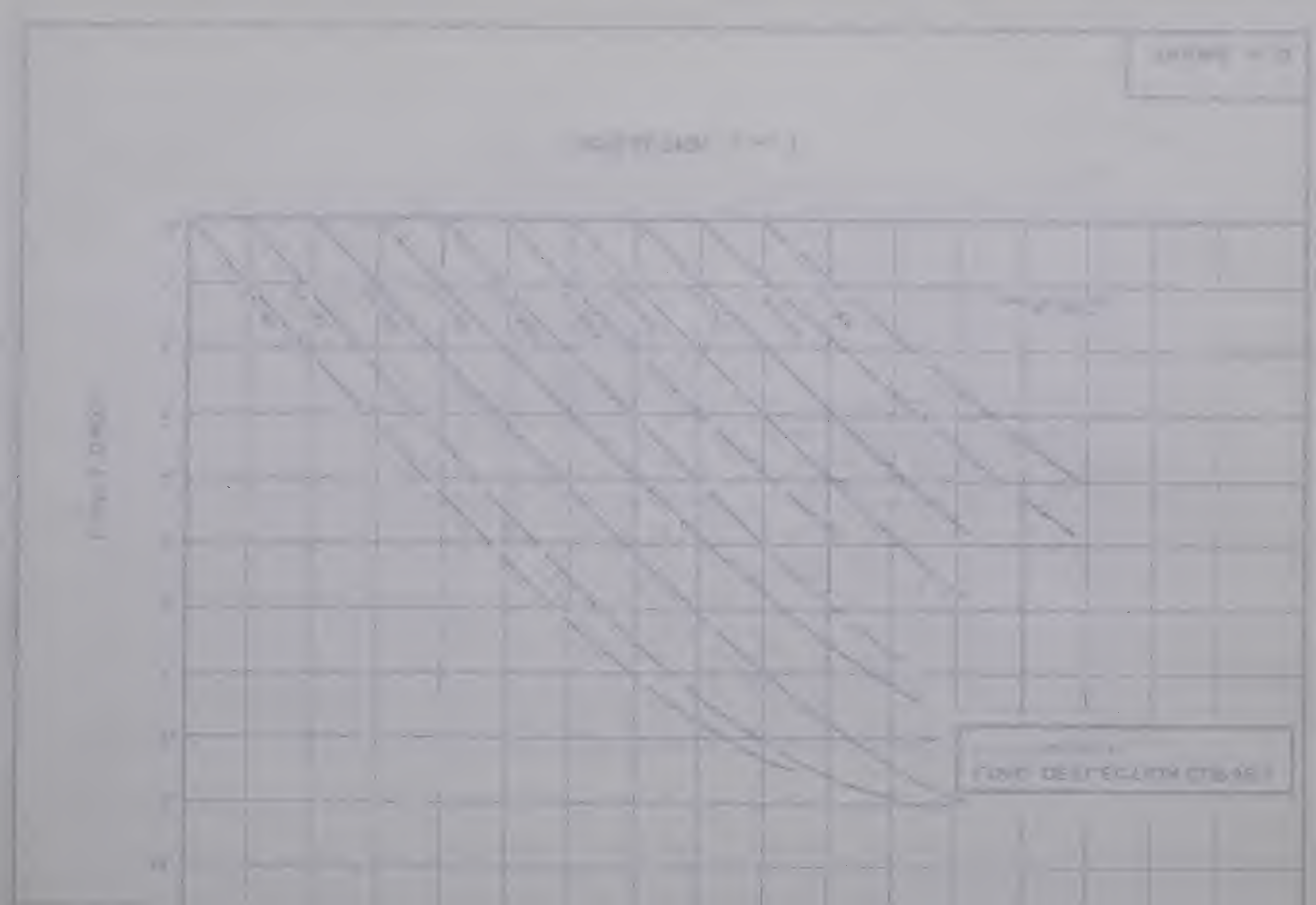

LOAD DEFLECTION CURVES

GAUGES 2 AND 4

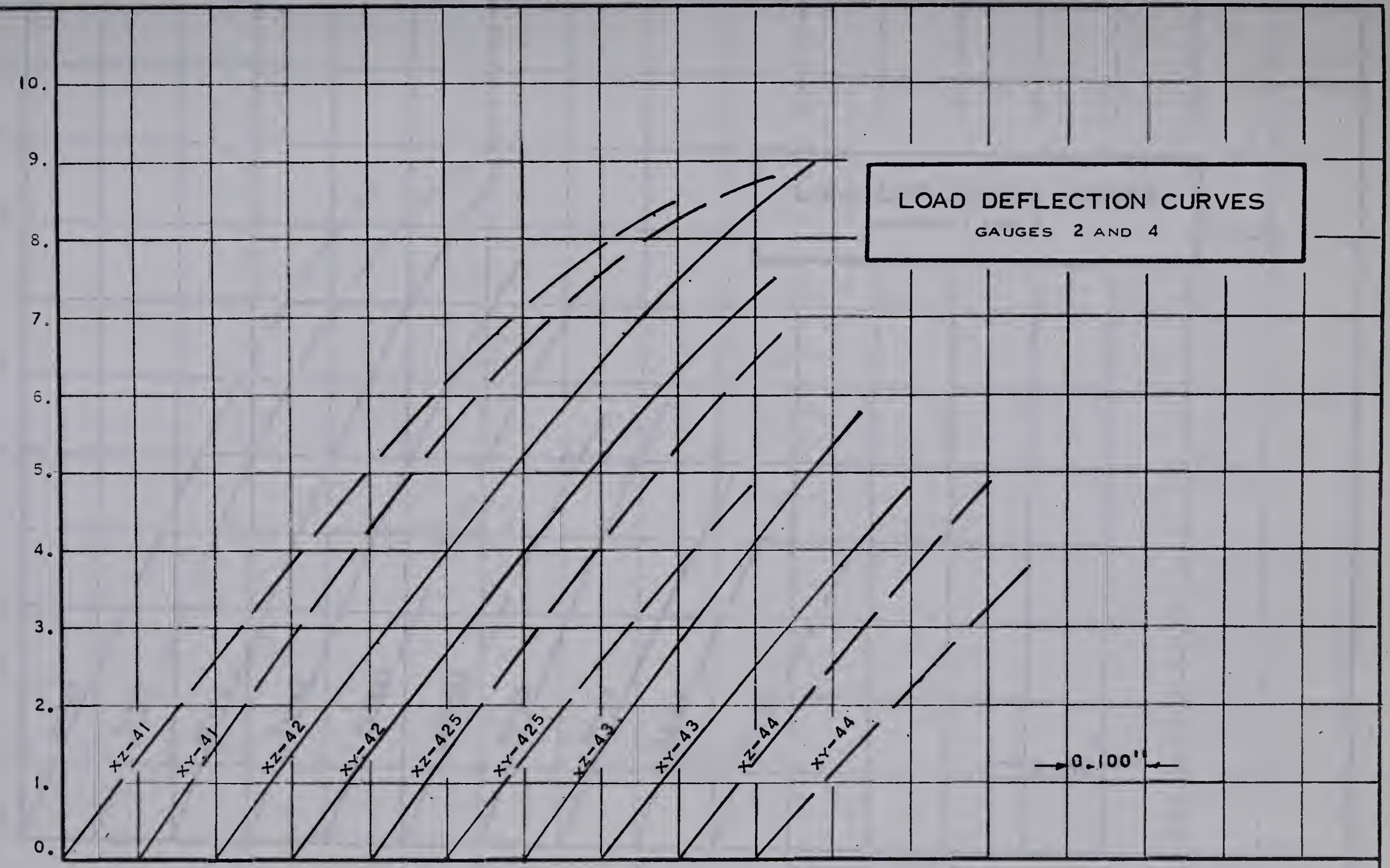

FIGURE 6.23

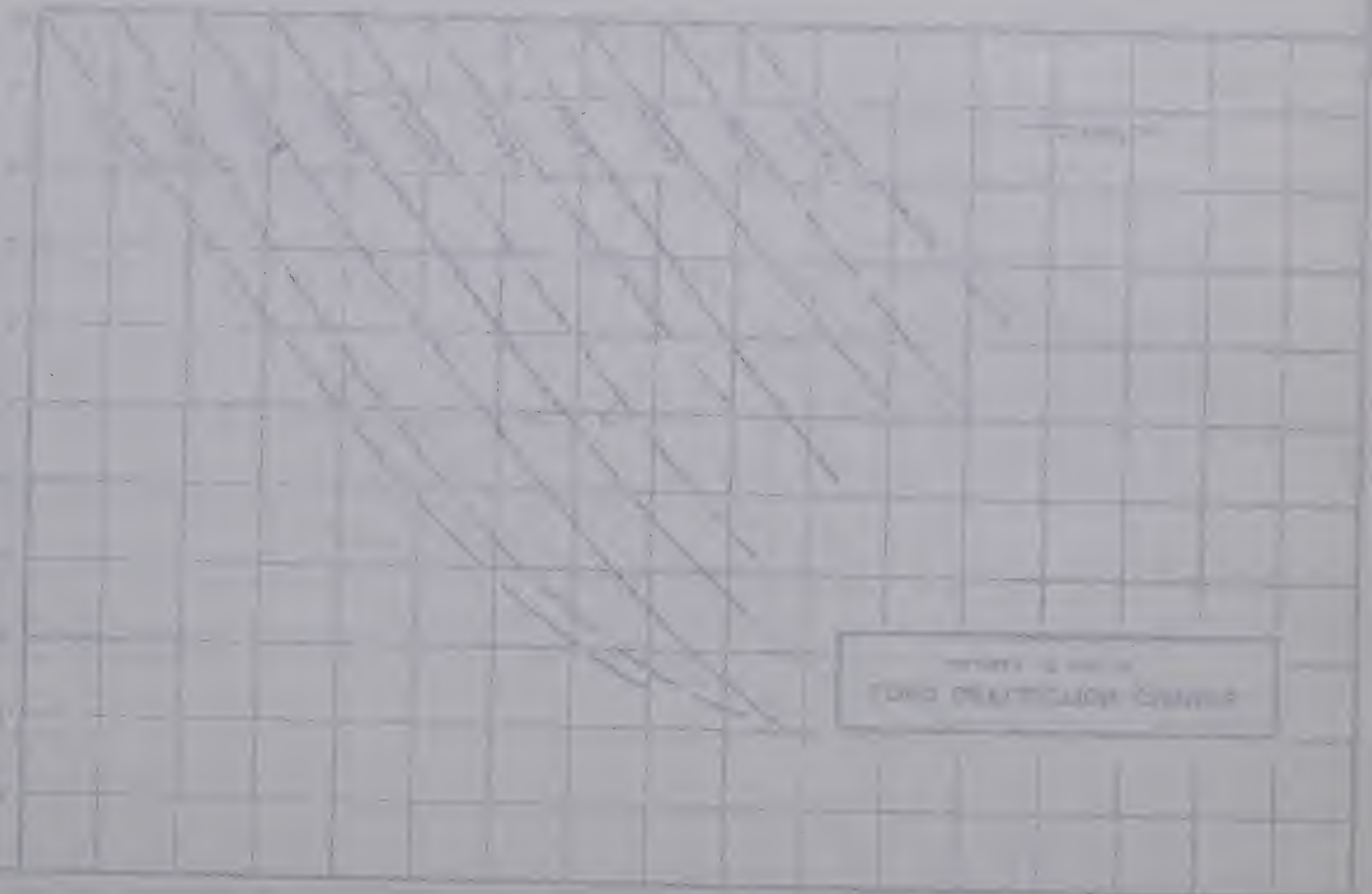

LOAD DEFLECTION CURVES

GAUGES 1 AND 5

FIGURE 6.24

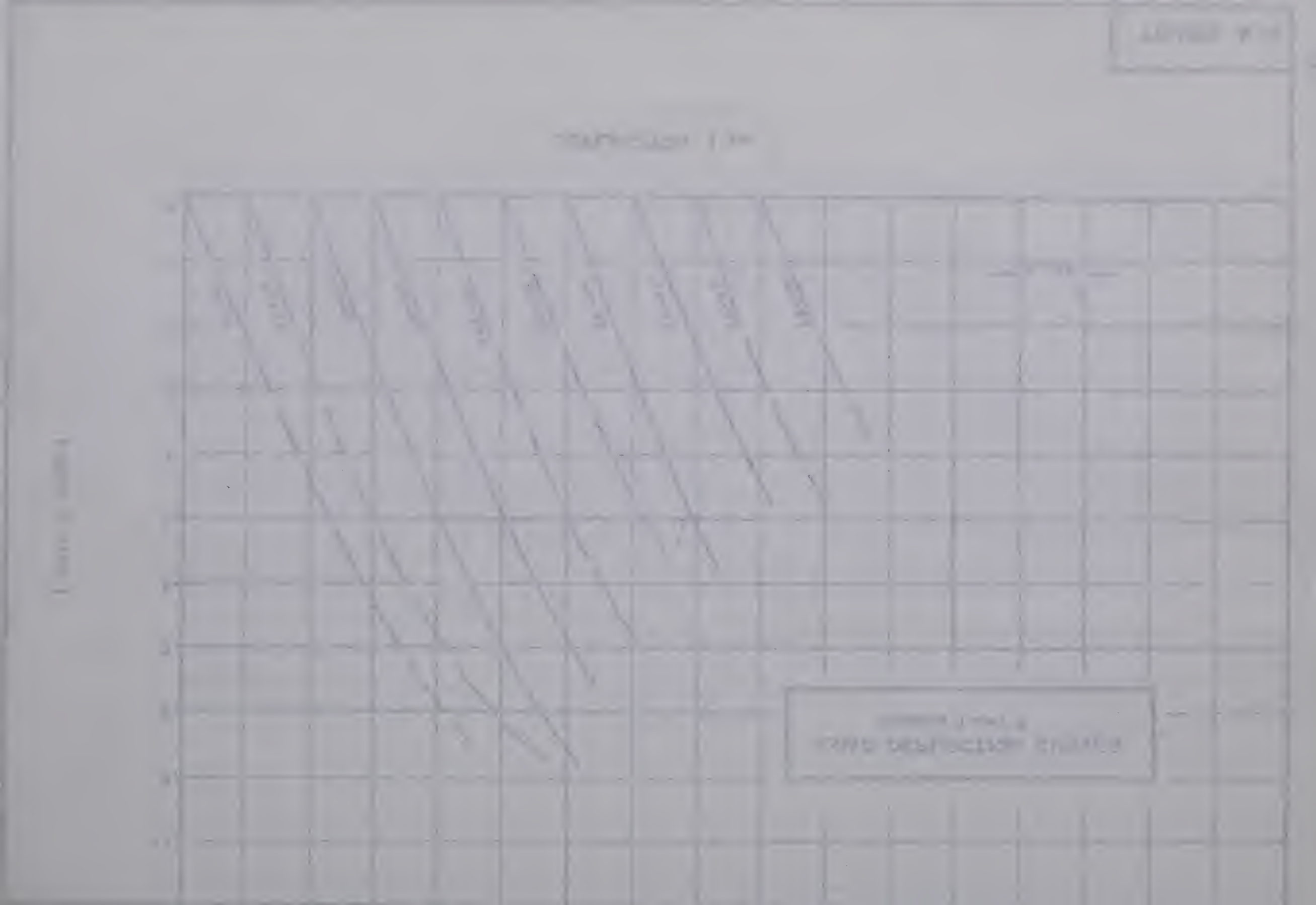

COMPUTED HORIZONTAL SHEAR STRESS DISTRIBUTIONS

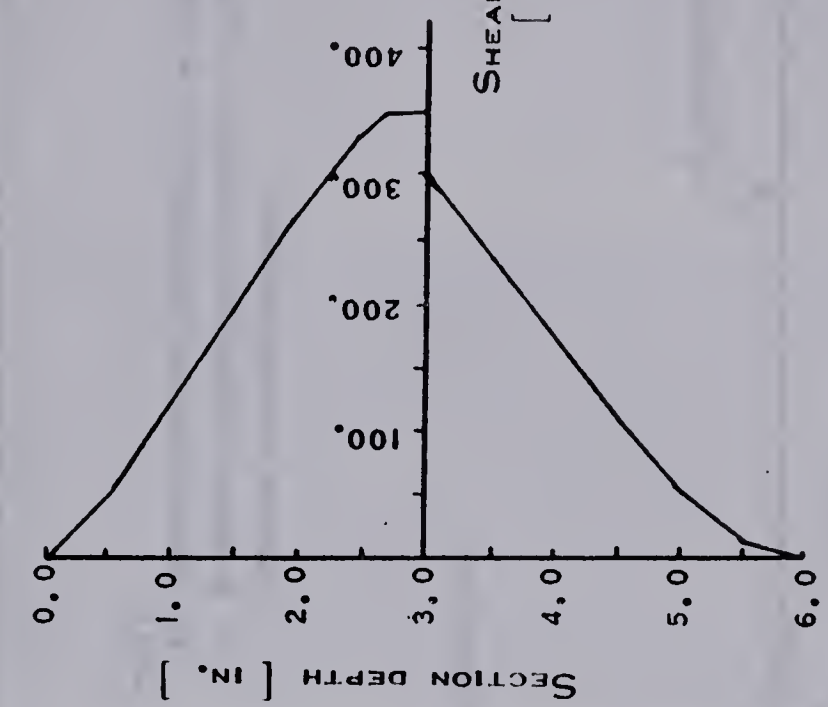

Beam XZ - 44 @ P 5000. lbs.
section 5 - 6

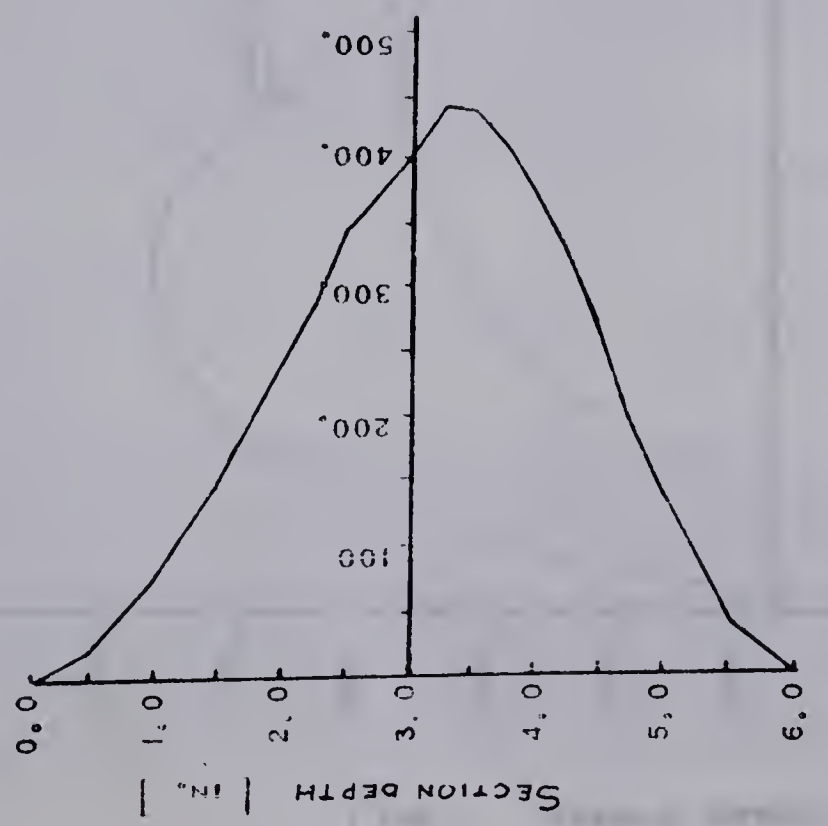

Beam XY - 425 @ P 5000. lbs.
section 5 - 6

FIGURE 6.25

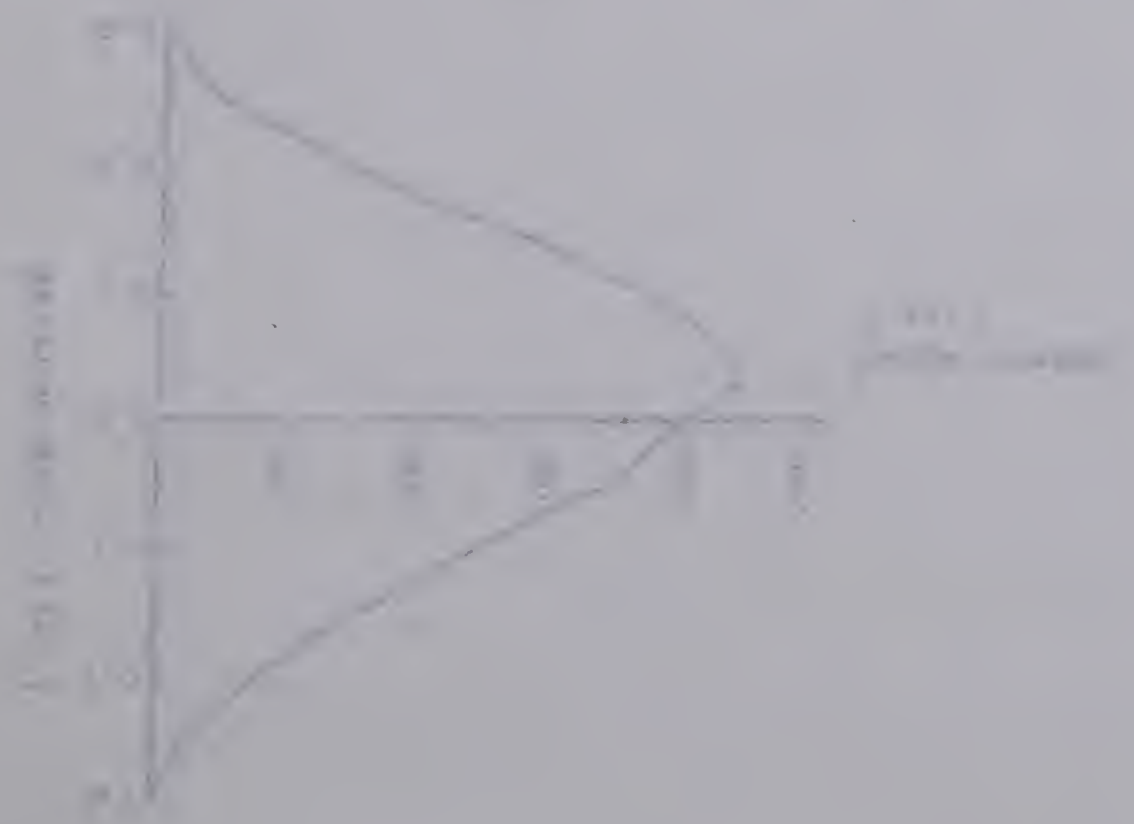

DISTRIBUTIONS OF HORIZONTAL SHEAR STRESS

NOTE
1. DISTRIBUTIONS FOR BEAM XY – 425 @ P=5000. LBS.
2. ● SHEAR STRESSES OBTAINED FROM EXPERIMENTAL STRAIN DISTRIBUTIONS.

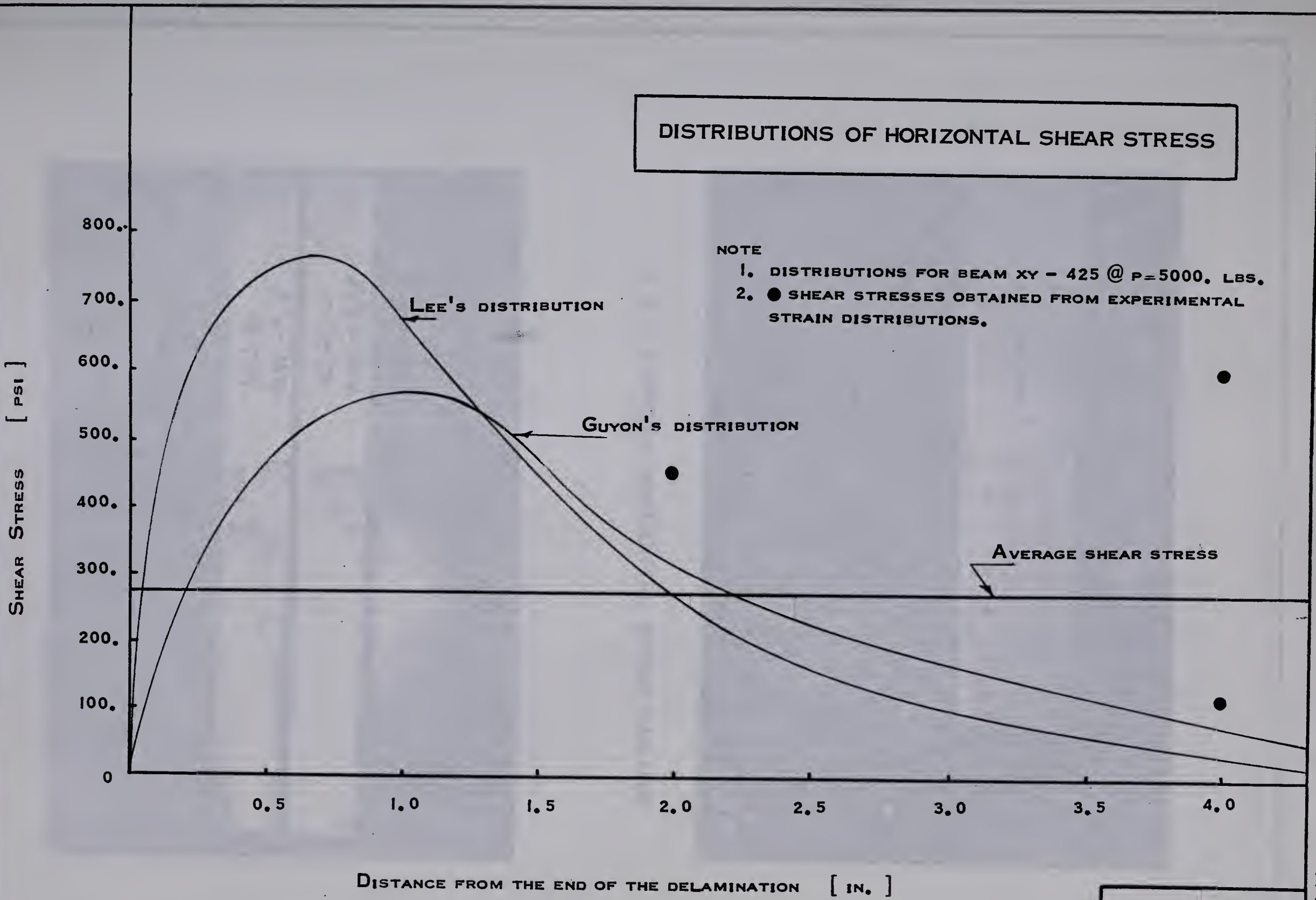

FIGURE 6.26

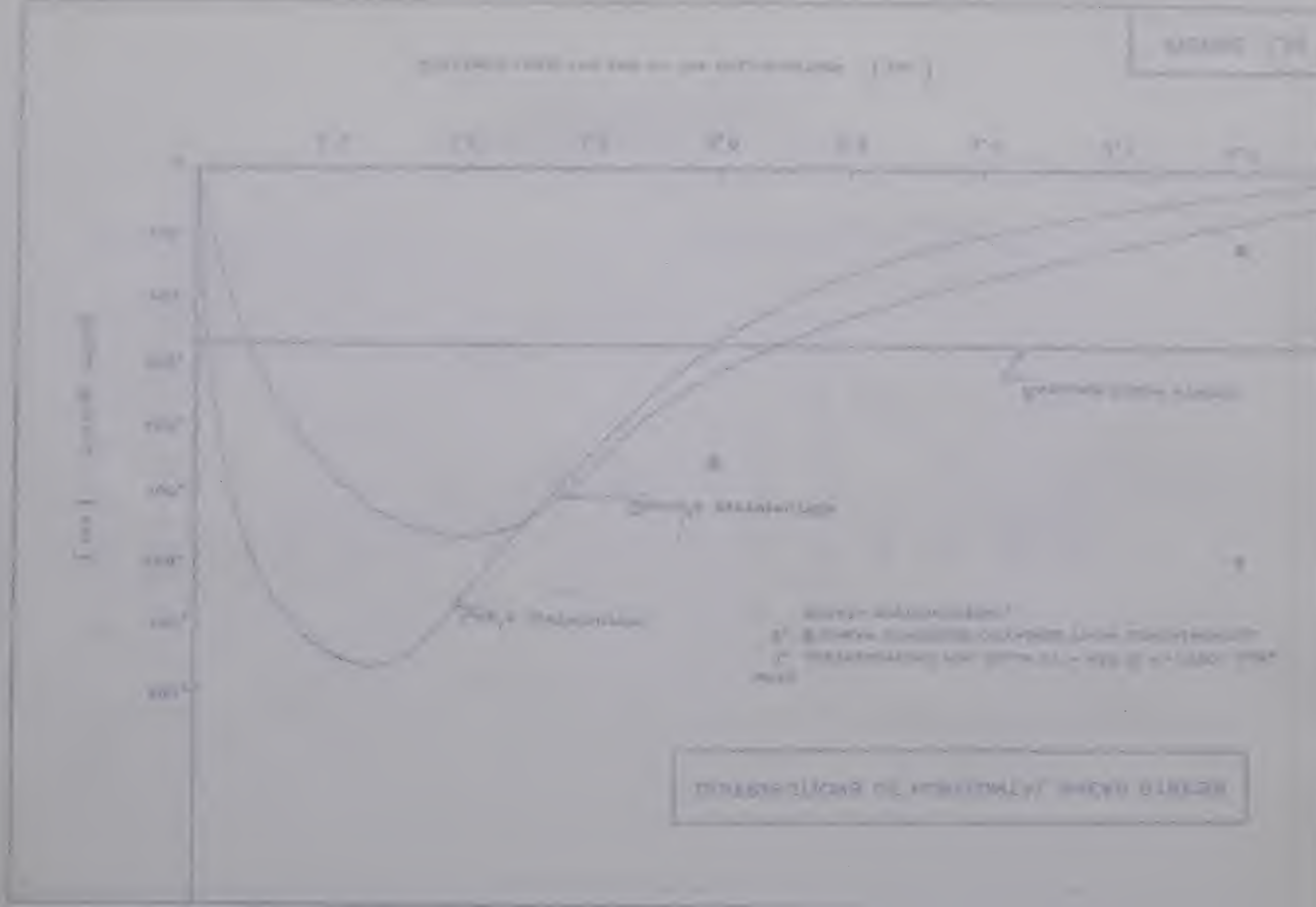

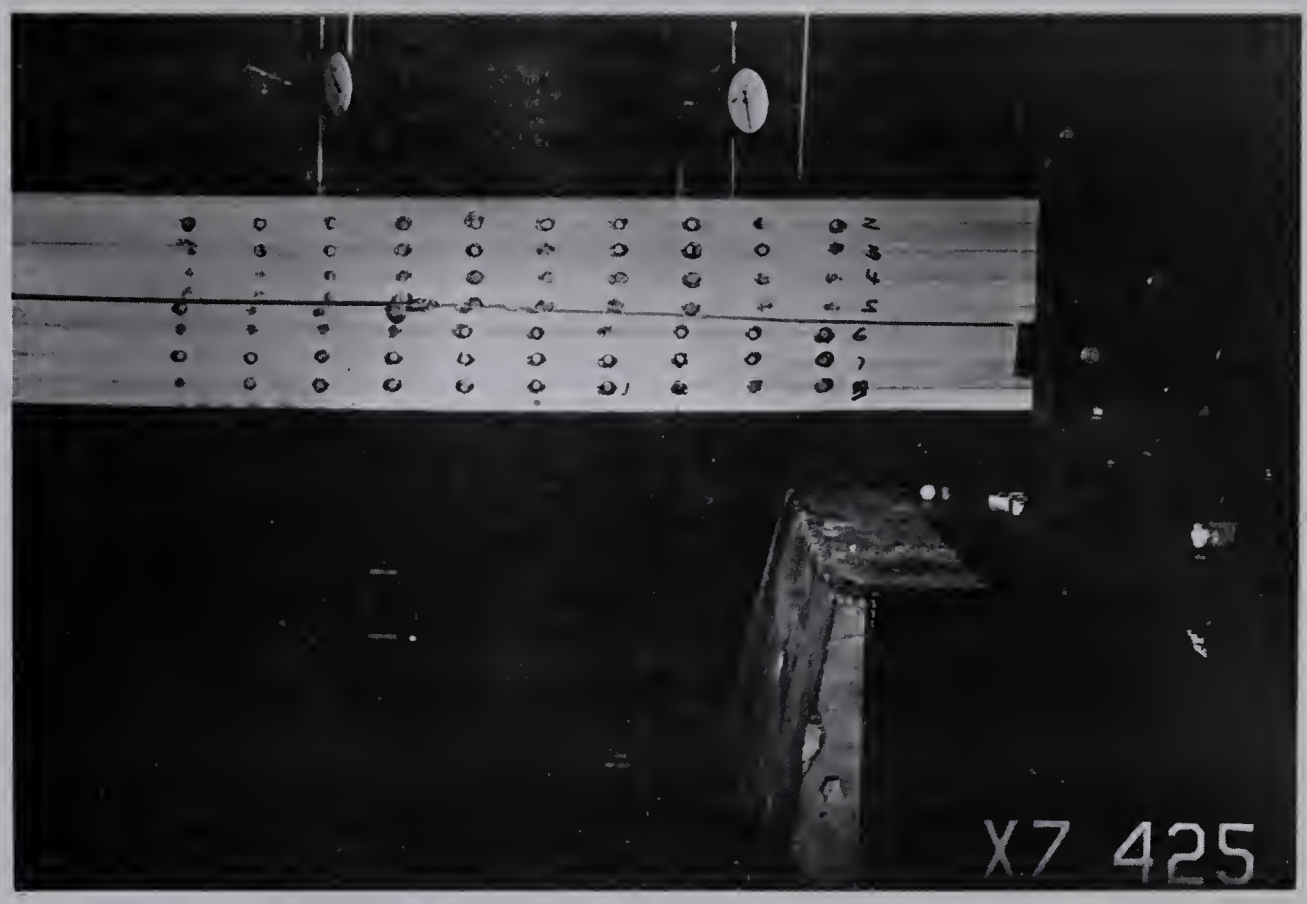

[A] TYPICIAL HORIZONTAL SHEAR FAILURE

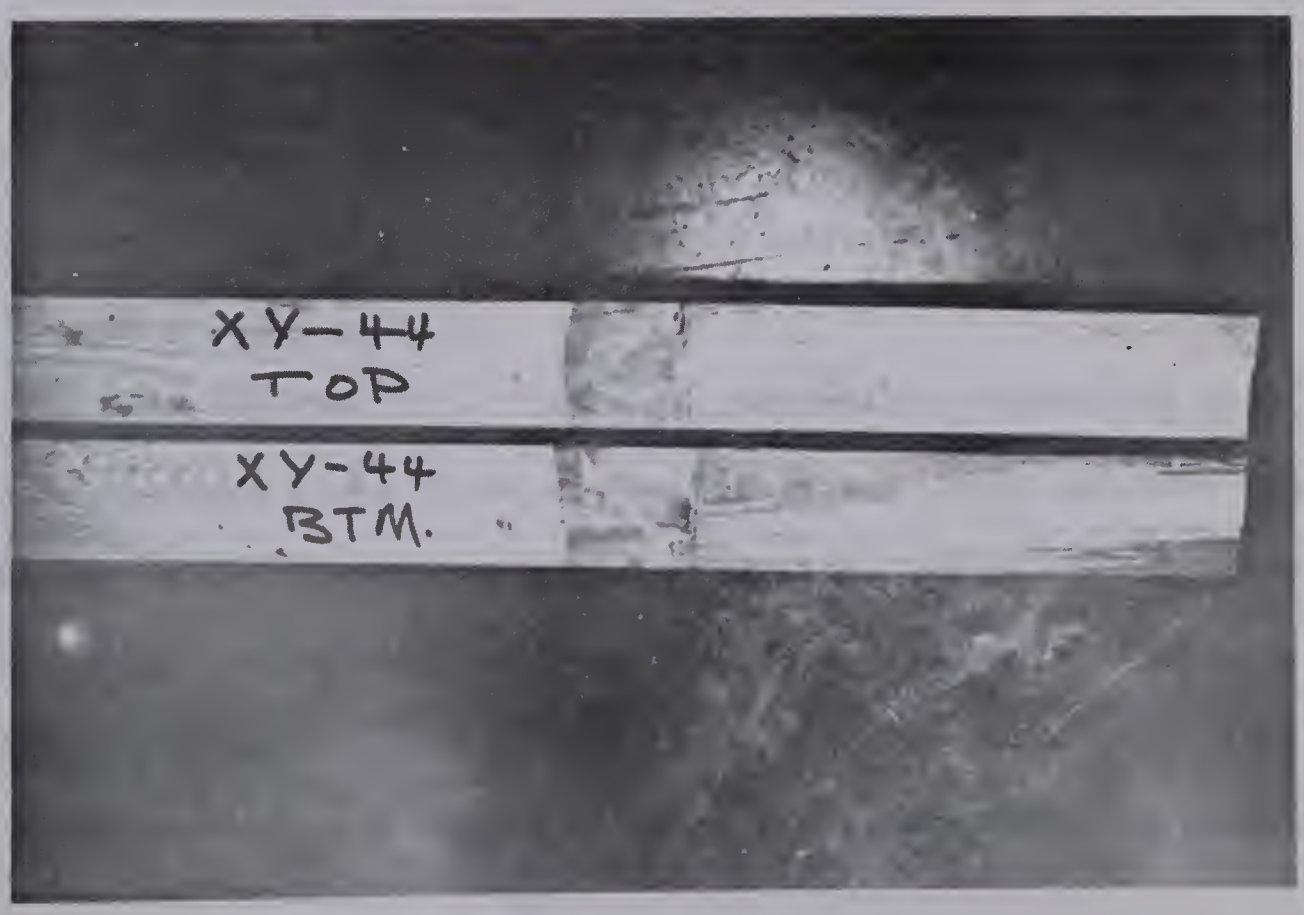

[B] HORIZONTAL SHEAR FAILURE SURFACE

PLATE 6.1

CHAPTER VII

DISCUSSION OF TEST RESULTS

7-1 Material Properties

Examination of the tension and compression test results (FIGURES 6.1, 6.2 and TABLE VI-1) indicate a slight difference exists between the average compressive and tensile moduli of elasticity parallel to grain. Tests performed at the United States Forest Products Laboratory have also showed a difference in the tensile and compressive moduli of elasticity. However, this difference was insignificant for Douglas Fir.

The value of the average modulus of elasticity (1.72×10^6 psi) for the control beams, computed from the initial tangents to the load-deflection curves, is lower than the moduli of elasticity determined from the tension and compression tests. Examination of FIGURES 6.14 to 6.18 illustrating theoretical and experimental strain distributions at delaminated sections imply a modulus of elasticity between 1.7×10^6 psi and 2.1×10^6 psi is appropriate.

The moisture content of the beam laminations determined upon completion of the beam tests agree exceptionally well with moisture content values obtained prior to fabrication. The specific gravity values obtained after tests exhibit a definite tendency towards a maximum specific gravity at the mid-depth laminations, decreasing to a minimum at the outer laminations. However, a limited number of beams did contain dense material

in the outer laminations.

7-2 Control Beams

In order to establish whether or not the two stage method of beam fabrication had a detrimental effect on beam shear strength, the control beam test results of this investigation and Strong's investigation are compared. In both these investigations beams of identical dimensions were manufactured from the same fabricating stock. However, the beams tested by Strong were manufactured by normal fabricating procedures. The thirteen control beams in Strong's investigation sustained an average horizontal shear stress of 391 psi prior to failure by four typical failure modes. The three beams failing in horizontal shear failed at an average horizontal shear stress of 377 psi. Examination of TABLE VI-2 indicates all the control beams in this present investigation developed horizontal shear stresses comparable to Strong's beam results. Therefore, the two stage method of beam manufacture did not have an apparent effect on horizontal shear strength.

Qualitatively the strain distributions of control beam X-003 (FIGURE 6.3) appear to satisfy the normal assumption of a linear distribution of strains. This is more evident when a comparison is made with the distributions obtained by Ramos (FIGURE 1.6). The strain distributions obtained from control beam X-003 do not contain the abrupt variations in strain through the depth of the section, which are present at a number of the sections in the beams tested by Ramos.

At all sections in control beam X-003 the outer tensile strains

are about ten percent larger than the corresponding compressive strains. Therefore, in order to satisfy equilibrium, this difference would imply that the compressive elastic modulus is slightly larger than the tensile elastic modulus.

At sections 1 to 4 of control beam X-003, the neutral axis shifted upwards from the centroidal axis of the beam. Examining TABLE VI-3 with respect to the specific gravity of the laminations in this control beam, indicates laminations above the centroidal axis have an average specific gravity (0.579) higher than the laminations below (0.522). Doyle, McBurney and Drow (1946) found that an increase in specific gravity resulted in an increase in the modulus of elasticity. A transformed section concept based on a varying modulus of elasticity would explain the upward shift of the neutral axis.

A computer program (APPENDIX B) was used in an attempt to determine the horizontal shear stress from longitudinal strain distributions in control beam X-003. This analysis, considering equilibrium of the top and bottom portions of the beam, usually produces two incompatible values of shear stress at the neutral axis. Furthermore, for all loads the shear stresses at the neutral axis of the instrumented sections generally deviate widely from theoretical values, as shown in TABLE VI-6B.

7-3 Delaminated Beams

i. Strains and Shear Stresses at Intact Sections

In a homogeneous, isotropic, rectangular beam a linear distribution of longitudinal strain is valid at the transverse sections

along the beam length. In order to satisfy equilibrium at any transverse section, the shear stress distribution is a second degree parabola having a maximum ordinate at the neutral axis. This maximum shear stress is 1.5 times the average transverse shear stress.

The presence of a discontinuity at the mid-depth of a beam, such as a delamination, results in a shear stress concentration in the vicinity of this discontinuity. To simultaneously satisfy this condition of a shear stress concentration and equilibrium of the cross section, a non-linear distribution of flexural stresses must exist across the section. If the outer fiber flexural stress is below the proportional limit stress, the strain distribution will be in direct proportion to the flexural stress distribution. Therefore, sections which are plane before bending do not remain plane, but warp as a result of bending. Under this condition the maximum shear stress at the neutral axis will be in excess of 1.5 times the average shear stress, as shown in FIGURE 2.2.

FIGURES 6.4 to 6.13 illustrate the longitudinal strain distributions measured in the instrumented delaminated beams. From these distributions it is very evident, by the extent of the non-linearity in strains, or warping of sections, that a definite shear stress concentration must exist in the vicinity of the delamination.

FIGURES 6.4 and 6.9 indicate parabolic strain distributions exist at section 4 in beams XZ-41 and XY-41, which contain 1'-0" long delaminations. As the distance from the end of the delamination increases the strains approach a linear distribution. Beams XZ-42 and XY-42 (FIGURES 6.5 and 6.10), containing 2'-0" long delaminations, exhibit marked parabolic strain distributions at sections 4 to 6. Similarily,

the extent and magnitude of the parabolic strain distributions are shown for beams XZ-425 and XY-425, containing 2'-6" long delaminations, in FIGURES 6.6 and 6.11. In both of these beams section 4 at the end of the delamination is warped to such an extent that magnitude of the strains in the outer two laminations approach a constant value across these laminations. As a consequence, a larger amount of the total transverse shear at the section will be carried by the central portion of the beam. In beams XZ-43 and XY-43, with 3'-0" long delaminations (FIGURES 6.7 and 6.12), parabolic strain distributions exist at sections 4 to 8. FIGURE 6.19B, typical for all delaminated beams, indicates the fairly uniform progression of strains at an intact section, through the full range loads to failure. The strain distributions in beams XZ-44 and XY-44, containing 4'-0" long delaminations (FIGURES 6.8 and 6.13) are peculiar. At sections 4 and 5 the strain increases from the neutral axis to a maximum at the quarter depth before decreasing towards the outer laminations. In the delaminated portions of these beams the compression and tension flexural forces are largely concentrated near the delamination plane, as shown by the strains in FIGURE 6.18. This immediate proximity of the larger portion of these longitudinal forces to the neutral surface will result in substantial horizontal shear stress concentrations at intact sections, in the vicinity of the delamination. This would then explain the extensive warping observed in these beams.

It is therefore evident that the longer the delamination or larger the ratio of delamination length to beam length (D/L ratio) the more the strain distribution, in the vicinity of the delamination, deviates from a linear distribution. In beams with low D/L ratios the

longitudinal strain is a maximum at the outer fibers, decreasing almost linearly to zero at the neutral axis. For larger D/L ratios the strains at intact sections in the vicinity of the delamination become parabolic. For these large D/L ratios the strains in delaminated sections at the end of the delamination are a minimum at the outer fibers, increasing to a maximum at the delamination. Guyon's and Lee's influence lines (Figure 1.4) indicate loads at lower eccentricities produce larger shear stresses on the neutral surface. Therefore, beams with high D/L ratios will develop large shear stress concentrations. This explains the pronounced warping observed at these cross-sections. Similarly, beams with low D/L ratios having the larger portion of the longitudinal fiber forces at large eccentricities, will develop less severe shear stress concentrations resulting in moderate warping.

Using the computer program in APPENDIX B, an attempt was made to compute the horizontal shear stress distributions between transverse beam sections, for all loads to failure. In the analysis of every section a second degree parabola is fitted to each set of five recorded longitudinal strains above and below the neutral axis. The flexural stresses at each section are determined from the defined strains together with a modulus of elasticity having a value equal to the average of the compressive and tensile moduli. The shear stress distribution, between any two successive sections, is then obtained by considering the horizontal equilibrium of thirty elements through the depth of the top and bottom halves of the beam. For the vast majority of the sections in all the beams this analysis usually produces two different values of shear stress at the neutral axis. (TABLE VI-6). FIGURE 6.25 indicates

the horizontal shear stress distributions at sections where compatability of shear stress at the neutral axis is approached. These distributions when compared to the normal parabolic distribution indicate the presence of a definite shear stress concentration at the neutral axis. For all beams the values listed in TABLE VI-6A indicate that at the neutral axis there are no reasonable gradients in shear stresses, between intact sections in the vicinity of the delaminations. Therefore, the extent of the horizontal shear stress concentrations cannot be determined from these computed shear stresses.

Even though the strain distribution in the vicinity of the delamination is complicated, it should be possible to obtain valid shear stress values from this type of analysis on longitudinal strains. In this investigation a second degree parabola is fitted to the recorded strains, but in very few cases do these five strains define a perfect parabola. A slight variation in any one of these five strains influences the equation of the best fit parabola to a considerable degree. Due to the nature of the computations, a small variation in strain distribution produces a large accumulative error in the shear stress at the neutral axis. Perhaps better results would be obtained if deeper beams were instrumented and tested. With a large number of strain readings over the depth of the section a more accurate strain distribution might be obtained. Theoretical and experimental shear stress values, which different computational methods indicate to exist in beam XY-425, are illustrated in FIGURE 6.26. The theoretical shear stresses computed by Guyon's and Lee's influence coefficients (APPENDIX C) indicate sizable shear stress concentrations exist for a distance of d/3 (2 inches) away

from the end of the delamination. For greater distances these two methods yield shear stresses which are lower than the average horizontal shear stress, computed on the undelaminated neutral surface. This trend is common for all D/L ratios. At a distance d/3 from the end of the delamination, the two compatible values of the shear stress at the neutral axis are about twenty-five per cent greater than the average shear stress. However, since the occurrence of this compatibility of shear stresses at the neutral axis is an exception rather than the rule, no conclusions can be drawn with respect to the magnitude of the stress concentration. In examining the strain distributions obtained for the delaminated beams (FIGURES 6.4 to 6.13), the extent of section warping indicates shear stress concentrations do exist at sections situated further than d/3 away from the end of the delamination. For low D/L ratios warping extends to d/2 (3 inches) from the end of the delamination while for high D/L ratios warping extends to 3/2 d (9 inches).

In the delaminated beams a vast majority of sections exhibit outer tensile strains about ten per cent greater than corresponding compressive strains. This tendency, present at all loading stages, suggests a slightly higher modulus of elasticity in compression than in tension.

At strains much below compression yielding, the neutral axis in a number of beams shifted down towards the tension face of the beam. As for the control beam X-003, a reasonable explanation of this trend would be a transformed section based on an increased modulus of elasticity with an increase in specific gravity. Examination of TABLE VI-5 indicates

that the majority of beams, in which this shift occurred have denser laminations in the lower portion of the beam as compared to the top. Therefore, the neutral axis of the transformed section would be located below the centroidal axis of the beam.

FIGURE 6.20 gives a comparison of strains determined by the 2-inch Demec gauge and SR-4 Type A-3 strain gauges. The minute differences in values obtained can be attributed to observation errors.

ii. Strains in Delaminated Sections

The method developed by Huggins, Aplin and Palmar for determining stress distributions in delaminated sections was employed to determine theoretical strain distributions shown in FIGURES 6.14 to 6.18. A modulus of elasticity of 1.72×10^6 psi, obtained from the control beam tests, was used in the calculations. The flexural stress distributions, which are different for beams with different D/L ratios, must be compatible with the equilibrium of the particular section under consideration. Therefore, the value of the elastic modulus applied to the theoretical stress distribution will only affect the magnitude of the theoretical strains and not the actual distribution of these strains across the section.

Beams XZ-41 and XY-41, containing 1'-0" long delaminations, show very good agreement between theoretical and experimental strain distributions (FIGURE 6.14). For beams XZ-42 and XY-42, with 2'-0" long delaminations, the theoretical and experimental strain distributions are in good agreement for sections 1 and 2 (FIGURE 6.15). At section 3 in both beams the experimental strain distribution is not geometrically

similar to the theoretical distribution. Experimental strain distributions for beams XZ-425 and XY-425 differ considerably from the theoretical distributions (FIGURE 6.16). However, the agreement is generally very good for beams XZ-43 and XY-43, containing 3'-0" long delaminations (FIGURE 6.17). FIGURE 6.24A indicates the strains at delaminated section 3 increase almost uniformly with increase in load. The strain distributions for beams XZ-44 and XY-44, containing 4'-0" long delaminations, agree with theoretical values at the outer fibers. Progressing towards the delamination plane this agreement begins to diverge.

At most delaminated sections the measured strains were of lower magnitude than the theoretical strains. This difference would be rectified if a higher modulus of elasticity, as indicated by compression and tension test specimens, is used.

An examination of beams having the same delamination length, but a different type of delamination, indicates there is no significant difference in the strain distributions at delaminated sections. This implies that friction, in the wood contact type of delamination, has no apparent effect on the forces in the delaminated sections. In beams having low D/L ratios agreement between experimental and theoretical strain distributions is generally good. However, for higher D/L ratios this correlation diverges. The initial assumption of plane sections remaining plane after bending is definitely not valid for sections at the termination of the delamination. The pronounced warping of the sections for high D/L ratios is most likely responsible for the deviation in the strain distributions.

For most beams the correlation between experimental and theoretical strain distributions improved at sections removed from the end of the delamination. The deviation of the theoretical strains from the actual strains near the end of the delamination affects the magnitude of the shear stress concentrations, computed using Guyon's or Lee's influence lines.

CHAPTER VIII

CONCLUSIONS AND RECOMMENDATIONS

8-1 Conclusions

The most significant conclusions based on the results of this investigation are summarized as follows:

1. Non-linear longitudinal strain distributions at intact sections of delaminated beams indicate shear stress concentrations exist in the vicinity of a delamination. The extent of this non-linearity in strain is more pronounced in beams having large delamination length to beam length ratios.
2. It is not possible to accurately compute shear stresses from equilibrium considerations using longitudinal strain distributions obtained in this investigation. The relatively small number of strains recorded across the beam section do not satisfactorily define the strain distribution.
3. The theoretical and experimental strain distributions at delaminated sections agree reasonably well for low delamination to beam length ratios. However, this correlation decreases with increasing delamination length to beam length ratios.
4. At delaminated sections it appears that there is no appreciable friction between the contacting delamination surfaces.

8-2 Recommendations

The results of this investigation indicate that tests on deeper beams may be warranted. An increased section depth may facilitate a more accurate determination of the longitudinal strain distribution across the section.

The possibility of developing further theoretical shear stress distributions from non-linear longitudinal strain distributions should be investigated.

BIBLIOGRAPHY

1. Dietz, A.G.H., Grinsfelder, H. and Reissner, E., "Glue-Line Stresses in Laminated Wood" Transactions of the American Society of Mechanical Engineers, Volume 48, 1946.

2. Canadian Standards Association, "0122-1959 Specification for Glued-Laminated Softwood Structural Timber" Second Edition 1959.

3. Huggins, M.W., Aplin, E.N., and Palmer, T.H.C., "Static and Repeated Load Tests of Delaminated Glulam Beams" Ontario Joint Highway Research Programme, Report No. 32, July 1964.

4. Guyon, Y., "Prestressed Concrete" Volume I. London, Contractors Record Ltd. 1960.

5. Iyengar, S.R. "Two-Dimensional Theories of Anchorage Zone Stresses in Post-Tensioned Prestressed Beams". Journal of the American Concrete Institute, October 1962.

6. Lee, C.S. "Shear Stress in the Vicinity of Delaminations" MASc. Thesis 1964, University of Toronto.

7. Ramos, A.N., "Stress-Strain Distributions in Douglas-Fir Beams Within the Plastic Range". Forest Products Laboratory Report No. 2231, 1961.

8. Doyle, D.V., McBurney, R.S. Drow, D.T., "The Elastic Properties of Wood", Forests Products Laboratory Report Nos. 1528 D and E, 1946.

9. Strong, J.M., "The Effect of Delamination on Shear Strength of Glulam Beams" M.Sc. Thesis 1964, University of Alberta.

APPENDIX A

DETERMINATION OF MOISTURE CONTENT AND SPECIFIC GRAVITY

Specimens were weighed prior to being dried in an oven at 100°C for 36 hours. Upon removal from the oven the specimens were placed in a desiccation cabinet for 2 hours and then weighed. The volume of the specimen was obtained by a mercury displacement method. A container was filled with mercury until the volume of mercury equaled the exact volume of the container. The specimen was then immersed in the mercury and the mercury which overflowed from the container was weighed. Repeating this procedure for any one specimen indicated the maximum volumetric deviation of displaced mercury specimen was one percent. Moist weight, dry weight and weight of displaced mercury were read into the IBM 7040 Digital Computer and the moisture content and specific gravity were calculated by the program on page A2.

```
$IBSYS
$JOB            180027   E. F. COLLINS    PROGRAM  ONE
$TIME           2,1000
$IBJOB REDUCE
$IBFTC RESULTS NODECK
C      COMPUTATION OF MOISTURE CONTENT AND SPECIFIC GRAVITY
       COMMON MW(8,15),DW(8,15),WM(8,15),SG(8,15),MC(8,15)
       INTEGER B
       REAL MW,MC
       DO 500 B=1,13
       READ(5,100) (MW(L,B),DW(L,B),WM(L,B),L=1,4)
       READ(5,100) (MW(L,B),DW(L,B),WM(L,B),L=5,8)
       WRITE(6,201)
       DO 501 L=1,8
   779 MC(L,B)=(MW(L,B)-DW(L,B))/DW(L,B)
   778 SG(L,B)=DW(L,B)*13.55/WM(L,B)
   501 WRITE(6,200)L,MW(L,B),DW(L,B),WM(L,B),MC(L,B),SG(L,B)
   500 CONTINUE
   201 FORMAT(5HLBEAM)
   200 FORMAT(1X,I5,5F10.3)
   100 FORMAT(1X,2F4.1,F6.1,2F4.1,F6.1,2F4.1,F6.1,2F4.1,F6.1)
       STOP
       END
$ENTRY          RESULTS
```

APPENDIX B

COMPUTER PROGRAM FOR SHEAR STRESSES

The reduction of strain gauge readings and the subsequent computations in determining shear stresses are time consuming and repetative. Therefore, solutions were obtained by means of a computer program. This program was written in Fortran IV for the IBM 7040 Digital Computer. A very simplified flow-chart and the actual program as shown on pages B2 to B8.

FLOW CHART FOR SHEAR STRESS COMPUTER PROGRAM

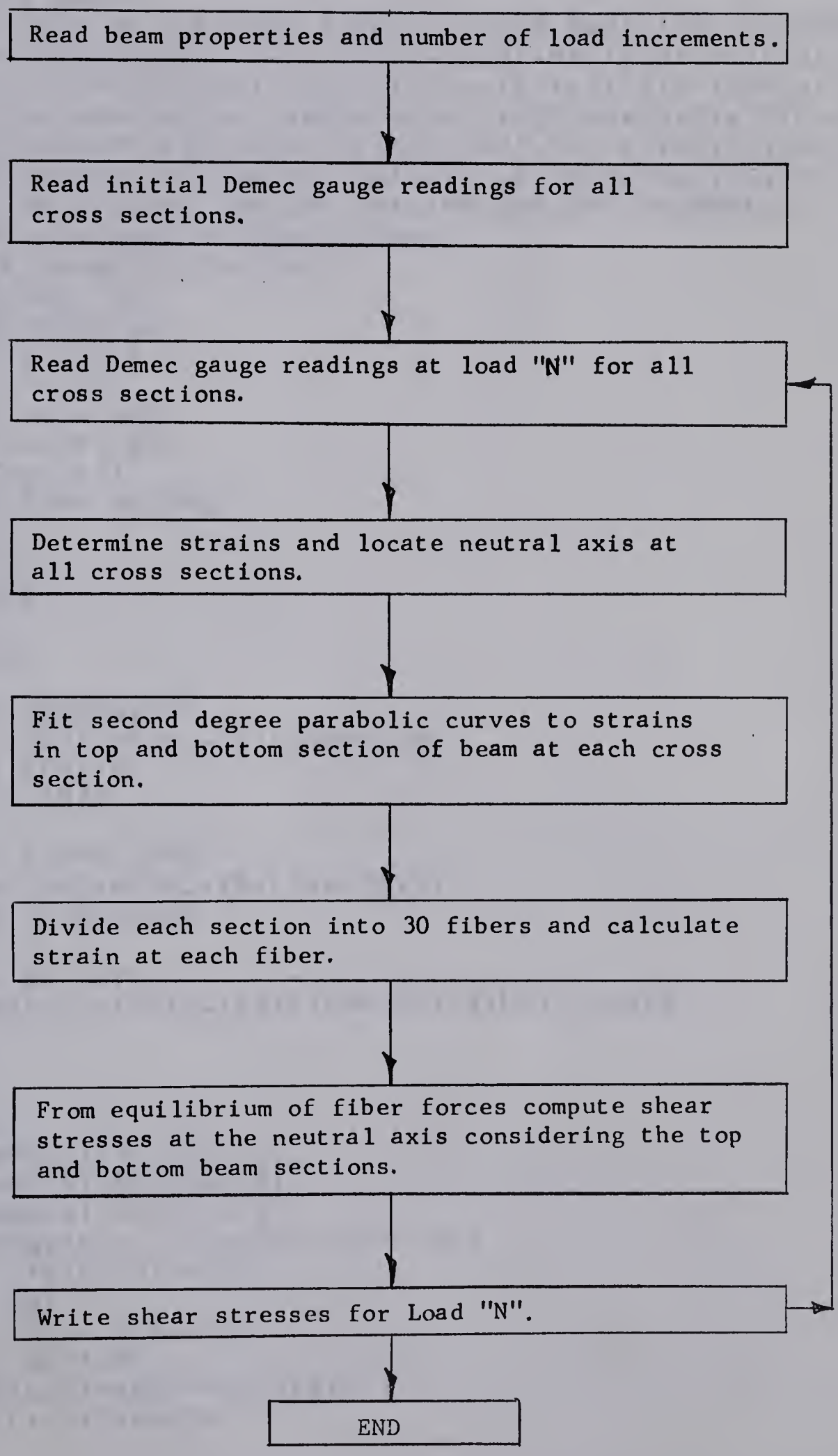

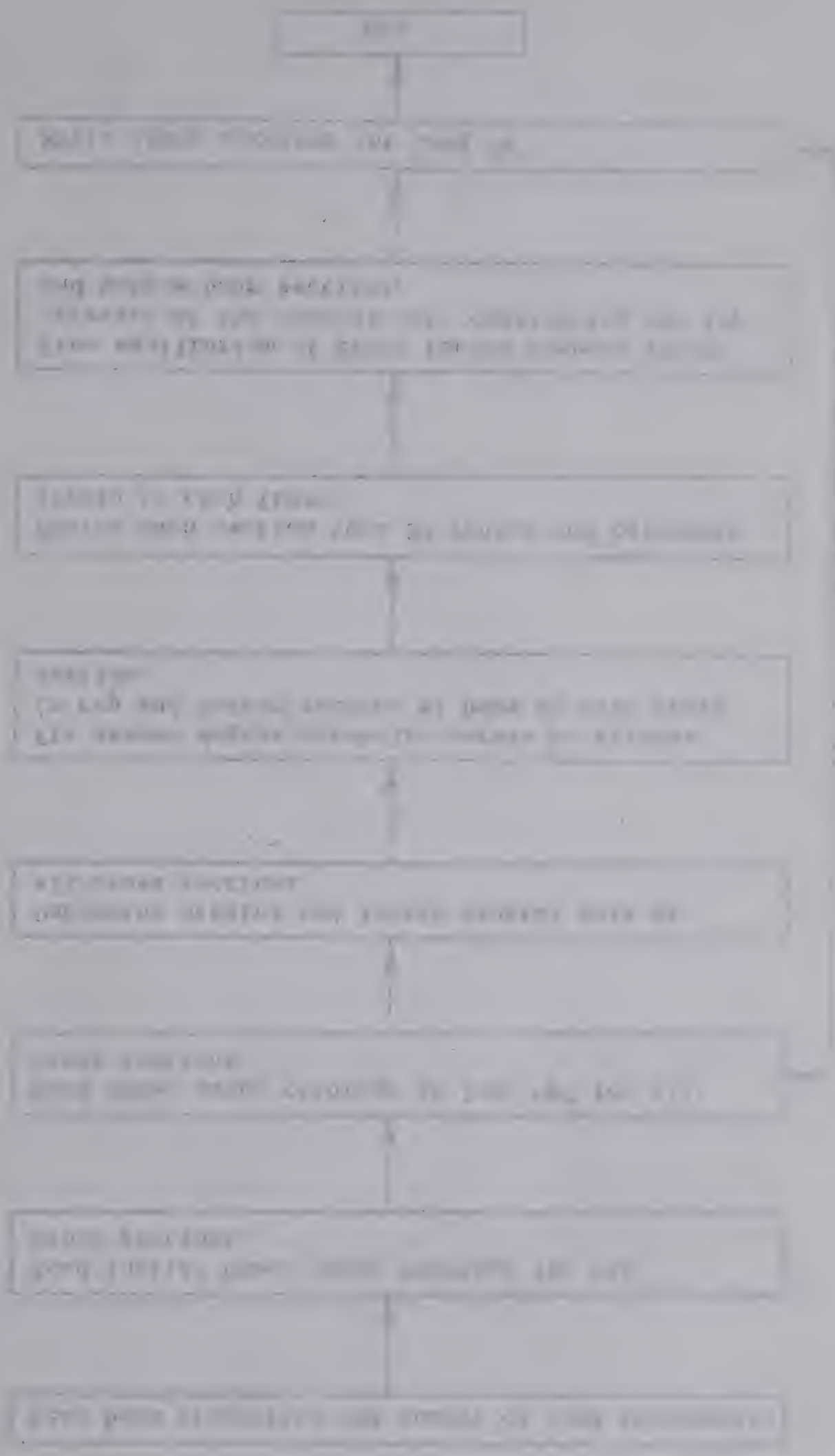

```
$IBSYS
$JOB            180027    E. F. COLLINS    PROGRAM TWO
$TIME           8,5000
$IBJOB REDUCE
$IBFTC RESULTS NODECK
C      COMPUTATION OF SHEARING STRESSES FROM EQUILIBRIUM CONSIDERATIONS
       COMMON P(12),DR(10,12,2),ST(10,12,2),NA(12,2),NA2(12,2),
      1X(10,12,2),Y(10,12,2),YS(63,12,2),YST(63,12,2),XB(63,12,2),
      2F(63,12,2),M(63,12,2),XBC(63,12,2),YSC(63,12,2),YSTC(63,12,2),
      3FC(63,12,2),MC(63,12,2),DFC(63,12,2),YVC(63,12,2),SVC(12,2),
      4NES,NEF,NP,N11,N121,N222,N241,E,EC,ET,D,B,NX,L,XS,XSL,LO,N10,DNA,
      5C,GL,TL,GLX,H,NGAI,NGA,XX,XXX,AMR,BMR,CMR,DC,NNA(12)
       REAL P,NX,NA,NA2,NF,NGA,NF2,NF3
       INTEGFR XS,GL,XSL,H,X2,C
       READ(5,101) NB
       READ(5,105)EC,ET
       READ(5,106)D,B
       READ(5,101)NP
       DO 200 NBC=1,NB
       WRITE(6,109) NBC
  109  FORMAT(1X,I7)
       READ(5,100) NES,NEF
       NX=30.
       DC=0.10
       TL=D/8.0
       N11=1
       N241=62
       L=1
       DO 201 XS=NES,NEF
  201  READ(5,103)(DR(GL,XS,L),GL=1,9)
       DO 202 LC=2,NP
       WRITE(6,102)
       L=2
       DO 300 XS=NES,NEF
  300  READ(5,103)(DR(GL,XS,L),GL=1,9)
       DO 203 XS=NES,NEF
       LO=1
       DO 204 GL=1,9
  204  ST(GL,XS,L)=(DR(GL,XS,L)-DR(GL,XS,LO))*0.038
       N4=4
       N5=5
       N6=6
       N10=10
       ST4=(ABS(ST(N4,XS,L)))
       ST5=(ABS(ST(N5,XS,L)))
       ST6=(ABS(ST(N6,XS,L)))
       IF(ST(N5,XS,L).LE.0.00) GO TO 253
       DNA=-TL*ST5/(ST5+ST4)
       GO TO 281
  253  DNA=TL*ST5/(ST5+ST6)
  281  DO 254 GL=1,9
  254  ST(GL,XS,L)=ABS(ST(GL,XS,L))
       NA(XS,L)=D/2.0+DNA
```

```
      NA2(XS,L)=D-NA(XS,L)
      GLX=NA(XS,L)+TL
      NF=NA(XS,L)/TL+1.0
      NI=NF
      DO 282 GL=1,NI
      GLX=GLX-TL
      X(GL,XS,L)=GLX
  282 Y(GL,XS,L)=ST(GL,XS,L)
      H=1
      NGAI=NI+1
      N10=NI+1
      X(N10,XS,L)=0.0
      Y(N10,XS,L)=0.0
      NGA=NGAI
      CALL SRP1
      CALL SRP2
      CALL SRP3
      NF2=9.0-NF
      NI2=NI+1
      NI3=NF2
      NF3=NI3
      GLX=NA2(XS,L)-NF3*TL
      DD2=D*0.5
      DD3=NA(XS,L)
      DD4=ABS(DD2-DD3)
      IF(DD4.EQ.0.00) GLX=0.75
      NGAI=11-NI2
      NGA=NGAI
      N9=1
      DO 283 GL=NI2,9
      N9=N9+1
      X(N9,XS,L)=GLX
      Y(N9,XS,L)=ST(GL,XS,L)
  283 GLX=GLX+TL
      H=2
      N10=1
      X(N10,XS,L)=0.0
      Y(N10,XS,L)=0.0
      CALL SRP1
      CALL SRP2
      CALL SRP3
  203 CONTINUE
      CALL SRP4
      DO 303 C=N11,N241
  303 WRITE(6,104)(XBC(C,XS,L),YVC(C,XS,L),XS=2,NEF)
  202 CONTINUE
  200 CONTINUE
  100 FORMAT(1X,2I3)
  101 FORMAT(1X,I3)
  102 FORMAT(1HK)
  103 FORMAT(1X,9F7.3)
  104 FORMAT(1X,F11.2,F7.1,F11.2,F7.1,F11.2,F7.1,F11.2,F7.1,F11.2,F7.1,
     1F11.2,F7.1)
```

```
  105 FORMAT(1X,2F8.0)
  106 FORMAT(1X,2F5.2)
  107 FORMAT(1X,10F6.0)
      STOP
      END
$IBFTC ABCD1    NODECK
      SUBROUTINE SRP1
      COMMON P(12),DR(10,12,2),ST(10,12,2),NA(12,2),NA2(12,2),
     1X(10,12,2),Y(10,12,2),YS(63,12,2),YST(63,12,2),XB(63,12,2),
     2F(63,12,2),M(63,12,2),XBC(63,12,2),YSC(63,12,2),YSTC(63,12,2),
     3FC(63,12,2),MC(63,12,2),DFC(63,12,2),YVC(63,12,2),SVC(12,2),
     4NES,NEF,NP,N11,N121,N222,N241,E,EC,ET,D,B,NX,L,XS,XSL,LO,N10,DNA,
     5C,GL,TL,GLX,H,NGAI,NGA,XX,XXX,AMR,BMR,CMR,DC,NNA(12)
      REAL  AMR,BMR,CMR,M1,M2,M3,M4,M5,M6,M7,M8,DD,EE,BB,CC,X,Y,NGA
      INTEGER G,C,L,XS
      M1=0.0
      M2=0.0
      M3=0.0
      M4=0.0
      M5=0.0
      M6=0.0
      M7=0.0
      M8=0.0
      DO 600 G=1,NGAI
      M1=M1+Y(G,XS,L)
      M2=M2+X(G,XS,L)
      M3=M3+((ABS(Y(G,XS,L)))**2.0)
      M4=M4+((ABS(X(G,XS,L)))**2.0)
      M5=M5+((ABS(X(G,XS,L)))**3.0)
      M6=M6+((ABS(X(G,XS,L)))**4.0)
      M7=M7+(X(G,XS,L)*Y(G,XS,L))
  600 M8=M8+((ABS(X(G,XS,L)))**2.0)*(Y(G,XS,L))
      DD=(NGA*(M4*M6-M5*M5))-(M2*(M2*M6-M5*M4))+(M4*(M2*M5-M4*M4))
      EE=( M1*(M4*M6-M5*M5))-(M7*(M2*M6-M5*M4))+(M8*(M2*M5-M4*M4))
      BB=(NGA*(M7*M6-M8*M5))-(M2*(M1*M6-M8*M4))+(M4*(M1*M5-M7*M4))
      CC=(NGA*(M4*M8-M5*M7))-(M2*(M2*M8-M5*M1))+(M4*(M2*M7-M4*M1))
      AMR=EE/DD
      BMR=BB/DD
      CMR=CC/DD
      RETURN
      END
$IBFTC ABCD2    NODECK
      SUBROUTINE SRP2
      COMMON P(12),DR(10,12,2),ST(10,12,2),NA(12,2),NA2(12,2),
     1X(10,12,2),Y(10,12,2),YS(63,12,2),YST(63,12,2),XB(63,12,2),
     2F(63,12,2),M(63,12,2),XBC(63,12,2),YSC(63,12,2),YSTC(63,12,2),
     3FC(63,12,2),MC(63,12,2),DFC(63,12,2),YVC(63,12,2),SVC(12,2),
     4NES,NEF,NP,N11,N121,N222,N241,E,EC,ET,D,B,NX,L,XS,XSL,LO,N10,DNA,
     5C,GL,TL,GLX,H,NGAI,NGA,XX,XXX,AMR,BMR,CMR,DC,NNA(12)
      REAL NX,M,MI,ME,NA,NA2
      INTEGER H,XS,XX,XXX,X1,C,XX1
      X1=63
      IF (H.EQ.2)GO TO 602
```

```
      C1=NA(XS,L)/DC
      N1=C1
      C3=N1
      N12=N11+1
      XX=N11
      XXX=N1+2
      N121=XXX
      NNA(XS)=N121
      XX1=0
      E=EC
      GO TO 603
  602 XX1=XXX+1
      N222=XX1
      XX=N222
      XXX=N241
      C2=N1+1
      XB(X1,XS,L)=C2*DC-NA(XS,L)-DC
      E=ET
  603 YB(X1,XS,L)=0.0
      YST(X1,XS,L)=0.0
      M(X1,XS,L)=0.0
      DO 601 C=XX,XXX
      IF(C.EQ.N12) GO TO 608
      IF(C.EQ.XX1) GO TO 611
      IF(C.EQ.N11) GO TO 636
      XB(C,XS,L)=XB(X1,XS,L)+DC
      DC1=1.0
      GO TO 610
  608 XB(C,XS,L)=NA(XS,L)-C3*DC
      DC1=ABS(XB(C,XS,L))/DC
      GO TO 610
  611 XB(C,XS,L)=C2*DC-NA(XS,L)
      DC1=ABS(XB(C,XS,L))/DC
  610 YS(C,XS,L)=CMR*((ABS(XB(C,XS,L)))**2.0)+BMR*XB(C,XS,L)+AMR
      YST(C,XS,L)=YS(C,XS,L)*E
      F(C,XS,L)=(YST(C,XS,L)+YST(X1,XS,L))*0.5*DC*B*DC1
      M(C,XS,L)=F(C,XS,L)*(XB(C,XS,L)-0.5*DC*DC1)+M(X1,XS,L)
      GO TO 601
  636 F(C,XS,L)=0.0
      M(C,XS,L)=0.0
      YS(C,XS,L)=0.0
      YST(C,XS,L)=0.0
      XB(C,XS,L)=0.0
  601 X1=C
      RETURN
      END
$IBFTC ABCD3   NODECK
      SUBROUTINE SRP3
      COMMON P(12),DR(10,12,2),ST(10,12,2),NA(12,2),NA2(12,2),
     1X(10,12,2),Y(10,12,2),YS(63,12,2),YST(63,12,2),XB(63,12,2),
     2F(63,12,2),M(63,12,2),XBC(63,12,2),YSC(63,12,2),YSTC(63,12,2),
     3FC(63,12,2),MC(63,12,2),DFC(63,12,2),YVC(63,12,2),SVC(12,2),
     4NES,NEF,NP,N11,N121,N222,N241,E,EC,ET,D,B,NX,L,XS,XSL,LO,N10,DNA,
     5C,GL,TL,GLX,H,NGAI,NGA,XX,XXX,AMR,BMR,CMR,DC,NNA(12)
      REAL NA
```

```
      INTEGER XX,XXX,X2,K,XS,L,H
      IF(H.EQ.2) GO TO 850
      XX=N11
      Z=1.0
      XXX=N121
      X2=N121
      K=-1
      GO TO 852
  850 XX=N222
      XXX=N241
      Z=-1.0
      K=1
      X2=XX
      GO TO 852
  852 DO 851 NN=XX,XXX
      XBC(NN,XS,L)=NA(XS,L)-XB(X2,XS,L)*Z
      YSC(NN,XS,L)=YS(X2,XS,L)
      YSTC(NN,XS,L)=YST(X2,XS,L)
      FC(NN,XS,L)=F(X2,XS,L)
      MC(NN,XS,L)=M(X2,XS,L)
  851 X2=X2+K
      RETURN
      END
$IBFTC ABCD4    NODECK
      SUBROUTINE SRP4
      COMMON P(12),DR(10,12,2),ST(10,12,2),NA(12,2),NA2(12,2),
     1X(10,12,2),Y(10,12,2),YS(63,12,2),YST(63,12,2),XB(63,12,2),
     2F(63,12,2),M(63,12,2),XBC(63,12,2),YSC(63,12,2),YSTC(63,12,2),
     3FC(63,12,2),MC(63,12,2),DFC(63,12,2),YVC(63,12,2),SVC(12,2),
     4NES,NEF,NP,N11,N121,N222,N241,E,EC,ET,D,B,NX,L,XS,XSL,LO,N10,DNA,
     5C,GL,TL,GLX,H,NGAI,NGA,XX,XXX,AMR,BMR,CMR,DC,NNA(12)
      INTEGER XS1,XS,C,CC
      DO 704 XS=2,NEF
      XS1=XS-1
      K1=N11
      K2=NNA(XS)
      K3=K1
      K4=K2
      K5=1
      K6=-1
      GO TO 719
  719 C=K1+K6
      DO 702 CC=K3,K4
      C=C+K5
      IF(C.EQ.K1) GO TO 709
      IF(C.EQ.K2) GO TO 710
      GO TO 713
  709 DFC(C,XS,L)=(FC(C,XS1,L)-FC(C,XS,L))/(2.0*B)
      YVC(C,XS,L)=0.0
      SVC(XS,L)=DFC(C,XS,L)
      GO TO 702
  710 YVC(C,XS,L)=SVC(XS,L)
      GO TO 702
  713 DFC(C,XS,L)=(FC(C,XS1,L)-FC(C,XS,L))/(2.0*B)
      YVC(C,XS,L)=SVC(XS,L)
```

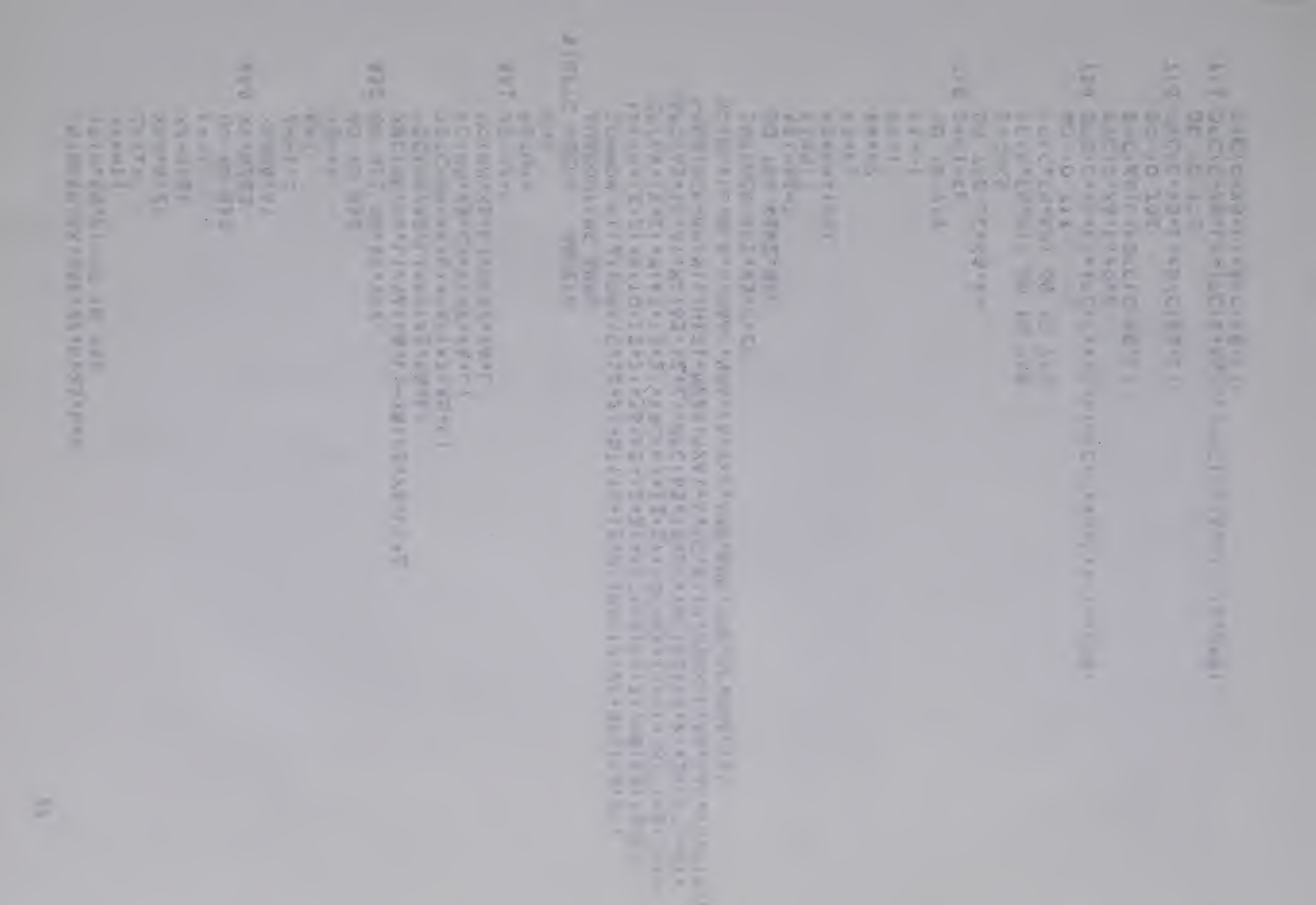

```
      SVC(XS,L)=DFC(C,XS,L)+SVC(XS,L)
  702 CONTINUE
      IF(K1.EQ.N11) GO TO 720
      GO TO 704
  720 K1=N241
      K2=0
      K3=NNA(XS)
      K4=N241
      K5=-1
      K6=1
      GO TO 719
  704 CONTINUE
      RETURN
      END
$ENTRY          RESULTS
```

APPENDIX C

CALCULATION OF THEORETICAL SHEAR STRESS CONCENTRATIONS

The calculations of the theoretical shear stress concentrations (FIGURE 6.26), based on Guyon's and Lee's methods, are outlined in this appendix. The following sample calculations illustrate the determination of the horizontal shear stress, based on Lee's method, at a distance d/6 (1/2 inch) from the end of the delamination in beam XY-425.

The distribution of flexural stresses across a section at the end of the delamination must be obtained by the simultaneous solution of Equations 1.1 and 1.4 as follows:

$$R_L (a + z) - M_T - M_B - \frac{Cd}{2} = 0 \qquad (1.1)$$

$$\frac{2z}{dE} \left(\frac{C}{A_T} + \frac{T}{A_B}\right) = \frac{1}{EI_T} \left[M_{TX} - \frac{V_{TX}^2}{4} \right]_{x=0}^{x=2} \qquad (1.4)$$

where

$a = 21.0$ in.

$a_1 = 1.0$ in.

$z = 15.0$ in.

$b = 3.0$ in.

$d = 6.0$ in.

$k = 0.5$

$A_T = A_B = 9.0$ in.^{2}

$A = 18.0$ in.^{2}

$I = 54.0$ in.^{4}

$I_T = I_B = 6.75$ in^4

$R_L = 2500$ lbs.

Since $k = 0.5$

$$M_B = M_T$$

$$C = T$$

$$V_T = V_B = 0.5\ R_L$$

Substituting these values into Equations 1.1 and 1.4:

$$110 - 2M_T - 3C = 0 \qquad (1.1A)$$

$$20.8 - 2.22M_T + 1.11C = 0 \qquad (1.4A)$$

Solving:

$$C = T = 17.8 \text{ kips}$$

$$M_T = M_B = 18.25 \text{ in-kips}$$

At the end of the delamination where x = 15 in.:

$$M_{TX} = M_T - V_T X$$

$$M_{TX} = M_{BX} = -0.50 \text{ in-kips}$$

The flexural stresses in the top and bottom delaminated portions are:

$$f = \frac{C}{A_T} + \frac{M_T d}{4I_T}$$

$$f_{max.} = \pm 1{,}987 \text{ psi at the delamination}$$

$$f_{min.} = \pm 1{,}967 \text{ psi at the outer fibers}$$

The average horizontal shear stress on the undelaminated surface is:

$$v_{ave} = \frac{C}{b(a_1 + a)} = 270 \text{ psi}$$

In order to compute the shear stress concentration on the neutral surface at d/6 from the end of the delamination, each delaminated beam portion is divided into ten elements. Influence coefficients (FIGURE 1.7) are obtained for each element knowing its distance from the neutral axis. The shear stress at the neutral axis due to the influence of a single element is:

$$v_n = \frac{0.05 \text{ bd } f_n C_n}{bd}$$

$$= 0.05 \, f_n C_n$$

where v_n = element "n" shear stress

f_n = element "n" fiber stress

C_n = element "n" influence coefficient

For the twenty elements through the depth of the beam the total shear stress is:

$$v = 0.05 \sum_{n=1}^{n=20} f_n C_n$$

Since the computations for the two delaminated portions are identical

$$v = 0.10 \sum_{n=1}^{n=10} f_n C_n$$

The computations are tabulated below in TABLE C1.

TABLE C1

LEE'S SHEAR STRESS CONCENTRATION AT d/6

Element	f_n (psi)	C_n	$f_n C_n$
1	1968	-0.30	- 590
2	1970	-0.35	- 689
3	1972	-0.20	- 394
4	1974	-0.10	- 197
5	1976	0.05	99
6	1978	0.18	356
7	1980	0.45	890
8	1982	0.93	1843
9	1984	2.05	4067
10	1986	1.02	2035
		$\sum_{n=1}^{n=10} f_n C_n$ =	7420

$$v_{d/6} = 0.10 \times 7420 = 742 \text{ psi}$$

Similar computations were performed for other sections and the results recorded in FIGURE 6.25.